

**SYNTHESIS, CHARACTERIZATION AND
ENCAPSULATION STUDIES OF MULTIDENTATE
LIGANDS AND THEIR ORGANOTIN COMPLEXES**

NUR ADIBAH BINTI MOHD AMIN

**FACULTY OF SCIENCE
UNIVERSITY OF MALAYA
KUALA LUMPUR**

2019

**SYNTHESIS, CHARACTERIZATION AND
ENCAPSULATION STUDIES OF
MULTIDENTATE LIGANDS AND THEIR
ORGANOTIN COMPLEXES**

NUR ADIBAH BINTI MOHD AMIN

**DISSERTATION SUBMITTED IN FULFILMENT OF
THE REQUIREMENTS FOR THE DEGREE OF MASTER
OF SCIENCE**

**DEPARTMENT OF CHEMISTRY
FACULTY OF SCIENCE
UNIVERSITY OF MALAYA
KUALA LUMPUR**

2019

UNIVERSITY OF MALAYA
ORIGINAL LITERARY WORK DECLARATION

Name of Candidate: Nur Adibah binti Mohd Amin

Matric No: SGR150061

Name of Degree: Master of Science

Title of Dissertation: Synthesis, Characterization and Encapsulation Studies of Multidentate Ligands and Their Organotin Complexes

Field of Study: Inorganic Chemistry

I do solemnly and sincerely declare that:

- (1) I am the sole author/writer of this Work;
- (2) This Work is original;
- (3) Any use of any work in which copyright exists was done by way of fair dealing and for permitted purposes and any excerpt or extract from, or reference to or reproduction of any copyright work has been disclosed expressly and sufficiently and the title of the Work and its authorship have been acknowledged in this Work;
- (4) I do not have any actual knowledge nor do I ought reasonably to know that the making of this work constitutes an infringement of any copyright work;
- (5) I hereby assign all and every rights in the copyright to this Work to the University of Malaya ("UM"), who henceforth shall be owner of the copyright in this Work and that any reproduction or use in any form or by any means whatsoever is prohibited without the written consent of UM having been first had and obtained;
- (6) I am fully aware that if in the course of making this work, I have infringed any copyright whether intentionally or otherwise, I may be subject to legal action or any other action as may be determined by UM.

Candidate's Signature

Date:

Subscribed and solemnly declared before,

Witness's Signature

Date:

Name:

Designation:

SYNTHESIS, CHARACTERIZATION AND ENCAPSULATION STUDIES OF MULTIDENTATE LIGANDS AND THEIR ORGANOTIN COMPLEXES

ABSTRACT

The chemistry of organotin(IV) complexes with multidentate ligands have been the subject of interest because of their potential as an effective antitumor agent. It has been found that the biochemical activity is influenced by the structure of resulting complexes and the numbers of organic groups bind to the tin centre. In this thesis, the work emphasis has been dedicated to synthesis new multidentate ligands and diorganotin(IV) complexes and formulate compound that showing best therapeutic activity. Therefore, a series of multidentate ligands and diorganotin(IV) complexes containing various carbonyl groups as substituents were prepared from the respective ligands with various substituted dibenzyltin(IV) dihalides. The chemical structures of the multidentate ligands and complexes have been characterized and confirmed by melting point, Fourier transform infrared (FT-IR), proton and carbon nuclear magnetic resonance (^1H and ^{13}C NMR), ultraviolet and visible (UV-vis) absorption spectroscopies. The carbon, hydrogen, nitrogen and sulphur (CHNS) elemental analyser was used to determine the elemental composition. In the **C10** complex preparation step, crystalline byproduct was formed and its crystalline structure has been identified using X-ray crystallography. Besides that, five ligands and ten complexes have been successfully synthesized. From the structure elucidation data, the coordination of ligands and complexes took place through azomethine nitrogen and phenolic oxygen. For the study of anticancer properties, a selected ligand and corresponding diorganotin(IV) complexes have been tested against several human cancer cell lines specifically breast (MCF-7), lung (A549) and prostate (PC-3). The anticancer screening results showed that most of the

complexes had greater therapeutic activity compared to *cis*-platin. The findings also revealed that complex 2,3-*bis*((*N*)-(2,4-dihydroxybenzylidene)amino) maleonitrile di(*p*-chlorobenzyl)tin, **C9** exhibited significantly better activity towards MCF-7 than the other organotin(IV) derivatives. Hence, **C9** was chosen for further study on its encapsulation and release. The formulation was prepared using thin film hydration method in phosphate buffered saline (PBS) pH 7.4 as a medium. The properties of the formulation such as the zeta potential, particle size and size distribution profile of the carriers were measured by dynamic light scattering (DLS). The morphology of carrier was visualized by field emission scanning electron microscope (FESEM). The solution of encapsulated-**C9** was centrifuged to determine the percentage encapsulation efficiency (%EE). The concentration of **C9** in supernatant and sediment were obtained from the measurement with UV-vis spectroscopy. A cationic and non-ionic surfactant mixture was used as drug carrier. The results of formulation showed an average size of 128 ± 22 nm with 100% intensity, 0.5 polydispersity index and the zeta potential is -16 ± 1 mV. From the FESEM image, it was observed that nanoparticles exist in a spherical shape. High encapsulation efficiency and drug loading have been obtained as >90% and 90% respectively. Moreover, *in vitro* drug release studies showed the release of the drug was observed as soon as the test started but less than 20%, and then followed by a sustained release for 60 days. The amounts of percentage cumulative drug release were found to be 75%. Based on these results, can be conclude that the organotin(IV) complex based on multidentate ligand might be a potential as slow release drug for cancer chemotherapy.

Keywords: multidentate ligands, anticancer, surfactant, encapsulation

SINTESIS, PENCIRIAN DAN KAJIAN ENKAPSULASI LIGAN MULTIDENTAT DAN KOMPLEKS ORGANOTIN

ABSTRAK

Kimia kompleks organotin(IV) dan ligan multidentat telah menjadi subjek utama kerana potensi mereka sebagai agen antitumor yang berkesan. Didapati, aktiviti biokimia dipengaruhi oleh struktur kompleks yang terbentuk dan bilangan kumpulan organik yang terikat di pusat timah. Dalam tesis ini, penekanan kerja dikhususkan untuk sintesis ligan multidentat dan kompleks diorganotin(IV) baru dan merumuskan sebatian yang menunjukkan aktiviti terapeutik yang terbaik. Oleh sebab itu, satu siri ligan multidentat dan kompleks diorganotin(IV) yang mengandungi pelbagai kumpulan karbonil sebagai terbitan telah disediakan daripada beberapa jenis ligan dan terbitan dibenzyltin(IV) dihalid. Ligan multidentat dan kompleks telah dicirikan dengan pelbagai kaedah seperti takat lebur, transformasi Fourier inframerah (FT-IR), proton dan karbon nuklear magnetik resonan (^1H dan ^{13}C NMR) dan spektroskopi nampak ultra lembayung (UV-Vis). Penganalisis unsur karbon, hidrogen, nitrogen dan sulfur (CHNS) telah digunakan untuk menentukan komposisi unsur. Dalam langkah penghasilan kompleks **C10**, produk sampingan berbentuk kristal telah terhasil dan struktur hablurnya telah dikenalpasti menggunakan kristalografi sinar-X. Selain dari itu, lima ligan dan sepuluh kompleks telah berjaya disintesis. Dari data penjelasan struktur, koordinasi ligan dan kompleks terbentuk melalui azomethin nitrogen dan fenolik oksigen. Bagi kajian sifat-sifat antikansernya, ligan dan kompleks diorganotin(IV) telah diuji dengan beberapa jenis sel kanser manusia iaitu payudara (MCF-7), peparu (A549) dan prostat (PC-3). Hasil saringan pemeriksaan antikanser menunjukkan bahawa kebanyakan kompleks mempunyai aktiviti terapeutik yang lebih baik berbanding dengan *cis*-platin.

Penemuan ini juga mendedahkan bahawa kompleks 2,3-bis((N)-(2,4-dihydroxybenzylidene)amino) maleonitrile di(*p*-chlorobenzyl)timah, **C9** menunjukkan aktiviti yang lebih baik terhadap MCF-7 berbanding dengan terbitan organotin(IV) yang lain. Justeru itu, **C9** telah dipilih untuk kajian enkapsulasi dan pelepasan. Perumusan disediakan dengan menggunakan kaedah penghidratan filem nipis dalam larutan penimbal fosfat (PBS) pH 7.4 sebagai medium. Sifat rumusan seperti potensi zeta, saiz partikel dan profil taburan saiz diukur menggunakan alat penyebaran cahaya dinamik (DLS). Morfologi pembawa digambar menggunakan pelepasan medan mikroskopi pengimbasan elektron (FESEM). Larutan mengandungi **C9**-terkandung telah diempar untuk menentukan peratus kecekapan enkapsulasi (%EE). Kepekatan **C9** dalam supernatan dan sedimen diperolehi dari pengukuran menggunakan UV-vis spektroskopi, kemudian, dikira berdasarkan lengkung penentukuran. Oleh itu, peratusan kecekapan pengkapsulan dan pemuatan ubat boleh diperolehi. Campuran surfaktan kationik dan tak ionik digunakan sebagai pembawa ubat. Keputusan formulasi menunjukkan purata saiz 128 ± 22 nm dengan keamatan 100%, 0.5 indeks kepoliserakan dan potensi zeta adalah -16 ± 1 mV. Dari imej FESEM, ia menunjukkan bahawa zarahnano wujud dalam bentuk sfera. Kecekapan pengkapsulan dan pemuatan ubat yang tinggi telah diperolehi dengan masing-masing >90% dan 90%. Kajian *in vitro* menunjukkan pelepasan ubat diperhatikan sebaik sahaja ujian dimulakan tetapi kurang dari 20%, kemudian diikuti dengan pelepasan yang berterusan selama 60 hari. Jumlah peratusan pelepasan ubat terkumpul didapati 75%. Berdasarkan hasil kajian ini, dapat disimpulkan bahawa kompleks organotin(IV) berasaskan ligan multidentat berpotensi sebagai ubat perlepasan perlahan untuk kemoterapi kanser.

Kata kunci: ligan multidentat, antikanser, surfaktan, enkapsulasi

ACKNOWLEDGEMENTS

First and foremost, I am grateful to Allah for giving me opportunity and strength to complete this research. I would like to express my sincerest appreciation to both of my supervisors, Dr. Rusnah Syahila for the drug formulation, encapsulation and characterisation and Dr. Lee See Mun for the synthesis and biological studies. Without their help, this dissertation could not have been completed. I extend my gratitude to Professor Dr. Lo Kong Mun for his keen interest, continuous support and his kind help in providing facility, checking thesis and manuscript.

I would also like to thank my beloved friends and staff of University of Malaya for their moral support and their listening ears to all the problems I have faced throughout this research. Special thanks to my dearest family for giving me advices and encouragement to complete my masters.

And last but not least, many thanks to University of Malaya (PPP grant, PG239-2016A) and UMRG grant (RP17A-14AFR) and Ministry of Higher Education of Malaysia for offering me a scholarship and giving me financial support which enabled me to pursue my studies.

TABLE OF CONTENTS

Abstract	iii
Abstrak	v
Acknowledgements	vii
Table of Contents	viii
List of Figures	xii
List of Tables.....	xiii
List of Symbols and Abbreviations.....	xv
List of Appendices	xvii
CHAPTER 1: INTRODUCTION.....	1
1.1 Research Background	1
1.2 Significance and Problem Statements of the Research.....	2
1.3 Motivation.....	4
1.4 Research Objectives.....	5
1.5 Thesis Outline.....	6
CHAPTER 2: LITERATURE REVIEW.....	8
2.1 Introduction.....	8
2.2 General Overview of Organotin Compounds.....	8
2.2.1 Applications of Organotin Compounds.....	9
2.2.2 Organotin(IV) complexes with Schiff base ligands containing N ₂ O ₂ -donor atoms	10
2.3 General Overview of Multidentate Ligands	13
2.4 Characterization Techniques for Organotin Complexes.....	18
2.4.1 Infrared Spectroscopy.....	18

2.4.2	Nuclear Magnetic Resonance (NMR) Spectroscopy.....	19
2.4.2.1	¹ H NMR Spectroscopy.....	19
2.4.2.2	¹³ C NMR Spectroscopy.....	20
2.4.2.3	¹¹⁹ Sn NMR Spectroscopy.....	20
2.4.3	CHNS Elemental Analysis.....	21
2.4.4	UV-vis Spectroscopy.....	21
2.4.5	X-ray Crystallography.....	22
2.4.6	Thermogravimetric Analysis.....	25
2.5	Encapsulation Studies.....	25
2.5.1	General Overview of Drug Carrier.....	25
2.5.2	Methods to Prepare Drug Carrier.....	30
2.5.3	Drug Administration.....	32
2.5.4	Characterization of Formulated Drug.....	35
2.6	Concluding statement.....	38
CHAPTER 3: METHODOLOGY.....		39
3.1	Introduction.....	39
3.2	Materials.....	39
3.3	Physical Measurement of Multidentate Ligands, Substituted Dibenzyltin Compounds and Organotin Complexes.....	40
3.4	Synthesis of Multidentate Ligands.....	40
3.5	Synthesis of Organotin Compounds.....	42
3.6	Synthesis of Diorganotin(IV) Complexes.....	43
3.7	Biological Activities of Selected Ligand and Complexes.....	44
3.8	Encapsulation Studies.....	45
3.8.1	Sample Preparation.....	46

3.8.2	Size Distribution Analysis and Zeta Potential.....	46
3.8.3	Morphological Analysis	47
3.8.4	Determination of Encapsulation Efficiency and Drug Loading.....	47
3.8.5	<i>In vitro</i> Drug Release Study	48
CHAPTER 4: RESULTS AND DISCUSSION		49
4.1	Introduction.....	49
4.2	Characterization Data of Ligands, Organotin Compounds and Complexes.....	49
4.3	Infrared (IR) spectra data.....	55
4.4	Nuclear Magnetic Resonance (NMR) Spectral Data.....	57
4.4.1	¹ H NMR spectra of ligands and complexes.....	58
4.4.2	¹³ C NMR spectra of ligands and complexes	64
4.5	Carbon, Hydrogen and Nitrogen (CHN) Elemental Analysis	67
4.6	Electronic Spectra	67
4.7	X-ray crystallography	69
4.7.1	Synthesis and crystallization	70
4.7.2	Structural commentary	70
4.7.3	Database survey.....	73
4.8	Cytotoxic Activity	74
4.9	Encapsulation Studies of Selected Complex	78
4.9.1	Particles Size Distribution and Zeta Potential.....	78
4.9.2	Drug Encapsulation Efficiency and Drug Loading	82
4.9.3	Morphology Analysis	84
4.9.4	<i>In vitro</i> Drug Release Study	85
CHAPTER 5: CONCLUSIONS.....		88

References	90
List of Publications and Papers Presented	111
Appendices	113

University of Malaya

LIST OF FIGURES

Figure 2.1 : Structural formula of organotin compounds.....	8
Figure 2.2 : The proposed structure of diorganotin(IV) complex with Schiff base ligands.	10
Figure 2.3 : Structures of diorganotin(IV) complexes.	12
Figure 2.4 : Structure of [<i>N,N'</i> -bis(5-bromo-salicylidene)-1,3-diaminopropane] copper(II).	16
Figure 2.5 : Ni- <i>Salpn</i> films.	17
Figure 3.1 : Preparation of sample.	46
Figure 4.1 : Preparation of Schiff base ligands.	49
Figure 4.2 : Preparation of diorganotin(IV) Schiff base complexes.	50
Figure 4.3 : ¹ H NMR spectra of <i>N,N'</i> -bis(salicylidene)-1,3-diaminopropane, L3.	58
Figure 4.4 : ¹ H NMR spectra of <i>N,N'</i> -bis(5-chloro-salicylidene)-1,3-diaminopropane di(<i>p</i> -chlorobenzyl)tin, C3.	61
Figure 4.5 : Formation of crystal of by-product of complex C10 in NMR tube.	70
Figure 4.6 : Structure of trans-dichloridobis(dimethyl sulfoxide- κO)bis(4-fluorobenzyl- κC^1)tin(IV).	71
Figure 4.7 : The molecular structure of coordination trans-dichloridobis(dimethyl sulfoxide- κO)bis(4-fluorobenzyl- κC^1)tin(IV).	72
Figure 4.8 : Bar chart showing the comparison of the IC ₅₀ value of L5 and its diorganotin(IV) complexes.	75
Figure 4.9 : The particle size distribution of the complex C9.	79
Figure 4.10 : FESEM image of formulation complex C9.	84
Figure 4.11 : <i>In vitro</i> drug release profile of complex C9 formulation in 60 days.	85

LIST OF TABLES

Table 3.1 : The amount of starting materials to synthesise the compounds.	44
Table 4.1 : Analytical data of ligands.	51
Table 4.2 : Analytical data of organotin compounds.	52
Table 4.3 : Analytical data of organotin complexes.	53
Table 4.4 : Infrared spectra data for ligands L1 to L5.	56
Table 4.5 : Infrared spectra data for complexes C1 to C10.	57
Table 4.6 : ^1H NMR chemical shifts for ligands L1 to L3.	59
Table 4.7 : ^1H NMR chemical shifts for ligands L4 & L5.	60
Table 4.8 : ^1H NMR chemical shifts for complexes C1 to C4.	62
Table 4.9 : ^1H NMR chemical shifts for complexes C5 to C10.	63
Table 4.10 : ^{13}C NMR chemical shifts for ligands L1 to L3.	65
Table 4.11 : ^{13}C NMR chemical shifts for ligands L4 & L5.	65
Table 4.12 : ^{13}C NMR chemical shifts for complexes C1 to C4.	66
Table 4.13 : ^{13}C NMR chemical shifts for complexes C5 to C10.	66
Table 4.14 : CHN elemental analysis of complexes C9 & C10.	67
Table 4.15 : Electronic spectra data of ligands L1 to L5.	69
Table 4.16 : Electronic spectra data of complex C1 to C10.	69
Table 4.17 : Selected geometric parameters (\AA , $^\circ$).	71
Table 4.18 : Crystallographic and refinement details for trans-dichloridobis(dimethyl sulfoxide- κO)bis(4-fluorobenzyl- κC^1)tin(IV) ^a	73
Table 4.19 : Selected geometric parameters (\AA , $^\circ$) for molecules of the general formula $\text{R}_2\text{SnX}_2(\text{DMSO})_2$	74
Table 4.20 : Anticancer result of L5 and its complexes.	77

Table 4.21 : Particle size distribution, polydispersity index (PDI) and zeta potential of complex C9.....	78
Table 4.22 : Encapsulation efficiency and drug loading of complex C9.....	82

University of Malaya

LIST OF SYMBOLS AND ABBREVIATIONS

A549	:	Human lung carcinoma cancer cell line
bzCl	:	dibenzyltin dichloride
C1	:	<i>N,N'</i> -bis(5-bromo-salicylidene)-1,3-diaminopropane di(<i>p</i> -bromobenzyl)tin
C2	:	<i>N,N'</i> -bis(5-bromo-salicylidene)-1,3-diaminopropane di(<i>p</i> -fluorobenzyl)tin
C3	:	<i>N,N'</i> -bis(5-chloro-salicylidene)-1,3-diaminopropane di(<i>p</i> -chlorobenzyl)tin
C4	:	<i>N,N'</i> -bis(salicylidene)-1,3-diaminopropane dibenzyltin
C5	:	2,3-bis((<i>N</i>)-(2-hydroxybenzylidene)amino)maleonitrile di(<i>p</i> -bromobenzyl)tin
C6	:	2,3-bis((<i>N</i>)-(2-hydroxybenzylidene)amino)maleonitrile di(<i>p</i> -fluorobenzyl)tin
C7	:	2,3-bis((<i>N</i>)-(2-hydroxybenzylidene)amino)maleonitrile di(<i>p</i> -methylbenzyl)tin
C8	:	2,3-bis((<i>N</i>)-(2,4-dihydroxybenzylidene)amino)maleonitrile di(<i>p</i> -bromobenzyl)tin
C9	:	2,3-bis((<i>N</i>)-(2,4-dihydroxybenzylidene)amino)maleonitrile di(<i>p</i> -chlorobenzyl)tin
C10	:	2,3-bis((<i>N</i>)-(2,4-dihydroxybenzylidene)amino)maleonitrile di(<i>p</i> -fluorobenzyl)tin
DLS	:	Dynamic light scattering
DMEM	:	Dulbecco's modified eagle medium
DMSO	:	Dimethylsulfoxide
DMSO- <i>d</i> ₆	:	Deuterated dimethylsulfoxide
DNA	:	Deoxyribonucleic acid
DTAB	:	Dodecyl trimethylammonium bromide
EE	:	Encapsulation efficiency
FESEM	:	Field emission scanning electron microscope
FTIR	:	Fourier-transform infrared

IR	:	Infrared
L1	:	<i>N,N'</i> -bis(5-bromo-salicylidene)-1,3-diaminopropane
L2	:	<i>N,N'</i> -bis(5-chloro-salicylidene)-1,3-diaminopropane
L3	:	<i>N,N'</i> -bis(salicylidene)-1,3-diaminopropane
L4	:	2,3-bis((<i>N</i>)-(2-hydroxybenzylidene)amino)maleonitrile
L5	:	2,3-bis((<i>N</i>)-(2,4-dihydroxybenzylidene)amino)maleonitrile
MCF-7	:	Human breast cancer cell line
MeOH	:	Methanol
MTT	:	3-(4,5-dimethylthiazol-2-yl)-2,5-diphenyltetrazolium bromide
PBS	:	Phosphate buffer saline
PC-3	:	Human prostate cancer cell line
PDI	:	Polydispersity index
PTX	:	Paclitaxel
PVC	:	Polyvinyl chloride
RPMI	:	Roswell park memorial institute
TGA	:	Thermogravimetric analysis
UV-vis	:	Ultraviolet-visible
4Br	:	di(<i>p</i> -bromobenzyl)tin dibromide
4Cl	:	di(<i>p</i> -chlorobenzyl)tin dichloride
4F	:	di(<i>p</i> -fluorobenzyl)tin dichloride
4CH ₃	:	di(<i>p</i> -methylbenzyl)tin dichloride

LIST OF APPENDICES

Appendix A : IR spectra of ligands and complexes.....	113
Appendix B : ^1H NMR spectra of ligands and complexes.....	121
Appendix C : ^{13}C NMR spectra of ligands and complexes.....	129
Appendix D : Electronic spectra of ligands and complexes.	137
Appendix E : CHN elemental analysis.	142

University of Malaya

CHAPTER 1: INTRODUCTION

1.1 Research Background

Cancer remains the top leading disease that is fatal particularly in developing countries. Most of the cancer cases can be cured using treatments such as surgery, chemotherapy and radiotherapy. Platinum-based drugs, for instance, *cis*-platin, oxaliplatin, nedaplatin, and carboplatin are the common drugs widely used for cancer treatment. These drugs are the coordination complexes of platinum. In the form of chemotherapeutic agent, *cis*-platin is the leading metal-based drugs which have been used for more than three decades in the treatment of cancer (Wang & Guo, 2013; Zucali *et al.*, 1976). However, platinum-based drugs are related to severe side effects due to poor water solubility and systemic toxicities including nephrotoxicity, neurotoxicity and ototoxicity (Argyriou *et al.*, 2008; McWhinney *et al.*, 2009). These limitations have encouraged the investigation of several scaffolds to act as vectors for targeted delivery of platinum-based anticancer complexes (Butler & Sadler, 2013). Hence, attempts are being made to develop an alternative medicine that can be used for the treatment of drug resistant cancer.

Among the non-platinum metal based drugs, organotin(IV) complexes have captured the attention of many scientists in the past several decades as antitumor chemotherapeutic agents (Yang *et al.*, 2016). Organotin(IV) complexes exhibit the most potential in antitumor activities as compared to other main-group metal compounds and transition metals. Studies have shown that bioactive organotin(IV) complexes have a potential as chemotherapeutic drugs due to their apoptotic inducing character and also great interaction with deoxyribonucleic acid (DNA) (Cima & Ballarin, 1999; Pellerito *et al.*, 2005). Literature also revealed that they showed better toxicity behaviour as compared to the *cis*-platin (Cagnoli *et al.*, 1998; Varela-Ramirez *et al.*, 2011).

The choice of coordinated ligand is crucial in the biological effects of organotin(IV) complexes such as solubility and bioavailability (Fani *et al.*, 2015). The coordinated ligands with tin atom not only can diminish the drawbacks, but can embellish the biochemical activity of organotin(IV) complexes (Kumar *et al.*, 2009). The coordination of azomethine linkage with organotin(IV) compounds are considered as privileged ligands due to their remarkable biological properties (Pellerito, 2002). This may be due to the fact that an additional of C=N bond is capable to impede the enzyme activity since the enzymes depend on the linkage for their activity (Sirajuddin *et al.*, 2012). Moreover, the azomethine can enhance the biological activity by the influence of structural factors such as solubility, dipole moment and cell permeability (Li & Shen, 2000).

Besides that, organotin(IV) complexes are not only discovered as promising anticancer agent, but they exhibited a wide range in biological activities such as antibacterial, antifungal, antiviral and anti-inflammatory properties (Dawara & Singh, 2011; Khan *et al.*, 2004). Moreover, the organotin(IV) complexes have been utilised in various chemical behaviour as an excellent catalyst (Yin *et al.*, 2007; Yin *et al.*, 2005). As an example, organotin(IV) carboxylates complexes act as catalyst in transesterification reaction and organotin(IV) amine complexes are applied as latent catalysts for epoxy resins (Sirajuddin *et al.*, 2015; Smith, 1997).

1.2 Significance and Problem Statements of the Research

Over the past few years, commercial drugs such as paclitaxel and doxorubicin have been utilised for several cancer treatments such as breast, lymphoma and ovarian. One of the major challenges for cancer treatment with chemotherapeutic drugs is the non-selective of active ingredients towards the targeting site. Thus, the main goal for researchers is to reformulate an existing drug that can detect the cancer cells and eliminate the toxicity. Conventional chemotherapy fails to distinguish the cancerous

cells selectively without damaging the normal body cells. This problem has caused severe impacts to the cancer patients including organ damage. It happens in impaired treatment with a lower dose and results in low chances for survival due to the failure of delivering the anticancer drugs to the tumour site (Mousa & Bharali, 2011). Recently, targeted drug delivery systems with nanoparticles for cancer treatment appeared as an ideal alternative and promising solution to increase the selectiveness and to reduce systemic side effects of cancer treatment (de Vos *et al.*, 1998; Gasser *et al.*, 2011).

Many strategies have been suggested to combat the limitations and problems including the modification of a drug by adding surfactants and encapsulating the active ingredient within a nanoparticle. This improvement will enhance the stability of drugs and offer a better protection to the normal tissue before the drugs reach the targeted site. This encapsulation technique can provide an adequate drug concentration at a controlled rate to permit an effective dose to the patient. Besides that, this encapsulation technique is able to reduce the frequency of drug administration taken by the patient and allows them to experience more uniform effect of the drugs. Treatment of cancer by using nanotechnology contributes a great benefit for cancer patients as it provides efficient delivery to the targeted site and can minimise the side effects such as toxicity.

Thus, this study is focusing to prepare organotin(IV) complexes derived from multidentate ligands containing various carbonyl group as substituents based on dibenzyltin(IV) dihalides. We are interested in preparing multidentate ligands and diorganotin(IV) complexes. There are a few questions of whether the tin plays an important role as an anticancer drug. Will the ligands show similar biological properties as its diorganotin(IV) complexes? For what type of cancer these diorganotin(IV) complexes are more effective? Is it possible to encapsulate the complexes? How much is the encapsulation and the loading efficiencies of the diorganotin(IV) complexes? What is the size of the particle loaded with diorganotin(IV) complexes? Is this

compound released at a rapid or slow rate?

This thesis attempts to find solutions to the problems raised. Thus, this study is focusing on the preparation of organotin(IV) complexes derived from multidentate ligands for greater complex stability and investigating how good is their performance as anticancer drugs.

1.3 Motivation

The present study was focused to the synthesis of substituted dibenzyltin compounds with various multidentate ligands prepared from a condensation reaction of 1,3-diaminopropane, diaminomaleonitrile and salicylaldehyde derivatives.

This section discusses the two factors that motivate the research undertaken in this study. Firstly, we were very interested to design and synthesize a new series of diorganotin(IV) complexes with tetradentate ligands containing azomethine linkage and phenolic oxygen which involve a different substitution group. Then, the influence of substitution group in complexes on the biological activity was determined. There have been numerous of studies on organotin(IV) complexes since they have shown evidence of wide range of biological activities such as antibacterial, antifungal, anticancer agents. A new series of diorganotin(IV) complexes probably show potential in many applications. Secondly, we were concerned to encapsulate the compounds by adding certain surfactant to enhance their performance as anticancer drugs. This is because encapsulation of drug is one of the best techniques to limit the major drawback such as toxicity and also facilitating better delivery of drug molecules to the targeted site. Thus, these two factors motivate us to further investigate their biological activity and drug release study.

1.4 Research Objectives

The scope of this work can be divided in two parts: First, the synthesis and characterization of multidentate ligands and diorganotin(IV) complexes. Second, the selected diorganotin(IV) complex is further studied for its drug formulation and release.

The research objectives can be summarised as follows:

- a) To prepare five type multidentate ligands and diorganotin(IV) complexes.

All the ligands are not the new discovery and the preparation method of the ligands are based on the reported literature. Three multidentate ligands were prepared from the reaction of 1,3-diaminopropane with salicylaldehyde, 5-bromosalicylaldehyde or 5-chlorosalicylaldehyde. Subsequently, complexation of the respective ligands produces four new diorganotin Schiff base complexes. Another two ligands were obtained from the reaction of diaminomaleonitrile with salicylaldehyde or 2,4-dihydroxybenzaldehyde. Afterward these two ligands were used to prepare six new diorganotin(IV) complexes.

- b) To analyse and determine the structural features of the ligands and complexes.

Spectroscopic methods such as Fourier transform infrared (IR), proton and carbon nuclear magnetic resonance (^1H and ^{13}C NMR) and carbon, hydrogen and nitrogen (CHN) analyser had been applied to analyse, determine and confirm the structures of the prepared ligands and their diorganotin(IV) complexes. Ultraviolet and visible (UV-vis) spectroscopy was applied to study the electronic properties of the synthesized compounds. For the crystalline compounds, single crystal X-ray diffraction has been carried out to determine the structures.

- c) To evaluate the biological activity of the selected ligand and diorganotin(IV) complexes.

In this research, only one complex was selected for the encapsulation and drug release study as we assumed the outcome will be similar because of the resemblance in structures and molecular sizes. Thus, we were only choosing one type of ligand and three types of complexes for cytotoxicity study. The cytotoxicity study was conducted against human breast cancer cell line (MCF-7), human lung carcinoma cancer cell line (A549) and human prostate cancer cell line (PC-3) for its anticancer properties.

- d) To study the encapsulation and drug release performance of the selected complex.

One complex with the best therapeutic activity based on the findings in part “c” was selected for encapsulation and drug release study. The prepared formulation was characterized in terms of their particle size, polydispersity index, zeta potential, morphology, percentage of encapsulation efficiency and drug loading. In addition, the *in vitro* drug release was studied by using dialysis tubing method.

1.5 Thesis Outline

Chapter 1 presents the introduction and background of the current research. Apart from that, significance and problem statements of the research are explained in Chapter 1. Motivation, research objectives and scope of work are also included. Chapter 2 describes the literature review of organotin(IV) complex with multidentate ligand and their applications. A description on characterization techniques that involved for structural features of organotin(IV) complex and also a general brief about the formulation studies are included in this Chapter 2. Chapter 3 describes the experimental

procedures to prepare ligands and complexes and its characterization methods and formulation part. Chapter 4 discusses the overall results from the characterization techniques used throughout this work. Finally, Chapter 5 concludes the research output and includes suggestion of works with respect to the objectives of this thesis.

University of Malaya

CHAPTER 2: LITERATURE REVIEW

2.1 Introduction

This chapter will reflect a concise overview and application of organotins and multidentate ligands as both are the main component of this research. Moreover, this chapter will discuss regarding various techniques that are available to characterize the compounds. Review on encapsulation studies is also included in this chapter.

2.2 General Overview of Organotin Compounds

Organotin chemistry has been growing rapidly in 1900s, after the discovery of Grignard reagents which are useful in producing Sn-C bond. Generally, organotin compounds can be classified into four major types depending on the number of Sn-C bonds (Song *et al.*, 2006). Organotin compounds containing one Sn-C bond are known as monoorganotin while those with two, three, and four Sn-C bonds are called di-, tri-, and tetraorganotin compounds respectively. The structural formula of the four types of organotin compounds are shown below in **Fig. 2.1**. Tetravalent organotin compounds have the general formula R_nSnX_{4-n} where $n = 1$ to 4; R is any organic group and X is an anionic species (halide, oxide, hydroxide, carboxylate, or thiolate) or a group attached to tin through oxygen, sulphur, nitrogen, halogen, etc.

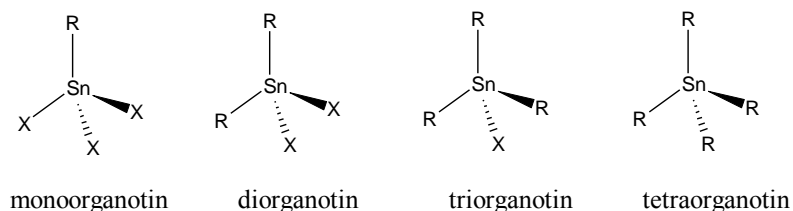


Figure 2.1 : Structural formula of organotin compounds.
[Adapted from (Okawara & Wada, 1967)]

2.2.1 Applications of Organotin Compounds

The uses of organotins have developed rapidly after the discovery of the first organotin compound by Frankland in 1849. Organotin compounds show a diverse range in industrial, biocidal and agricultural applications. Depending on the number of organic groups, monoorganotin compounds have rather limited applications. Organotin with one organic group such as methyltin, butyltin, octyltin and monoesters are utilised as heat stabilisers in manufacturing of plastic (Frye *et al.*, 1964). On the other hand, they are also used as catalysts in the binder of adhesives, sealants, jointing compounds and coatings. Although monoorganotin compounds have no biocidal activity and have very low toxicity towards mammals, they are widely used in glass coating (Zhao *et al.*, 2008).

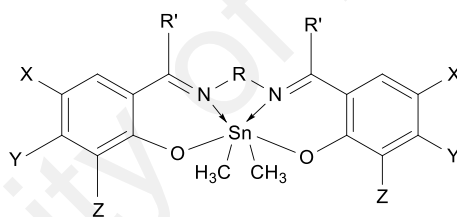
Diorganotins are commonly used as polyvinyl chloride (PVC) heat stabilisers in polymer manufacturing. As catalyst, the diorganotins are usually more favourable as compared to monoorganotin. They are used in the making of polyurethane, polysiloxane and for a variety of reactions at carboxyl centres (Silva & Bordado, 2004). Moreover, compounds such as dibutyltin dioctoate and dibutyltin dilaurate are normally used as catalyst in vulcanizing silicone rubber (Cervantes *et al.*, 2012). The room temperature curing silicones are applied in producing dental impressions and encapsulating electronic parts. Diorganotin compounds also have been exploited in veterinary application such as anthelmintic. For example, dibutyltin dilaurate is used for expelling parasitic worms in poultry.

Triorganotins are the most toxic organotin compounds which are used as industrial biocides (Saxena, 1987). The most commonly known source is tributyltins (TBT) compound which has been widely expanded in agriculture including pesticides and fungicides. Tributyltins are also versatile as preservative for textiles, paper, wood pulp, leather and electrical equipment. In the early 1960s, tributyltin compounds have been applied as anti-biofouling paint to impede the growth of barnacles, algae and marine

organisms (Balls, 1987). However, there are many arguments on the use of the compound because of the serious toxicity to marine life (Gibbs & Bryan, 2009). Tetraorganotin compounds are mostly used as precursor and starting material for the producing of other tin-organic compounds.

2.2.2 Organotin(IV) complexes with Schiff base ligands containing N₂O₂-donor atoms

Kianfar and Abroshan have synthesized a series of dimethyltin(IV) dichloride with Salen type N₂O₂ Schiff base ligands, in which the Schiff bases have been used as a neutral tetradentate ligand through its O or N atoms (Kianfar & Abroshan, 2013). These complexes have been synthesized from Schiff bases as donors with Me₂SnCl₂ as an acceptor in chloroform.



	R'	R	X	Y	Z
Salen	(CH ₂) ₂	H	H	H	H
Salpn	(CH ₂) ₃	H	H	H	H
Salbn	(CH ₂) ₄	H	H	H	H
Salophen	C ₆ H ₆	H	H	H	H
3MeOSalen	(CH ₂) ₂	H	H	H	MeO
4-MeOSalen	(CH ₂) ₂	H	H	MeO	H
5-MeOSalen	(CH ₂) ₂	H	MeO	H	H
5-BrOSalen	(CH ₂) ₂	H	Br	H	H
Me ₂ Salen	(CH ₂) ₂	CH ₃	H	H	H

Figure 2.2 : The proposed structure of diorganotin(IV) complex with Schiff base ligands.

This review explained spectral and thermodynamic studies of novel 1:1 complex formation dimethyltin(IV) dichloride as acceptor with Salen type Schiff base ligands such as Salen, 3-MeOSalen, 4-MeOSalen, 5-MeOSalen, 5-BrSalen, Me₂Salen, Salpn, Salbn and Salophen, as donor ligands in chloroform solvent (**Fig. 2.2**). The researchers have investigated the effects of different electronic and steric behaviours by comparing the spectral and the thermodynamic properties of Schiff base ligands. By considering the formation constants and the thermodynamic free energy, ΔG , they have concluded that the formation constant changes according to the following trend for Schiff bases due to the electronic factor:



From other literatures, a study on the synthesis and characterization of a new series of diorganotin(IV) complexes of the type R_2SnL_2 (R=Me, Et, Bu, Ph, Bz and L= 2-[(9H-Purin-6-ylimino)]-phenol) has been reported (Rehman *et al.*, 2009). From the Equation (1), the complexes have been synthesized through the proposed ratio 2:1 stoichiometry between the organotin moiety and Schiff base ligands.



R = methyl, ethyl, phenyl and benzyl

All the diorganotin(IV) complexes have been screened against various microorganisms and fungi such as *Staphylococcus aureus* and *Bacillus subtilis* (as gram positive bacteria) and *Pseudomonas aeruginosa*, *Escherichia coli* and *Salmonella typhi* (as gram negative bacteria) while for fungi are *Aspergillus niger*, *Fusarium oxysporum*,

and *Aspergillus flavus*. From the bactericidal activity, it was clearly showed that the complexes were more toxic towards Gram positive strains than Gram negative strains. Whereas the results of the antifungal studies showed that the mixed-ligand complexes were more toxic than their parent ligand against the same microorganisms. Additionally, the efficiency of all the complexes as potential antitumor drug has been tested *in vitro* on the KB cell line, derived from a human epidermoid carcinoma. Rehman and his co-workers have concluded that *bis*(2-[(9*H*-Purin-6-ylimino)]-phenolate)diethyltin(IV) complex was found to have promising antitumor activity.

Dey and his co-workers have been synthesized and characterized diorganotin(IV) complexes with six tetradentate Schiff base ligands containing N₂O₂ donor atoms (**Fig. 2.3**). The Schiff bases, H₂L, were derived from salicylaldehyde, 3-methoxysalicylaldehyde (*o*-vanillin), 1-phenyl-3-methyl-4-benzoyl-5-pyrazolone and diamines such as *o*-phenylenediamine and 1,3-propylenediamine. The structure of complexes have been examined by single crystal X-ray diffraction. From the study, the tin atom has a distorted octahedral coordination, with the Vanophen ligand occupying the four equatorial positions and the *n*-butyl groups in the *trans* axial positions. Besides that, all the diorganotin(IV) complexes displayed six-coordinated distorted octahedral structures as they possess similar spectroscopic data (Dey *et al.*, 1999).

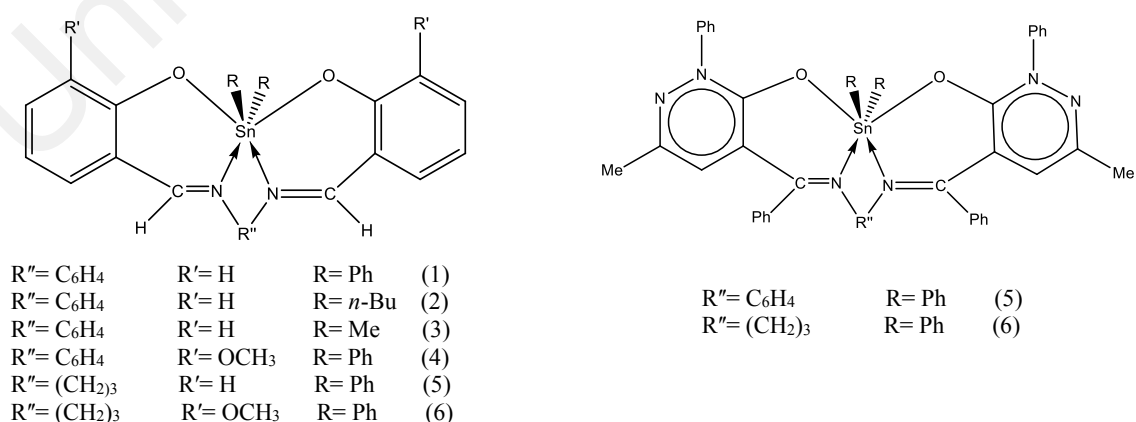


Figure 2.3 : Structures of diorganotin(IV) complexes.

From the literature review, studies on the synthesis and characterization organotin(IV) complexes with Schiff base ligands containing N₂O₂-donor atoms have not sufficient and requires more and deeper researches (Zarracino *et al.*, 2000). In view of the various interaction possibilities of the Schiff base ligands containing N₂O₂-donor atoms with organotin(IV) compounds, the author has undertaken this study for the purpose of synthesizing and characterizing organotin(IV) complexes with the proposed Schiff base ligands containing N₂O₂-donor atoms.

2.3 General Overview of Multidentate Ligands

Ligand is an ion or molecule which has donor electrons that can coordinate to central metal to form a coordination complex. Generally, ligand behaves as a Lewis base whereas Lewis acid is the central metal which can bind to form a covalent bond between them. The chemistry of ligands is very diverse and they can be coordinated to metal complexes in various coordination. Ligand that has one atom which binds to the metal was said to be monodentate or unidentate ligand. A ligand that has more than one electron donor atom was known as polydentate or multidentate ligand. The term of 'dentate' is referring to the ability of molecules to bind to a central metal ion and this is also known as denticity.

Recently, many researchers and chemists have great interest in structuring organometallic complexes with multidentate ligands (Burt *et al.*, 2014; Yin *et al.*, 2012). The synthesis of such ligands typically binds to the metal ion through phenolic oxygen, imine nitrogen, oxime oxygen or oxime nitrogen. The chelate effect of multidentate ligands with metals makes the compounds more versatile with a wide range of application. In addition, the presence of azomethine linkage is essential in enhancing the biological activity. Over the past few years, there have been many reports on their biological properties such as antibacterial (Majumdar *et al.*, 2017), antifungal (Kalshetty

et al., 2013), antioxidant (Kostova & Saso, 2013), anti-inflammatory (Nath *et al.*, 2013) and antiviral (Rogolino *et al.*, 2015). Recently, Kendre and her co-workers have reported that tetradentate Schiff base ligands derived from salicylaldehyde and ethylenediamine and La(III) complexes are active in antibacterial activity against selected gram-negative bacteria (*Escherichia coli*) and gram-positive bacteria (*Staphylococcus aureus*) (Kendre *et al.*, 2014). La(III) complexes and salen ligands also exhibited good antifungal activity against fungal strains (*Aspergillus niger* and *Alternaria*) as compared to the standard drugs. Thus, these evidences conclude that salen ligands complexes have great potential as antimicrobial agents.

On top of that, the presence of azomethine linkage in the ligands not only plays a significant role in enhancing the biological activity, but the azomethine makes the ligands work as a good corrosion inhibitor. Quan *et al.* reported that modification of self-assembled films of Schiff base with alkanethiol showed good efficiency to copper corrosion in 0.5 M NaCl solution. *N*-2-hydroxyphenyl-(3-methoxysalicylidiamine) was adsorbed on the surface of mild steel and a monolayer was formed on the surface spontaneously, thus, it was able to act as effective corrosion inhibitor (Quan *et al.*, 2001). In addition, Ananda and his co-workers studied the effect of corrosion inhibition of 2-(5-methoxy-2-hydroxybenzylideneamino)phenol (Ananda *et al.*, 2014). It was found that the multidentate ligand presented superior inhibition behaviour against corrosion of mild steel in a 0.1 M HCl solution. This was due to the coordination of azomethine linkage and phenolic group of the ligand and metal (Masroor, 2017).

Moreover, organometallic complexes with multidentate ligands have potential to act as chemotherapeutic agents. Ali and his co-researchers investigated the anticancer activity of Cu(II) and Ru(II) complexes with a new multidentate ligands derived from formaldehyde and ethylenediamine. It was found that the prepared complexes displayed strong binding interaction with DNA. Also, cytotoxicity profile of the prepared

complexes possess good anticancer activity against four human cancer cell lines includes colorectal (HT-29), breast (MDA-MB-231), cervical (HeLa) and liver (HepG-2) cancer cell lines (Ali *et al.*, 2012). Moreover, a novel series of diorganotin(IV) complexes of the Schiff base ligand derived from 7-methoxy-2-hydroxy-1-naphthaldehyde, 1,2-phenylenediamine and salicylaldehyde were successfully synthesized by Rehman and his co-researchers (Rehman *et al.*, 2016). Antitumor results against the established human oral epidermoid carcinoma cell line revealed that diethyltin(IV) complex showed the most promising cytotoxic results ($IC_{50} = 0.35 \mu M$) against the cell line as compared with *cis*-platin ($IC_{50} = 0.37 \mu M$). Apart from that, the docking studies revealed that these diorganotin(IV) complexes can bind favourably within *cis*-platin binding site and the binding energy of complex is more than that of *cis*-platin. In view of these facts, it was realized that organometallic complexes can be great candidature as anticancer agents.

In this study, attention is given on the preparation of a series of tetradentate Schiff base ligands. These types of ligands so-called salen ligands consist of four coordinating sites such as two group of azomethine nitrogen and two groups of phenolic oxygens giving an arrangement of N_2O_2 donor groups. The structure presents a remarkable mode of coordination with metal ions via four donor atoms. Hence, this type of tetradentate Schiff base ligands have been the subject of great interest for many researchers (Ajloo *et al.*, 2015; Osowole *et al.*, 2005; Shyamal *et al.*, 2014).

All the five type of tetradentate Schiff base ligands in this research are not a new discovery. They have been extensively discovered and studied since 1980s. For example, a number of researches regarding complexes of *N,N'*-bis(5-bromo-salicylidene)-1,3-diaminopropane, L1 and *N,N'*-bis(5-chloro-salicylidene)-1,3-diaminopropane, L2. Most of them have been synthesized and characterized both of the

ligands with transition metal such as Cu(II), Ni(II) and Fe(II) (Elmali *et al.*, 2000; Kabak *et al.*, 1999). These complexes have also been characterized by X-ray crystallography. Kabak *et al.* have synthesized a complex between copper(II) acetate monohydrate and *N,N'*-bis(5-bromo-salicylidene)-1,3-diaminopropane, L1 (Fig. 2.4). They have reported that the copper atom is coordinated by two imine nitrogen atoms and two phenol oxygen atoms from the imine-phenol ligand in a distorted square-planar coordination geometry. The distance of Cu-N and Cu-O are 1.967 Å and 1.914 Å respectively and the complex has a crystallographic twofold axis (Kabak *et al.*, 1999).

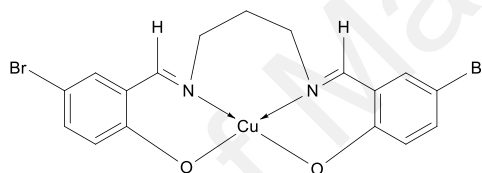


Figure 2.4 : Structure of [*N,N'*-bis(5-bromo-salicylidene)-1,3-diaminopropane]copper(II).

Moreover, metal-Schiff complexes with tetradentate ligand such as *N,N'*-bis(salicylidene)-1,3-diaminopropane, L3 is extensively studied as modifiers of electrodes by oxidative electrodeposition on a variety of conducting surfaces (Shagisultanova & Ardasheva, 2003). Modified electrodes based on films of Schiff base complexes are excellent candidates for sensing applications.

Martin and his co-workers have investigated the influence of the electrode material, glassy carbon, platinum, gold or indium tin oxide, on the electrodeposition of nickel-*N,N'*-bis(salicylidene)-1,3-propanediamine (Ni-*Salpn*) films in 1,2-dichloroethane (Martin *et al.*, 2015). From the study, they have concluded that the thinner Ni-*Salpn* films (Fig 2.5) have a more efficient orbital overlap and a more compact stacked

structure, being more stable in aqueous solution and display the most assuring electrochemical properties as modified electrodes for sensing applications.

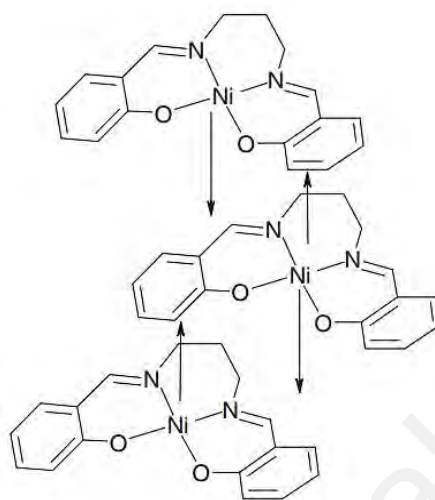


Figure 2.5 : Ni-Salpn films.

[Adapted from (Martin *et al.*, 2015)]

N,N'-bis(salicylidene)-1,3-diaminopropane also has been synthesized with various metal such as Pb(II) and Mn(II) for X-ray crystallography study and biological activity. (Elerman *et al.*, 1993; Kurtaran *et al.*, 2005; Sailaja *et al.*, 2003; Yardan *et al.*, 2015). Kurtaran *et al.* have reported that antibacterial and antifungal activities of the complexes are higher than the free ligand.

Several reports on the synthesis and characterization of metal complexes derived from 2,3-bis((*N*)-(2-hydroxybenzylidene)amino)maleonitrile, L4 and 2,3-bis((*N*)-(2,4-dihydroxybenzylidene) amino)maleonitrile, L5 have been reported. Takahashi and Iwamoto have been prepared a novel series of metal (Mn(II), Fe(III), Co(II), Ni(II), Cu(II), Zn(II) and Pd(II)) complexes of the Schiff base ligand derived from 2,3-diamino-cis-2-butenedinitrile (diaminomaleonitrile) and salicylaldehyde. This synthesis was a one-pot reaction which involve 1 : 1 : 2 stoichiometric addition in the solution containing the metal halide, the diamine, and the aldehyde (Takahashi & Iwamoto,

1981). These complexes have been characterized in their Raman spectra. From other review, cobalt chelates with 2,3-bis((N)-(2-hydroxybenzylidene)amino)maleonitrile, L4 has a potential as catalyst. The researchers have concluded that the complexes with Schiff base containing N₂O₂ donor atoms are the most active heterogenous catalysts for the valence isomerization of quadricyclane to norbornadiene (Dieter *et al.*, 1983; Wohrie & Buttner, 1985).

Even though all the five type of tetradentate ligands are not novel and have been widely studied, there are still no report related to synthesise of organotin complex with all those five ligands. The interesting about this research is all the ten type of organotin complexes with tetradentate ligands is the new series of complexes. Moreover, the difference between this research compared to others is the application part which is encapsulation and drug release study. The selected complex will be formulated to produce better drug delivery system.

2.4 Characterization Techniques for Organotin Complexes

The structural features of organotin complexes could be characterized by using several instrumental techniques. These techniques include infrared (IR) spectroscopy, nuclear magnetic resonance (NMR) spectroscopy, elemental analysis, UV-vis spectroscopy, X-ray crystallography, and thermogravimetric analysis (TGA).

2.4.1 Infrared Spectroscopy

Infrared spectroscopy has proved to be a useful method for the study of various functional groups in the organotin complex, even though it only provides little elemental information. Basically, the fundamental stretching vibrations involving tin atoms are found at frequencies below 650 cm⁻¹. The frequency of the Sn-C stretching vibrations is not particularly sensitive to change in the coordination number of tin (Poller, 1970). The di and tri-alkyltin compounds generally show two bands of asymmetric Sn-C vibration

essentially in the range 500-600 cm^{-1} and the second band at approximately 470-530 cm^{-1} due to symmetric Sn-C vibration band. Monoalkyltin compounds exhibit a single Sn-C stretching band.

The variations in the coordination number of tin will affect the Sn-X stretching modes (Agarwal & Rawat, 1985). In most diorganotin(IV) complexes, the Sn-Cl stretching are in the range of 327-328 cm^{-1} (Bukhari *et al.*, 2014). The medium peak appearing at 550-600 cm^{-1} in the respective spectra of the complexes is assigned to Sn-O bond. While Sn-N stretching shows weaker or medium intensity band at around 400-500 cm^{-1} (Lee *et al.*, 2015). The azomethine C=N of Schiff base band is usually observed at 1480-1690 cm^{-1} (Suydam, 1963). The frequency of O-H in free ligands is found at 3300 cm^{-1} and the disappearance of O-H stretching indicates the oxygen atom has bonded to the centre tin atom (Hong *et al.*, 2014).

2.4.2 Nuclear Magnetic Resonance (NMR) Spectroscopy

Nuclear magnetic resonance (NMR) is related to the property of the nucleus of an atom. The chemical shift depends appreciably on both the nature and position of the substituent. NMR analyses collectively provide highly valuable information and hence are used for the characterization of organotin complexes.

2.4.2.1 ^1H NMR Spectroscopy

In ^1H NMR spectroscopy, most of the azomethine protons of ligands displayed a sharp singlet peak in the region 8.00-9.00 ppm (Tümer *et al.*, 1999). As the ligand has been coordinated to the tin atom through the azomethine group, there is a upfield shift in the chemical shift of spectra of complexes (Dubey *et al.*, 2014). In the ^1H NMR spectra of complexes, appearance of azomethine proton signal due to $^3\text{J}(^{119}\text{Sn}-^1\text{H})$ coupling showing the imine nitrogen atom is bonded to tin (Khandani *et al.*, 2013). The phenolic

proton of the ligand usually displayed a weak peak around the region 9.00-15.00 ppm (Canpolat & Kaya, 2004; Mohamed *et al.*, 2009). The phenolic proton peak was disappeared upon coordination to the tin atom (Sirajuddin *et al.*, 2012).

2.4.2.2 ^{13}C NMR Spectroscopy

The ^{13}C NMR chemical shifts were found over a wider range between from 0-200 ppm. The chemical shifts depended on coordination number of tin, donor ability of solvent, position of carbon atom in alkyl or aryl groups and nature of organotin substituent. (Rehman *et al.*, 2009). The aryl and alkyl carbons of organotin compound can be easily identified by their ^{13}C NMR chemical shifts. For example, the chemical shifts for the alkyl carbons were lower, between 10-100 ppm while for aryl carbons, the chemical shifts were from 110-150 ppm. In the ^{13}C NMR spectra of organotin(IV) complexes, the azomethine carbon shifts to lower frequency. This indicated the coordination of nitrogen with tin atom (Muñoz-Flores *et al.*, 2014).

2.4.2.3 ^{119}Sn NMR Spectroscopy

Tin is a unique element as it has the greatest number of stable isotope and they are ^{115}Sn , ^{117}Sn and ^{119}Sn , which yield narrow signal over a very wide chemical shift range. In the study of organotin complexes, the ^{119}Sn NMR is the most preferred nucleus of tin. This is because ^{119}Sn NMR is slightly more sensitive and most abundant. Each type of tin compound has its chemical shift range from -1900 ppm to 700 ppm. The ^{119}Sn chemical shift values give information about the environment around the tin atom. In all complexes, ^{119}Sn spectra show only a sharp singlet indicating the formation of single species.

The chemical shifts of organotin compound depend on the coordination number of tin atoms. In addition, the δ values (^{119}Sn) will increase with the increasing of coordination number of tin and usually will produce a large upfield shift (Nath *et al.*,

2010). For example, Pruchnik *et al.* suggested that the δ values from +200 to -60 for four-coordinate compound (Pruchnik *et al.*, 2003). For five-coordinate compounds, ^{119}Sn resonances are found to lie between -90 and -330 ppm while in the six-coordinate derivatives are between -125 and -515 ppm (Otera, 1981). Moreover, report on ^{119}Sn NMR spectroscopy revealed that the chemical shifts in seven-coordinate organotin compounds are more than 100 ppm (Otera *et al.*, 1980). There are several studies on the ^{119}Sn NMR spectroscopy to predict the coordination environment of tin in the complexes (Holeček *et al.*, 1983, 1986; Hunter & Reeves, 1968; Nádvorník *et al.*, 1984).

2.4.3 CHNS Elemental Analysis

CHNS elemental analyser can provide information on the weight percentage of carbon, hydrogen, nitrogen and sulphur in a compound (Rezl & Janák, 1973). Theoretical data will be used as a reference in comparing the actual weight of the element. This technique is convenient and reliable for checking the purity and determines the empirical formula of organotin complex (Mishra *et al.*, 2005; Rehman & Zahid, 2016).

2.4.4 UV-vis Spectroscopy

UV-vis spectroscopy is a study of interaction of matter with light. This study is related to the promotion of electrons from lower to higher energy state. In UV-vis spectroscopy, the ultraviolet region falls between in the range of 190-380 nm while the visible light is absorbed in the region 380-800 nm (Papadopoulos *et al.*, 2001). The electronic spectra of organotin complex usually exhibit three or four bands corresponding to the carbonyl group, azomethine group or phenyl group (Shujha *et al.*, 2010). The absorption bands are usually in the region between 260-400 nm (Jain *et al.*, 2013). After complexation, a new absorption band will appear in the region between

400-490 nm which is assigned to the ligand to metal charge transfer (Salam *et al.*, 2012).

2.4.5 X-ray Crystallography

X-ray crystallography is the most favoured research tool to obtain three-dimensional molecular structure from a crystal compound. A complex compound will be recrystallized to get a purified sample and exposed to x-ray beam. X-ray crystallography is widely used in the study of organotin compound since it can provide bond length of tin metal with other atoms, the bond angles, the crystal system, and can measure the distance between atoms in angstroms (de Sousa *et al.*, 2005; Muñoz-Flores *et al.*, 2014; Rocha *et al.*, 2016).

In order to obtain a suitable compound for X-ray diffraction study, the compound must undergo a process called purification. Purification is the main basis for synthesis of new compound and sometimes we need to apply proper techniques for isolation and purification so that we can obtain pure compound. There are several techniques of purification such as recrystallization, column chromatography, thin layer chromatography and sublimation.

a) Recrystallization

Recrystallization is a method of purifying a compound by eliminating any impurities that might be mixed with it. It operates efficiently when the compound is very soluble in a hot solvent, but very insoluble in the cold version of the same solvent. The compound must be a solid at room temperature. Recrystallization is the only technique that can generate absolutely pure and perfect single crystals of a compound. This technique is allowed to proceed very slowly and can take a week to months, to allow the crystal lattice to develop without the inclusion of any impurities. The pharmaceutical industry makes heavy use of recrystallization, since it is a

means of purification more easily scaled up than column chromatography (Ray *et al.*, 2011).

b) Column chromatography

Column chromatography is a versatile purification method used to separate compounds in a solution. The difference in polarity leads to variances in the rate at which the molecules travel through the column, which effectively separates the compounds from one another. Column chromatography's versatility and convenience has made it one of the most extensively used techniques for purifying compounds. Unlike recrystallization, compounds purified with column chromatography do not have to be solid. Column chromatography is also able of isolating a few compounds from a mixture. Another benefit of column chromatograph is that very little needs to be known about the compound's physical properties in order to use this purification process, making this technique very convenient when synthesizing or separating novel compounds, in which little is known about the compound.

c) Thin layer chromatography

Thin layer chromatography (TLC) is one of the most popular and widely used separation techniques because of its ease of use, cost-effectiveness, high sensitivity, speed of separation, as well as its capacity to analyze multiple samples simultaneously. TLC is composed of two phases, a mobile and a solid phase. The solid phase is a thin solid support that usually consists of Alumina or Silica. The mobile phase is a solvent that moves through capillary action right through the solid phase. In general, the solid phase is usually polar while the mobile solvent is non-polar relative to the solid phase. TLC can be utilized for separation, isolation, identification, and quantification of

components in a mixture. TLC remains a valuable and commonly used separation technique because of its features complementary to high-performance liquid chromatography (HPLC). Most of TLC applications use normal-phase methods for separation, whereas reversed-phase methods dominate in HPLC.

d) Sublimation

Sublimation is a purification technique, in which a solid is directly converted to vapor phase without passing through liquid phase. However, the compound must have a relatively high vapor pressure and the impurities must have significantly lower vapor pressures. By heating, the solid will be vaporized and become solid again when the vapor contacts with the cold surface. Some solid compounds, such as iodine, camphor, naphthalene, acetanilide, benzoic acid, can be purified by sublimation at normal pressure. Several compounds will sublime when heating under reduced pressure. There are many advantages for performing sublimation over other purification methods. This process is principally worked for micro scale purifications of solids because the loss of product is typically very minimal. Furthermore, this technique is appropriate for any heat sensitive compound. Thirdly, unlike recrystallization, solvents are not involved at all in the process, and most traces of any solvent are effectively removed.

It is essential to have compounds with highest purity to gain precise result for analytical data (UV, IR, NMR) & biological activity both *in-vivo* and *in-vitro*. This review proposes depth of knowledge on significance of purification of ligands and complexes with various techniques of isolation and purification of intermediate and final compounds.

2.4.6 Thermogravimetric Analysis

Thermogravimetric analysis is the study related to the changes in chemical and physical properties of the complexes with temperature (Broido, 1969). It is very significant to examine the thermal stability, decomposition and kinetics of complexes under various conditions taking place in the sample (Doyle, 1961). For organotin(IV) complexes, the thermal data presented two curves of degradation process. The first degradation process occurred at temperature around 250 °C and the second degradation occurred at 350 °C (Sainorudin *et al.*, 2015).

Among all the characterization techniques, only IR, ¹H NMR, ¹³C NMR, CHNS elemental analysis, UV-vis spectroscopies and X-ray crystallography and are done in this research. The selected characterization techniques are sufficient for identification and confirmation of all synthesized ligands and complexes.

2.5 Encapsulation Studies

Research on encapsulation of anticancer drugs with the support of nanoparticles hold impressive potential as an effective drug delivery system over last few years (Farokhzad & Langer, 2009). Encapsulating an anticancer drug in a nanoparticle proposes several benefits, such as a shield from degradation in the blood stream, decrease drug resistance, enhanced drug solubility, improved drug exposure time, reduced side-effects, enhanced their delivery from the blood vessels deep into the tumours, and create a uniform distribution of the chemotherapeutic drug to the targeted tissue (Bernabeu *et al.*, 2016).

2.5.1 General Overview of Drug Carrier

Drug carrier is a vital feature for the therapeutic purpose especially for breast cancer treatment. It serves to improve the selectivity and effectiveness in drug delivery system (Sutradhar & Amin, 2014). Moreover, it is important to deliver the drug to desired

targeted organ or tissue with minimum side effects (Jabir *et al.*, 2012). Carrier is widely used to enhance the drug performance via the encapsulation of active ingredient (Dutta, 2007; Kratz, 2008).

Drug carrier has many benefits in the process of drug delivery. Besides acting as vehicles in drug loading, drug carrier is important in protecting the drug against rapid degradation or elimination inside the human body (Tiwari *et al.*, 2012). It is also used to protect the non-targeted tissue from potential damage by the drug (Hussen & Heidelberg, 2016). Plus, the carrier can be targeted for a continuous release of drug over a period of time (Storm & Etten, 1997).

There are numerous drug carriers specifically for cancer therapy, such as polymeric micelles, hydrogels, dendrimers, carbon nanotubes, liposomes and vesicles.

a) Polymeric micelles

Polymeric micelles are synthetic polymers containing an inner core and the outer shell. They are formed by self-aggregation of AB-type diblock copolymers which are linked in a tandem form. The anticancer drugs are assimilated into the inner core of the micelle through physical entrapment and chemical conjugation. The inner hydrophobic core can physically entrap a large amount of poorly-water soluble anticancer drugs such as doxorubicin (DOX) (Nakanishi *et al.*, 2001), while the hydrophilic shell offers stability in an aqueous environment to the polymeric micelle (Discher & Eisenberg, 2002). Depending on chain lengths and chemical structures of the polymers, polymeric micelles can have either cylindrical or spherical shape. Literature revealed that most studies have focused on the spherical shape; while only a

few studies have dealt with filamentous shape systems (Christian *et al.*, 2009; Geng *et al.*, 2007).

b) Hydrogels

Hydrogels are defined as water-swollen which are composed of a hydrophilic structure. They are able to absorb large volume of liquid in their three-dimensional (3D) polymeric depending on density of the network joints and the properties of polymer used (Ahmed, 2015). Hydrogels display strong affinity and sensitivity to water (Wu *et al.*, 2017). They are unable to dissolve due to their polymeric crosslinking. Instead, the presence of macroporous gives superior swelling, thus offering a sponge-like structure (Tripathi & Melo, 2015). Hydrogels are also excellent in bio adhesive controlled release system, as they are capable in encapsulation of hydrophilic or hydrophobic drugs as well as biomacromolecules including DNA and proteins (Lin & Metters, 2006). An example for the use of anticancer drug-loaded hydrogels is the proposed delivery of doxorubicin (DOX) using thixotropic silk hydrogel in the treatment of breast cancer (Wu *et al.*, 2016).

c) Dendrimers

Dendrimers represents hyperbranched synthetic polymeric macromolecules which have multiple surface functional groups (Tomalia & Fréchet, 2002). Their arising as an ideal drug delivery vehicle is due to their unique features including monodispersity, membrane interaction, internal cavities, well-defined size and shape (Sharma *et al.*, 2017). Dendrimers interact with anticancer drugs by applying several ways which are electrostatic interactions, physical encapsulation and covalent conjugations (Singh *et al.*, 2016). The special

features of dendrimers enable them to reduce the carrier clearance and cross the membrane of cancer cells by macrophages (Perez-Herrero & Fernandez-Medarde, 2015).

d) Carbon nanotubes

Carbon nanotubes are cylindrical nanostructure which is composed by a group of fullerene family. They can be classified into two types, single-walled carbon nanotubes (SWCNTs) and multiwalled carbon nanotubes (MWCNTs). Single-walled carbon nanotubes are formed by wrapping of single graphene layer whereas multiwalled nanotubes are constructed by rolling up multiple sheets of graphite. In addition, they have capability to fill with drug molecules due to the presence of offer internal volume. Carbon nanotubes are one of the suitable candidates as a drug carrier. This is because they have very special properties such as high mechanical strength, ultralight weight, high thermal conductivity, high surface area, high electrical conductivity and metallic or semi-metallic behaviour (Chen *et al.*, 2017).

e) Liposomes and vesicles

Liposomes are microscopic spherical vesicles contain of central aqueous compartment surrounded by a bilayer of phospholipid. Vesicles are a general term for a self-enclosed amphiphilic. From the literature survey, vesicles are one of the most extensively used as a drug carrier in the enhancement of controlled drug release formulations. Vesicles have caught considerable attention owing to their efficiency in cell penetration, easiness of production, and the complete shield from degradation. They are able to encapsulate and effectively deliver both hydrophilic and hydrophobic drugs and may be applied

as a non-toxic vehicle for insoluble drugs. Hydrophilic drugs can be encapsulated inside the surrounded aqueous phase of the vesicles whereas hydrophobic core enable entrapped the oil-soluble drugs (Gireesh *et al.*, 2013).

Vesicles can form spontaneously from a single or mixture of two different surfactants. Safran and his co-researcher have stated that mixture of two surfactants can produce an equilibrium phase of large single bilayer vesicles (Safran *et al.*, 1990). In addition, most of the previous reports have revealed that thermodynamically stable vesicles are engaged with mixed surfactant or mixed counterion systems (Carnie *et al.*, 1979; Gabriel & Roberts, 1984). Thus, mixed surfactant systems show better performance than single surfactant systems (Shi *et al.*, 2013). Mixed surfactant systems have been widely explored due to their diverse applications in industries such as enhancing oil recovery, pharmaceutical as drug delivery vehicle, detergent and fabric softening (El-Batanoney *et al.*, 1999; Gaubert *et al.*, 2016; Senapati *et al.*, 2016). There are several types of mixed surfactant systems which are include nonionic-nonionic, anionic-anionic, cationic-cationic, nonionic-anionic, nonionic-cationic and cationic-anionic surfactant mixtures. From overall types of mixture, nonionic-cationic surfactant mixtures exhibited lower surface tension as compared to others which is due to the factor of synergistic effect (Bera *et al.*, 2013). An example of mixed surfactants that has been reported is amino acid based surfactants with cetyltrimethylammonium hydroxide (CTAOH) and dodecyl trimethylammonium hydroxide (DTAOH) which leads to the formation of vesicles (Ghosh *et al.*, 2016). From the report, it was revealed that mixed surfactant vesicles can be applied as drug delivery vehicle as they are found to be hemocompatible and do not cause any haemolysis.

Among the mixed surfactant vesicles, it is very crucial to consider the sugar-based ones. Mixed surfactant vesicles involving sugar-based surfactants give a good impact in drug delivery system as they are made from renewable raw materials, non-toxic and highly biodegradable (Hill & Rhode, 1999). In addition, sugar-based surfactants improve the water solubility of mixed surfactant vesicles and also increase the hydrophilicity (Blanzat *et al.*, 1999; Menger *et al.*, 1997). Consola and her co-workers have formulated an anti-inflammatory drug based on cationic vesicles with sugar-based surfactant. In the course of skin inflammation treatment, they proposed that sugar-based formulations have a potential in dermal delivery system for anti-inflammatory drug (Consola *et al.*, 2007).

In this context, we formulated mixtures of cationic and non-ionic surfactants to form vesicles as a drug carrier. From the evidence adapted from literature survey, we expected that mixed surfactant vesicles will present a better formulation.

2.5.2 Methods to Prepare Drug Carrier

There are various methods for the preparation of a drug carrier depending on their nature. The common methods to prepare a drug carrier are detergent analysis, solvent (ether or ethanol) injection, reverse phase evaporation (REV), and thin film hydration.

a) Detergent analysis

Detergent analysis is a common method to prepare unilamellar vesicles. This method has been applied for the preparation of drug carrier for chemotherapy and for the modification of poorly soluble membrane (Jiskoot *et al.*, 1986). The removal of detergent can be done by several techniques including gel permeation chromatography, adsorption using bio-beads, dialysis

and dilution. Detergent analysis by using absorbers is a good method as it can remove detergents with a very low critical micelle concentration (Kaur *et al.*, 2016). However, this method consumes large volumes of organic solvent which are toxic to human health and to the environment (Laouini *et al.*, 2012). Another potential disadvantage of this method is poor entrapment of any hydrophobic compounds (Meure *et al.*, 2008).

b) Solvent (ether or ethanol) injection

In solvent injection method, lipid is dissolved into an organic solvent such as ethanol or ether and followed by the injection of the suspension into an aqueous medium. The ethanol injection method was first discovered by Batzri and Korn in 1973 (Batzri & Korn, 1973). From the discovery, small vesicles which are under 100 nm are obtained without the process of sonication or extrusion (Stano *et al.*, 2004). The ether injection method contrast from the ethanol injection method as the ether cannot form homogenous mixture with aqueous phase. The ether injection method is able to produce high entrapment efficiency as compared to the ethanol injection method (Deamer & Bangham, 1976). This is because the removal of ether allowed the process to be performed for extended periods, forming a concentrated vesicle (Deamer, 1978).

c) Reverse phase evaporation (REV)

The reverse phase evaporation was introduced by Szoka and his researcher (Szoka & Papahadjopoulos, 1978). This method involves formation of drops of water which are enclosed by lipid. The mixture is dissolved in organic solvent and followed by an addition of aqueous medium. Then, sonication process is performed to produce inverted micelles. This method is able to obtain 65% of encapsulation efficiency in a medium of low ionic strength (Akbarzadeh *et al.*,

2013). The weakness of this method is the contact of the compound to be encapsulated with an organic solvent. These conditions are not suitable for fragile molecules and can lead to denaturation of some proteins (Meure *et al.*, 2008).

d) Thin film hydration

Hand shaken or thin film hydration was first described by Bangham in 1965 (Bangham *et al.*, 1965). This method includes dissolving of lipid in an organic phase and followed by elimination of the organic solvent via evaporation. Lipid film formed is hydrated with an aqueous medium and then, agitation process is performed to form sealed spherical structures. The disadvantage of this method is low encapsulation efficiency. However, Yalkowsky and Ran have modified the method by changing the organic solvent with halothane. From the research, more than 90% of encapsulation efficiency was obtained (Meure *et al.*, 2008).

Among these methods, thin film hydration is preferable to prepare drug carrier. Thin film hydration is the most widely used method to prepare vesicles (Pupo *et al.*, 2005; Tan *et al.*, 2002) and it is one of the simplest way to prepare drug carrier. Moreover, thin film hydration is a very straightforward method and excellent in upscaling feasibility. However, this method is not suitable for encapsulation of hydrophilic drugs and traces of organic solvent-critical for parenteral transport (Kreuter, 1994; Laouini *et al.*, 2012).

2.5.3 Drug Administration

Drug administration is defined as the route or path of active ingredient towards the targeting organ or tissue. The routes of administration can be generally classified according to the location of action. Each route has its own specific purpose, advantages and disadvantages. There are several types of drug administration for anticancer drug

which include intravenous administration, oral administration, and transdermal administration.

a) Intravenous administration

Intravenous administration involved injection directly into the vein. Intravenous injection is applicable for various type of cancer such as breast, lymphoma, gynaecologic and ovarian cancer (Ran *et al.*, 2015). The common anticancer drug carriers include emulsions, nanotubes and vesicles. The size of drug carrier that are administered intravenously should be less than 200 nm (Wong *et al.*, 2008). The advantages of intravenous administration are anticancer drugs can be delivered immediately into the blood stream and the effect of the drugs can act rapidly as compared to other routes. However, addition of active ingredients must be given continuously or the concentration of drugs must be increased to retain the effect of drug. The disadvantages for this administration include potential pain from the injection that leads to discomfort for the patient and it can be difficult to administer for obese patients.

b) Oral administration

Oral administration is consumption of drug that involves absorption through the gastrointestinal (GI) tract (Dong & Feng, 2005). Patients must swallow the drug either in solid or liquid form. This administration is suitable for ovarian, leukaemia, pancreatic and prostate cancer. Typical drug carriers for this administration include emulsions, microspheres and liposomes. The advantages of oral administrations are patients will not experience discomfort or pain and it can prevent any chances of infections caused by reuse of needles (Hussen & Heidelberg, 2016). Nevertheless, oral medication is very limited to certain types

of cancer and the process of drug absorption is very slow (Mazzaferro *et al.*, 2013). A drug that is orally administered may be degraded by stomach acid and enzymes unless an appropriate drug carrier is proposed for protection (Shaji & Patole, 2008).

c) Transdermal administration

In transdermal administration, the active ingredients are introduced on the skin surface and absorbed via the blood vessels into the bloodstream. The type of cancer which suitable for this administration include skin and prostate cancer. Compared to intravenous and oral administration, the drug carriers for transdermal administration are limited to emulsions and gels (Tanwar & Sachdeva, 2016). Transdermal administration can prevent the interference of gastrointestinal drug absorption and also able to transport a stable infusion of a drug over an extended period of time (Rabab, 2016). The main drawback of this administration is the drugs may not be well absorbed and undergo difficulty to penetrate through skin. Moreover, this administration is limited to nanosized drug in order to obtain efficient drug delivery system (Prausnitz & Langer, 2008).

As a concluding remark, the characteristic of the drug formulation must be suitable for intravenous administration. This is because the diorganotin(IV) complex is a hydrophobic drug and thin film hydration method is suitable technique for the preparation. Apart from that, this research aim is to formulate a drug for breast cancer treatment. Hence, the size of the encapsulated diorganotin(IV) complex must be below 200 nm.

2.5.4 Characterization of Formulated Drug

In order to confirm a successful formulated drug, some characteristic such as size of carrier, zeta potential, carrier morphology, encapsulation efficiency and *in vitro* drug release rate need to be examined.

a) Size analysis

The particle size and size distribution profile of carrier are usually determined by dynamic light scattering (DLS). Polydispersity index will evaluate the size distribution of carrier population. The smaller the PDI the more homogeneous the particles are distributed in the sample. This technique is very crucial to determine the exact size of drug carriers. Well distributed particle size is one of the key factors in enhancing the drug performance. For example, the size of the nanoparticles in drug delivery system should be small enough to escape capture by fixed macrophages (Cho *et al.*, 2008).

d) Zeta potential

Zeta potential is a parameter to measure the magnitude of electric charge near to the surface of potential cellular targets and normally determined by Zetasizer Nano (Zhang *et al.*, 2008). It is a good index to determine the interaction of drug carrier with its environment. Thus, zeta potential measurement is a convenient way to characterize electrostatic properties and one of the fundamental parameters to predict stability of colloidal systems. For example, if all the particles in suspension have a large negative or positive zeta potential, then they will tend to repel each other and they will be no tendency to aggregate (Clogston & Patri, 2011). However, if the particles have low zeta

potential values then they will be no force to prevent the particles flocculating (Laouini *et al.*, 2012).

e) Carrier morphology

The shape of the vesicles is another crucial factor to achieve a successful formulated drug. This is because the shape of the vesicles injected into the vein is significant for initiating an immune response (They *et al.*, 2009). Irregularly shaped microparticles have been established to promote tissue inflammation in comparison to the round shaped drug delivery systems. Due to this aspect, investigation of shape of carrier is a crucial element in effectiveness of drug delivery system. The morphology of carrier can be determined by field emission scanning electron microscope (FESEM) (Pramanik *et al.*, 2016), transmission electron microscope (TEM) (Peruzynska *et al.*, 2016) or scanning electron microscope (SEM) (Eldem *et al.*, 1991). Among all these methods, FESEM gives more advantages as compared to TEM and SEM. This is because FESEM provides better magnification resolution image and also able to diminish sample charging and damage.

f) Encapsulation and drug loading efficiency

Encapsulation and drug loading efficiency is one of the important parameters to obtain a successful formulated drug. Normally, encapsulation and drug loading are measured by UV-vis spectrophotometer (Fu *et al.*, 2005), high performance liquid chromatography (HPLC) (Awotwe *et al.*, 2012) or fluorescence absorbance (Xu *et al.*, 2017). The aims for this parameter are either improved delivery, or uptake by the target cells and decreasing the toxicity of the free drug to non-target organs.

Generally, to obtain this parameter, it requires the separation of free drug content. Then, the supernatant and encapsulated drug fraction will allow the calculation of encapsulation and drug loading efficiency (Ong *et al.*, 2016). The value of efficiency should be high enough to produce high entrapment drug concentration and preventing drug leakage. To acquire optimum efficiency of drug delivery system, parameters influencing the carrier and the drug need to be carefully considered during the early stages of development. In addition, the encapsulation and drug loading efficiency are influenced by solubility of the drug in water, the preparation process as well as the interaction between the drug molecules and drug carrier. These types of interaction consist of hydrophobic interaction, hydrogen bonding, electrostatic interaction, π - π stacking interaction and dipole-dipole interaction.

g) *In vitro* drug release

To ensure a better quality of drug performance, many attempts have been practiced developing a suitable *in vitro* release method for drug delivery system. The purpose of *in vitro* drug release study is to determine the rate of drug release. Practically, this study related on several factors such as absorption of drug through the nanoparticle matrix, size of nanoparticle, adsorbed drug or desorption of the surface-bound, drug solubility, degradation of nanoparticle matrix and diffusion or erosion processes (Singh & Lillard, 2009). Drug release study consists of variety methods including membrane diffusion methods such as continuous flow (Salmela & Washington, 2014), dialysis membrane (Nornoo & Chow, 2008) and sample and separation methods such as ultrafiltration (Cui *et al.*, 2006) and ultracentrifugation (Ricci *et al.*, 2006).

2.6 Concluding statement

As a conclusion, the chemistry of organotin(IV) complexes with multidentate ligands displays uniqueness in many points of view such as reactivity, biological activity, and structural features. Different type of donor atoms and number of coordination site able to influence their strength in bioactivity profiles. Moreover, there are many techniques and factors to build up a successful formulated drug such as size of drug, drug solubility, type of surfactant used, encapsulation efficiency and many more.

The interesting about this research is all the ten type of organotin complexes with tetradentate ligands is the new series of complexes. In addition, the difference between this research compared to others is the application part which is encapsulation and drug release study. Apart from that, there are still no report related with formulation of organotin complexes. Hence, this research is a good approach to introduce organotin complexes as a candidate of anticancer drug.

CHAPTER 3: METHODOLOGY

3.1 Introduction

This chapter will discuss on the chemicals and details of the instruments that are used in this research. Apart from that, methods to prepare the organotins and multidentate ligands are also included in this chapter.

3.2 Materials

The following commercial chemicals of reagent grade were used in the synthesis: salicylaldehyde, 5-bromosalicylaldehyde, 5-chlorosalicylaldehyde, 2,4-dihydroxybenzaldehyde, 1,3-diaminopropane, diaminomaleonitrile, tin powder, 4-bromobenzyl bromide, 4-chlorobenzyl chloride, 4-fluorobenzyl chloride, benzyl chloride, 4-methylbenzyl chloride and triethylamine. They were used without further treatment. All reagents were purchased from Merck, Acros Organics and Sigma-Aldrich.

For the formulation part, the chemicals that were used in the preparation of vesicles were: hexyldecyl-lactoside and dodecyl trimethylammonium bromide, DTAB.

The solvents used in the preparation of the drug were ethanol, dimethyl sulfoxide and phosphate buffer saline pH 7.4.

All the solvents such as methanol, ethanol, acetonitrile, toluene, acetone, chloroform, ethyl acetate, hexane, and dimethylsulfoxide were received as reagent grade and were used without purification.

3.3 Physical Measurement of Multidentate Ligands, Substituted Dibenzyltin Compounds and Organotin Complexes

The melting points of the compounds were measured using an Electrothermal digital melting point apparatus and were uncorrected. The infrared spectra for the compounds were recorded on a Perkin Elmer System 400 spectrophotometer from 4000 to 450 cm^{-1} at room temperature. The UV-vis spectra for the ligands and complexes were recorded in DMSO and methanol with a Shimadzu 2600 UV-vis spectrophotometer in the wavelength range of 190 to 600 nm. The ^1H and ^{13}C NMR spectra were recorded on FT-NMR Bruker AVN 400 MHz spectrophotometers and FT-NMR ECX 400MHz System JEOL spectrometer respectively, δ relative to SiMe_4 in $\text{DMSO-}d_6$ and CDCl_3 . Elemental analysis was carried out on a Thermofischer Scientific FlashSMART CHNS/O analyser.

The X-ray crystallographic intensity data were measured using Cu $K\alpha$ radiation graphite-crystal monochromator ($\lambda = 1.54184 \text{ \AA}$). The data were collected by using an Agilent Supernova, Dual Cu at zero, AtlasS2 diffractometer and *CrysAlis* PRO (Rigaku Oxford Diffraction). The programs that were used to solve structure were *SHELXS*, *SHELXL2014*, *ORTEP-3* for Windows and *DIAMOND*. Multi-scan absorption correction was applied to the data. The crystal structures were solved by direct methods and refined by full-matrix least-squares on F^2 .

3.4 Synthesis of Multidentate Ligands

N,N'-bis(5-bromo-salicylidene)-1,3-diaminopropane, L1

Preparation method of this ligand is based on the literature without modification (Elmali *et al.*, 2000). 4.03 g (0.02 mol) of 5-bromosalicylaldehyde was dissolved in 30 mL ethanol in a 250 mL flat-bottom flask. Then, 0.90 mL (0.01 mol) of 1,3-diaminopropane was added into the flask. The mixture was refluxed for 2 hours and a

dark yellow solution was obtained. The solution was cooled to room temperature and a light yellow precipitate was formed. The yellow precipitate was recrystallized from chloroform (lit. value; m.p. : 131-133 °C).

***N,N'*-bis(5-chloro-salicylidene)-1,3-diaminopropane, L2**

Synthesizing this ligand is also based on the same literature review to produce ligand L1 (Elmali *et al.*, 2000). A solution of 5-chlorosalicylaldehyde (3.19 g, 0.02 mol) was dissolved in 30 mL ethanol in a 250 mL flat-bottom flask. Next, 0.90 mL (0.01 mol) of 1,3-diaminopropane was added into the flask. A yellow solution was obtained upon the addition of mixture. The reaction mixture was heated under reflux for 2 hours and constantly stirred. The reaction mixture was allowed to cool to room temperature. Yellow crystals were obtained by the slow evaporation of ethanol solution at room temperature (lit. value; m.p. : 96-97 °C).

***N,N'*-bis(5-chloro-salicylidene)-1,3-diaminopropane, L3**

Preparation method of this ligand is based on the literature without modification (Shagisultanova & Ardasheva, 2003). 2.20 mL (0.02 mol) of salicylaldehyde and 1.00 mL (0.01 mol) of 1,3-diaminopropane were dissolved in 150 mL dry toluene in a 250 mL flat-bottom flask. The mixture was heated under reflux in a Dean-Stark apparatus for 6 hours to remove water formed during the reaction. The solution was cooled to room temperature and a light yellow solid was formed upon cooling. A yellow precipitate was filtered off and washed several times using hexane and dried under vacuum over silica gel overnight. The precipitate was recrystallized from methanol (lit. value; m.p.: 51-53 °C).

2,3-bis((N)-(2-hydroxybenzylidene)amino)maleonitrile, L4

Ligand L4 is prepared by referring the method described in literature review (Wohrie & Buttner, 1985). 2,3-bis((N)-(2-hydroxybenzylidene)amino)maleonitrile was prepared by stirring of 1.11 g (0.01 mol) of diaminomaleonitrile and 2.20 mL (0.02 mol) salicylaldehyde in 30 mL ethanol. The dark brown solution was obtained upon addition of mixture. The mixture was refluxed for 3 hours. Then, it was filtered and a light brown precipitate was obtained upon cooling to room temperature. The precipitate was recrystallized in ethanol (lit. value; m.p.: 230 °C (dec.)).

2,3-bis((N)-(2,4-dihydroxybenzylidene)amino)maleonitrile, L5

Dieter *et al.* have described the preparation of ligand L5 (Dieter *et al.*, 1983). From the literature, a hot ethanolic solution of 1.16 g (0.01 mol) of diaminomaleonitrile was added to 2.82 g (0.02 mol) of 2,4-dihydroxybenzaldehyde. The mixture was refluxed for 2-3 hours producing a reddish orange mixture at the end of the reaction. The mixture was filtered and a reddish orange precipitate was obtained upon cooling to room temperature. The solid product obtained was then recrystallized from methanol (lit. value; m.p. : 263 °C (dec.)).

3.5 Synthesis of Organotin Compounds

Preparation method is based on the literature without modification (Sisido *et al.*, 1961): 3 to 5 drops of water were added to 5.93 g (0.05 mol) of tin powder and kneaded together. The tin powder was suspended in 50 mL of toluene under efficient stirring and the mixture was heated to about 110 °C, which was the boiling point of toluene. Then, 6.40 g (0.05 mol) of benzyl chloride was dissolved in toluene and added drop wise into the suspension mixture for 3 minutes while refluxing was continued for an additional 3 hours. After that, fine colourless crystals started to appear on the surface of the solution.

The mixture was filtered while it was hot. The greyish residue which remained at the bottom of the flask was dissolved, extracted with acetone and filtered. The second filtrate and the solution were evaporated under diminished pressure producing a yellow solid. This method was repeated for synthesizing other organotin compounds.

3.6 Synthesis of Diorganotin(IV) Complexes

***N,N'*-bis(5-bromo-salicylidene)-1,3-diaminopropane di(*p*-bromobenzyl)tin, C1**

0.43 g (0.001 mol) of L1 and sodium ethoxide were dissolved with ethanol in a 50 mL flat-bottom flask. Clear light yellow solution was formed. The mixture was refluxed for 1 hour and 30 minutes. Then, 0.61 g (0.001 mol) of di(*p*-bromobenzyl)tin dibromide in 20 mL of ethanol was added. The mixture was further refluxed for 4 hours. The mixture was filtered and a light yellow precipitate was obtained upon cooling to room temperature.

2,3-bis((*N*)-(2-hydroxybenzylidene)amino)maleonitrile di(*p*-bromobenzyl)tin, C5

Et₃N was dissolved in hot ethanolic solution of 0.40 g (0.001 mol) of L4 in 50 mL flat-bottom flask. Clear light brown solution was formed. The reaction mixture was refluxed for 1 hour 30 minutes. Then, 0.61 g (0.001 mol) of di(*p*-bromobenzyl)tin dibromide in 20 mL of ethanol was added. The filtrate was evaporated and a light brown powder was formed from the mother liquor.

Similarly in preparing C1, compounds C2, C3 and C4 were prepared with sodium ethoxide as a base. Besides that, triethylamine was used for the preparation of compound C5. Similar procedure was applied to make compounds C6, C7, C8, C9 and C10. The details of the amount of starting materials to synthesise the compounds are listed in **Table 3.1**.

Table 3.1 : The amount of starting materials to synthesise the compounds.

Compounds	Ligand	Base	Organotin compound
C1	L1	Sodium ethoxide	di(<i>p</i> -bromobenzyl)tin dibromide (0.61 g, 0.001 mol)
C2	(0.43 g, 0.001 mol)		di(<i>p</i> -fluorobenzyl)tin dichloride (0.41 g, 0.001 mol)
C3	L2 (0.35 g, 0.001 mol)		di(<i>p</i> -chlorobenzyl)tin dichloride (0.44 g, 0.001 mol)
C4	L3 (0.28 g, 0.001 mol)		dibenzyltin dichloride (0.37 g, 0.001 mol)
C5	L4 (0.40 g, 0.001 mol)	Triethylamine	di(<i>p</i> -bromobenzyl)tin dibromide (0.61 g, 0.001 mol)
C6			di(<i>p</i> -fluorobenzyl)tin dichloride (0.41 g, 0.001 mol)
C7			di(<i>p</i> -methylbenzyl)tin dichloride (0.39 g, 0.001 mol)
C8	L5 (0.33 g, 0.001 mol)		di(<i>p</i> -bromobenzyl)tin dibromide (0.61 g, 0.001 mol)
C9			di(<i>p</i> -chlorobenzyl)tin dichloride (0.44 g, 0.001 mol)
C10			di(<i>p</i> -fluorobenzyl)tin dichloride (0.41 g, 0.001 mol)

3.7 Biological Activities of Selected Ligand and Complexes

L5, C8, C9 and C10 were sent to the Institute of Biological Sciences of University Malaya to investigate the anticancer properties. They were screened against several cancer cell lines, namely breast (MCF-7), lung (A549) and prostate (PC-3). The cytotoxicity experiment was evaluated by the 3-(4,5-dimethylthiazol-2-yl)-2,5-diphenyltetrazolium bromide (MTT) assay (Mosmann, 1983). Briefly, cells were maintained in basic culture medium, supplemented with 10% fetal bovine serum and 2% penicillin/streptomycin. For MCF-7, the type of medium used was Dulbecco's Modified Eagle Medium (DMEM) while PC-3 and A549 used Roswell Park Memorial Institute Medium (RPMI).

The cells were cultured at 37 °C under a humidified atmosphere in a CO₂ incubator. The cells were then seeded in a 96-well microtiter plate (Nunc, Germany) at a

concentration of 7000 cells per well and incubated in a CO₂ incubator at 37 °C. After 24 hours, the cells were treated with the samples and incubated for 72 hours. DMSO was used to dilute the samples and the final concentration of DMSO in each well was not more than 0.5% (v/v). At the end of the incubation period, 20 µL of MTT working solution (5 mg/ml) was added into each well and the 96-well microtiter plate was incubated for another three hours at 37 °C. The solution was then gently aspirated from each well and 200 µL of DMSO were added to solubilise the purple formazan crystals. The absorbance values were measured using a Multiskan GO micro plate spectrophotometer (Thermo Fisher Scientific Inc., Waltham, MA, USA) at 570 nm with 650 nm as a reference wavelength. The cytotoxic activity of each sample was expressed as the IC₅₀ value, which is the concentration of the test sample that causes 50% inhibition of cell growth. The viability of treated and control cells were calculated using the following formula (Senthilraja & Kathiresan, 2015):

$$\text{Cell viability} = (A_{\text{sample}} / A_{\text{control}}) \times 100\%$$

where A_{sample} and A_{control} is absorbance of the sample and control

3.8 Encapsulation Studies

In encapsulation studies, we evaluated different physiochemical characterization including size distribution analysis, zeta potential, morphological analysis, determination of encapsulation efficiency, drug loading and *in vitro* drug release study.

3.8.1 Sample Preparation

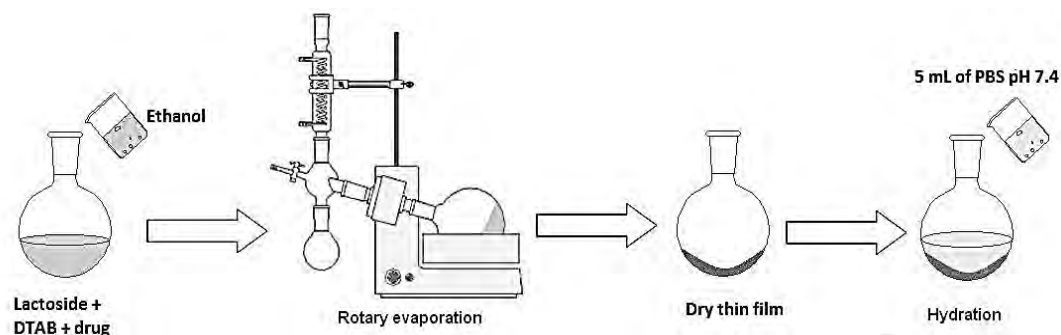


Figure 3.1 : Preparation of sample.

[Adapted and modified from (Araujo *et al.*, 2013)]

The preparation of sample is illustrated in **Fig. 3.1**. Mixture of cationic surfactant and non-ionic surfactant were prepared by thin film hydration methods. They were prepared by mixing DTAB : hexyldecyl lactoside in the ratio 30 : 70 respectively. The final concentration of compound in the formulation is fixed at five mM and the total concentration of the mixed surfactants is one mM. The compound and the surfactant were dissolved and mixed in an organic solvent such as ethanol to assure a clear and homogeneous mixture. The organic solvent was removed by rotary evaporator yielding a thin lipid film on the wall of a round bottom flask. The thin film was thoroughly dried to remove residual organic solvent by placing the flask overnight in a desiccator that has been vacuumed with vacuum pump. Then, the thin film was hydrated and agitated with 5 mL of phosphate buffer saline at concentration of pH 7.4. The hydrated film was further used to investigate related characterization on the formulated compound.

3.8.2 Size Distribution Analysis and Zeta Potential

The sample as prepared in **3.8.1** section was filtered through a polycarbonate membrane with pore size of 0.2 μm to remove any dust or large particles.

After that, the sample was examined to obtain the particle size and zeta potential. Dynamic light scattering (DLS) was used to measure the size distribution in this formulation. A light scattering was measured at a 173° angle to the incident beam. The zeta potential of the formulations was measured with the laser Doppler electrophoretic mobility measurements using the Zetasizer 2000 (Malvern Instruments Ltd., Malvern, U.K.) at a temperature of 25 °C. Analyses were done in triplicate. Zeta potential values and standard deviations (\pm S.D.) were elaborated directly from the instrument.

3.8.3 Morphological Analysis

A few drops of the sample as prepared in **3.8.1** were placed on a polycarbonate membrane without filtration. The sample was left overnight to dry and coated with platinum. Then, surface morphology of prepared nanocarrier was visualized by FESEM. The surface was scanned and photomicrographs were taken at an accelerating voltage of 30 kV.

3.8.4 Determination of Encapsulation Efficiency and Drug Loading

The percentage of encapsulation efficiency (%EE) and drug loading were determined by ultra-centrifugation method using Velocity 18R Refrigerated Centrifuge. The vesicles loaded with diorganotin(IV) complex as prepared in **3.8.1** was separated by centrifugation at 15000 rpm for 30 minutes and the process was repeated twice. The supernatant was analysed for the free drug content. The encapsulation efficiency and drug loading of drug carrier was calculated with the following formula:

$$\%EE = (T - C / T) \times 100\%$$

$$\%DL = [(T - C) / (T + S - C)] \times 100\%$$

where, %EE is the percentage encapsulation efficiency of drug carrier, %DL is the percentage drug loading, T is the total amount of drug in the initial suspension,

C is the amount of free drug in the supernatant, and S is the total amount of surfactant used (Yassin *et al.*, 2010).

3.8.5 *In vitro* Drug Release Study

The *in vitro* release of drugs from mixed vesicle system was measured by applying the dialysis bag method. Dialysis bags were soaked before use in buffer solution at room temperature for 12 hours to remove the preservative, followed by rinsing thoroughly in distilled water. An accurately measured amount of drug vesicular suspension was placed in a dialysis bag and then, the dialysis bag was suspended in 50 mL of PBS (pH 7.4), under gentle stirring.

The container that contained the dialysis bag was placed into a bulk volume of water at 37 °C, mimicking body temperature. At predetermined time intervals (from freshly prepared up to 60 days), 1 mL of the medium was withdrawn and assayed spectrophotometrically for drug content at 327 nm, the wavelength at which the maximum absorption for complex C9 using UV-vis spectrophotometer. The corresponding wavelength was the optimum wavelength which was obtained from the calibration curve of sample C9 in PBS. The volume of medium in the container was maintained with an equal volume of fresh PBS. The drug release was determined as the ratio in percentage of the amount of drug released at each time interval to the initial amount of drug encapsulated in the formulation. Experiments were done in duplicate and results were expressed as mean \pm standard deviation.

CHAPTER 4: RESULTS AND DISCUSSION

4.1 Introduction

This chapter will elaborate more on the findings that are obtained in this research. All the characterization data of compounds which cover synthesis and encapsulation parts are specified in this chapter. The data obtained will be compared to the previous literatures.

4.2 Characterization Data of Ligands, Organotin Compounds and Complexes

The general reaction scheme for the preparation of the two types of Schiff base ligands is shown in **Fig. 4.1** while the general scheme for the preparation of the complexes is shown in **Fig. 4.2**. The Schiff base ligands were used without extensive purification in the preparation of their organotin complexes since the ligands were obtained after recrystallization.

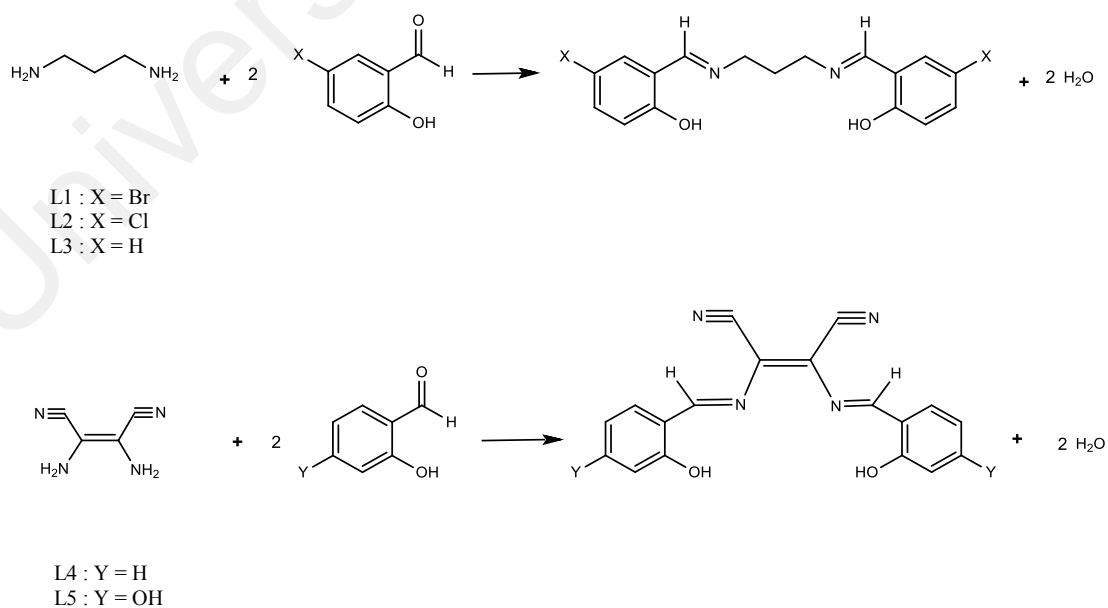


Figure 4.1 : Preparation of Schiff base ligands.

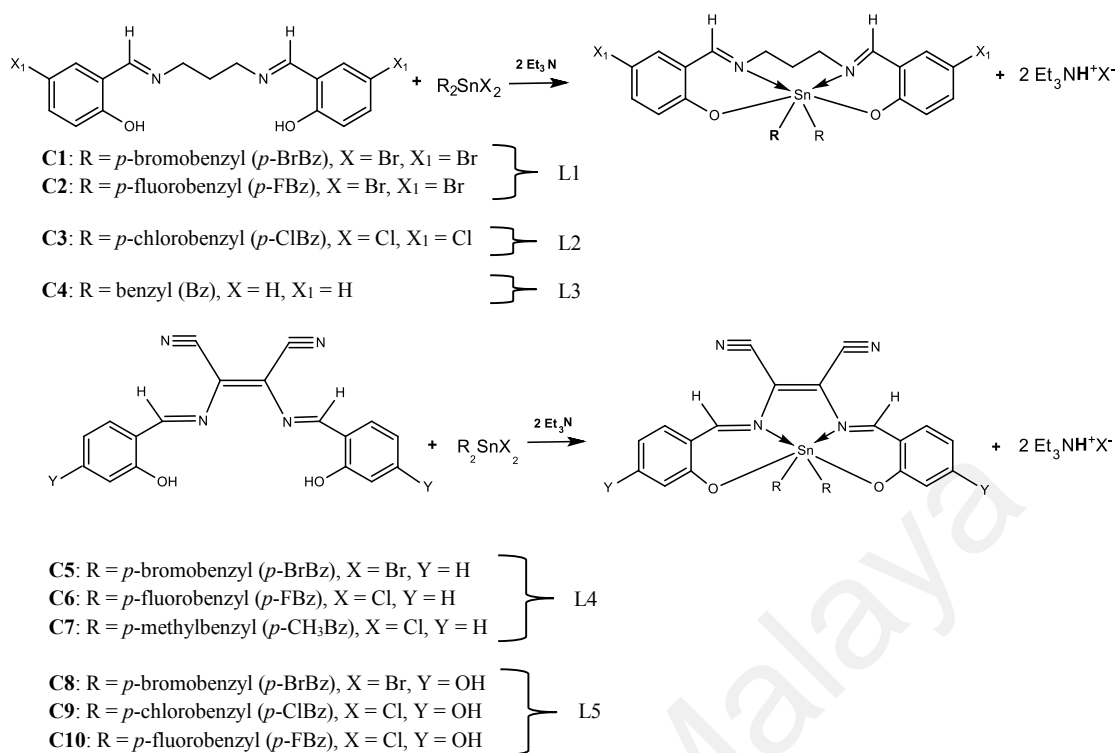


Figure 4.2 : Preparation of diorganotin(IV) Schiff base complexes.

Three multidentate ligands were prepared from the reaction of 1,3-diaminopropane with 5-bromosalicylaldehyde, 5-chlorosalicylaldehyde and salicylaldehyde. The ligands are named as L1, L2 and L3 respectively. Another two ligands were obtained from the reaction of diaminomaleonitrile with salicylaldehyde and 2,4-dihydroxybenzaldehyde and the products are called L4 and L5.

Subsequently, complexation of ligands L1, L2 and L3 produce four diorganotin(IV) Schiff base complexes named as C1, C2, C3 and C4. For the second types of ligands, these two ligands were used to prepare six diorganotin(IV) complexes which are known as C5, C6, C7, C8, C9 and C10. The details on physical appearances, melting points, and the yields are displayed in **Table 4.1** to **Table 4.3**.

Table 4.1 : Analytical data of ligands.

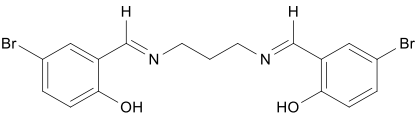
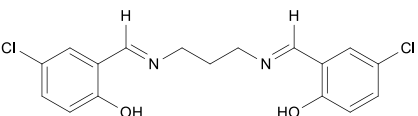
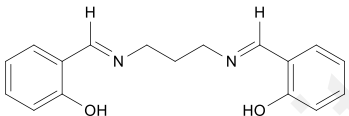
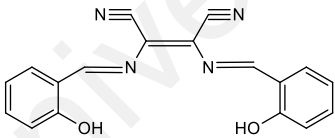
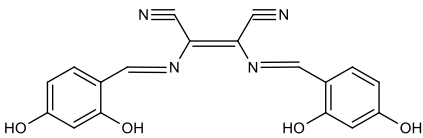
Ligand	Mass (g)	Percentage yield (%)	Melting point (°C)	Colour of ligand
<p>L1 <i>N,N'</i>-bis(5-bromo-salicylidene)-1,3-diaminopropane</p> 	3.56 g	81	132-134 °C	Light yellow solid
<p>L2 <i>N,N'</i>-bis(5-chloro-salicylidene)-1,3-diaminopropane</p> 	2.79 g	80	96-98 °C	Light yellow solid
<p>L3 <i>N,N'</i>-bis(salicylidene)-1,3-diaminopropane</p> 	2.17 g	77	50-52 °C	Light yellow solid
<p>L4 2,3-bis((<i>N</i>)-(2-hydroxybenzylidene)amino)maleonitrile</p> 	1.61 g	52	232 °C (dec.)	Light brown solid
<p>L5 2,3-bis((<i>N</i>)-(2,4-dihydroxybenzylidene)amino)maleonitrile</p> 	2.55 g	78	264 °C (dec.)	Reddish orange solid

Table 4.2 : Analytical data of organotin compounds.

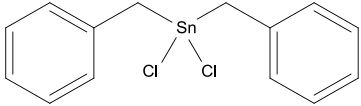
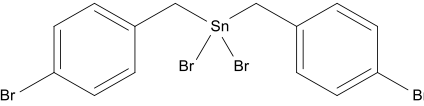
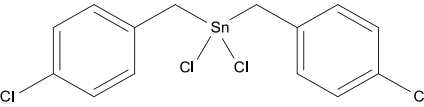
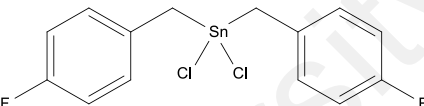
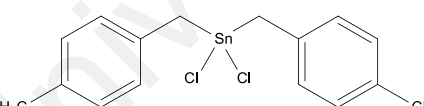
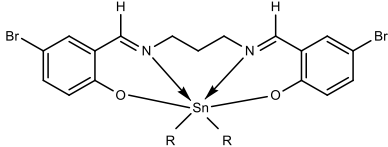
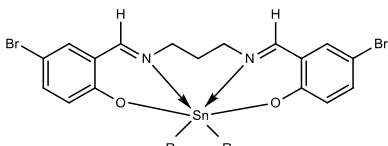
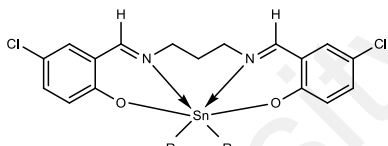
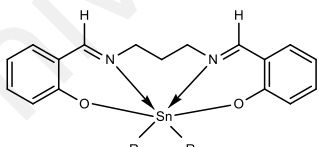
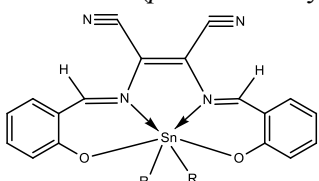
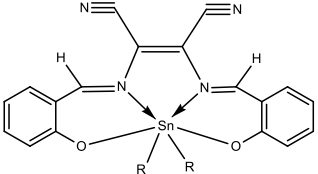
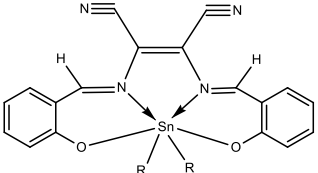
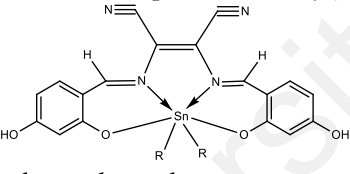
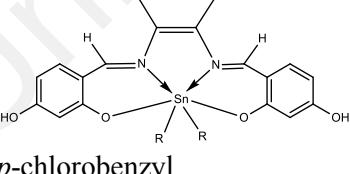
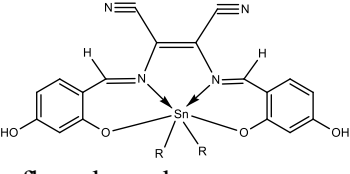
Organotin compound	Mass (g)	Percentage yield (%)	Melting point (°C)	Colour of compound
<p>BzCl dibenzyltin dichloride</p> 	5.61 g	10	165-168 °C	White solid
<p>4Br di(<i>p</i>-bromobenzyl)tin dibromide</p> 	6.49 g	21	175-177 °C	White solid
<p>4Cl di(<i>p</i>-chlorobenzyl)tin dichloride</p> 	8.41 g	13	206-208 °C	White solid
<p>4F di(<i>p</i>-fluorobenzyl)tin dichloride</p> 	19.65 g	32	168-170 °C	White solid
<p>4CH₃ di(<i>p</i>-methylbenzyl)tin dichloride</p> 	13.34 g	22	216-220 °C	White solid

Table 4.3 : Analytical data of organotin complexes.

Complex	Mass (g)	Percentage yield (%)	Melting point (°C)	Colour of ligand
<p>C1 <i>N,N'</i>-bis(5-bromo-salicylidene)-1,3-diaminopropane di(<i>p</i>-bromobenzyl)tin</p>  <p>R = <i>p</i>-bromobenzyl</p>	0.84 g	94	84-87 °C	Light yellow solid
<p>C2 <i>N,N'</i>-bis(5-bromo-salicylidene)-1,3-diaminopropane di(<i>p</i>-fluorobenzyl)tin</p>  <p>R = <i>p</i>-fluorobenzyl</p>	0.28 g	36	120-123 °C	Light yellow solid
<p>C3 <i>N,N'</i>-bis(5-chloro-salicylidene)-1,3-diaminopropane di(<i>p</i>-chlorobenzyl)tin</p>  <p>R = <i>p</i>-chlorobenzyl</p>	0.53 g	74	85-86 °C	Light yellow solid
<p>C4 <i>N,N'</i>-bis(salicylidene)-1,3-diaminopropane dibenzyltin</p>  <p>R = benzyl</p>	0.31 g	53	100-102 °C	Light yellow solid
<p>C5 2,3-bis((<i>N</i>)-(2-hydroxybenzylidene)amino)maleonitrile di(<i>p</i>-bromobenzyl)tin</p>  <p>R = <i>p</i>-bromobenzyl</p>	0.42 g	55	166-168 °C (dec.)	Light brown solid

Complex	Mass (g)	Percentage yield (%)	Melting point (°C)	Colour of ligand
<p>C6 2,3-bis((N)-(2-hydroxybenzylidene)amino) maleonitrile di(<i>p</i>-fluorobenzyl)tin</p>  <p>R = <i>p</i>-fluorobenzyl</p>	0.42 g	94	208-210 °C	Light brown solid
<p>C7 2,3-bis((N)-(2-hydroxybenzylidene)amino) maleonitrile di(<i>p</i>-methylbenzyl)tin</p>  <p>R = <i>p</i>-methylbenzyl</p>	0.40 g	63	Cannot be performed due to sticky appearance	Light brown solid
<p>C8 2,3-bis((N)-(2,4-dihydroxybenzylidene)amino) maleonitrile di(<i>p</i>-bromobenzyl)tin</p>  <p>R = <i>p</i>-bromobenzyl</p>	0.34 g	43	>360 °C (dec.)	Reddish brown solid
<p>C9 2,3-bis((N)-(2,4-dihydroxybenzylidene)amino) maleonitrile di(<i>p</i>-chlorobenzyl)tin</p>  <p>R = <i>p</i>-chlorobenzyl</p>	0.26 g	37	210-212 °C (dec.)	Dark brown solid
<p>C10 2,3-bis((N)-(2,4-dihydroxybenzylidene)amino) maleonitrile di(<i>p</i>-fluorobenzyl)tin</p>  <p>R = <i>p</i>-fluorobenzyl</p>	0.64 g	96	>360 °C (dec.)	Reddish brown solid

From the **Table 4.3**, some of the diorganotin(IV) complexes such as complex C2, C8 and C9 showed low of percentage yield. The low of percentage yield could have been caused by the purification steps. The purification steps will lower the yield, through losses incurred during the transfer of material between apparatus or imperfect separation of the product from impurities, which may necessitate the removal of fractions deemed insufficiently pure.

4.3 Infrared (IR) spectra data

The IR spectra of ligands and complexes can be found in section appendix at page 112 to page 119. **Table 4.4** and **Table 4.5** showed the spectra data of ligands and complexes. From the spectra of ligands, a strong broad peak of hydroxyl stretching frequencies was observed around 3064-3306 cm^{-1} . In the spectra of diorganotin(IV) complexes, a characteristic absorption of hydroxyl oxygen was disappeared. These findings are in agreement with theoretical data. This showed that the phenolic oxygen were participated in the coordination to the centre metal (Hong *et al.*, 2013).

All the Schiff base ligands exhibited a strong band of C=N stretching in the region 1623-1632 cm^{-1} as derived from the azomethine group. This was within the range reported for azomethine group in Schiff base ligands (Prasad *et al.*, 2010; Devi & Suman, 2017). In the spectra of complexes, the strong band of C=N stretching vibrations were found in the region between 1601-1619 cm^{-1} which was about 12-27 cm^{-1} lower than those reported for the Schiff base ligands. The weakening in the C=N bond led to the lowering of the C=N stretching frequencies in the diorganotin(IV) complexes (Ali *et al.*, 2008; Rehman *et al.*, 2009; Yearwood *et al.*, 2002). This is due to the shift of the electron density from the azomethine nitrogen and carbonyl moieties to the tin metal which cause the weakening of the double bond (Shujah *et al.*, 2014).

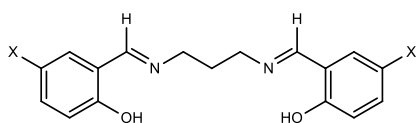
The C≡N stretching frequencies for ligands L4 and L5 are within the region of 2204-2234 cm⁻¹ meanwhile the phenolic C-O stretching frequencies exhibited in the region of 1276-1289 cm⁻¹. For the complexes, there are shifting about 8-24 cm⁻¹ for the phenolic C-O stretching. These results indicated that there was coordination between hydroxyl oxygen with the tin centre (Leovac *et al.*, 2005).

The presence of two new bands was observed in the lower frequency region of 456-586 cm⁻¹ for the diorganotin(IV) complexes. The absorption in the region of 500-590 cm⁻¹ had been assigned to the Sn-O stretching vibration which similar with literature (Amini *et al.*, 2016). According to published work by Varshney and her co-workers, the diorganotin(IV) complexes exhibited the Sn-N stretching frequencies in the region of 448-498 cm⁻¹ as the nitrogen lone pair of azomethine nitrogen bonded to the central tin atom (Varshney *et al.*, 1986). All the experimental results of Sn-C and Sn-N stretching frequencies were within the range reported by other researchers for diorganotin derivatives (Lee *et al.*, 2015; Li *et al.*, 2011).

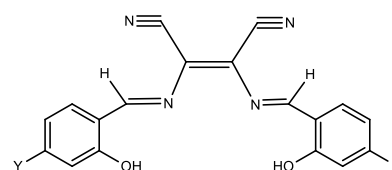
Table 4.4 : Infrared spectra data for ligands L1 to L5.

Ligand	Band assignment (cm ⁻¹)			
	ν (OH)	ν (C=N)	ν (C-O)	ν (C≡N)
L1	3064b	1632s	1276s	-
L2	3064b	1632s	1278s	-
L3	3051b	1631s	1277s	-
L4	3298b	1623s	1282s	2234s, 2204s
L5	3306b	1626s	1289s	2239s, 2212s

^as = strong, m = medium, w = weak, b = broad



L1 = Br
L2 = Cl
L3 = H

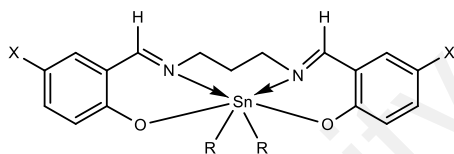


L4 = H
L5 = OH

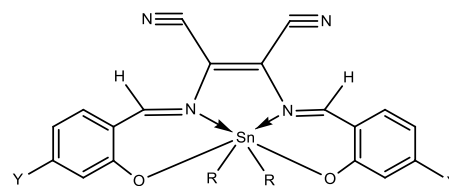
Table 4.5 : Infrared spectra data for complexes C1 to C10.

Ligand	Band assignment (cm ⁻¹)					
	ν (OH)	ν (C=N)	ν (C-O)	ν (C≡N)	ν (Sn-O)	ν (Sn-N)
C1	-	1603s	1252s	-	558m	457w
C2	-	1612s	1259s	-	548m	479w
C3	-	1604s	1255s	-	564m	459w
C4	-	1619s	1260s	-	586m	497w
C5	-	1607s	1270s	2234s, 2204s	535m	463m
C6	-	1601s	1272s	2235s, 2205s	534m	498w
C7	-	1603s	1274s	2237s, 2205s	534m	491w
C8	3305b	1603s	1270s	2241s, 2210s	544m	456m
C9	3306b	1603s	1272s	2239s, 2213s	543m	479m
C10	3307b	1599s	1275s	2241s, 2208s	536m	496m

^as = strong, m = medium, w = weak, b = broad



- C1: R = *p*-bromobenzyl (*p*-BrBz), X = Br
 C2: R = *p*-fluorobenzyl (*p*-FBz), X = Br
 C3: R = *p*-chlorobenzyl (*p*-ClBz), X = Cl
 C4: R = benzyl (Bz), X = H



- C5: R = *p*-bromobenzyl (*p*-BrBz), Y = H
 C6: R = *p*-fluorobenzyl (*p*-FBz), Y = H
 C7: R = *p*-methylbenzyl (*p*-CH₃Bz), Y = H
 C8: R = *p*-bromobenzyl (*p*-BrBz), Y = OH
 C9: R = *p*-chlorobenzyl (*p*-ClBz), Y = OH
 C10: R = *p*-fluorobenzyl (*p*-FBz), Y = OH

4.4 Nuclear Magnetic Resonance (NMR) Spectral Data

The NMR spectra of ligands and complexes can be found in section appendix at page 120 to page 135. The ¹H and ¹³C NMR spectra for the free ligands and complexes were recorded in deuterated DMSO or CDCl₃ due to the poor solubility of most of the complexes in deuterated solvents such as CD₃OD, CD₃CN and others. The information on what was the specific solvent used can be found in the summaries of physical and characterization data which are presented in the **Table 4.6 - Table 4.13**.

4.4.1 ^1H NMR spectra of ligands and complexes

The ^1H NMR spectra of ligands, L1, L2 and L3 showed a group of multiplet peak in the range of 3.70-3.74 ppm which confirmed the presence of $-\text{CH}_2-\text{CH}_2-$ group of 1,3-diaminopropane moiety. Another group of multiplet for L1, L2 and L3 appeared at 2.08-2.16 ppm due to the two protons of $-\text{CH}_2-$ group which has been displayed in **Fig. 4.3**. The aromatic proton of phenyl rings for all ligands was observed expected range which is around 6.26-8.00 ppm.

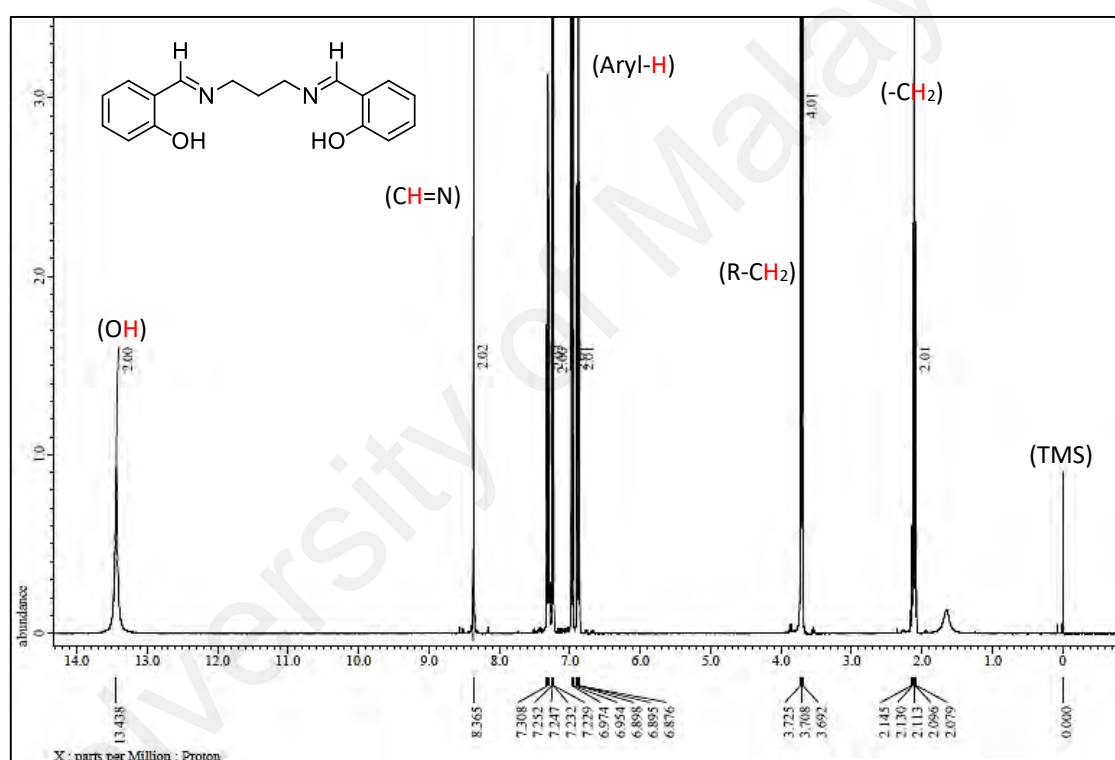


Figure 4.3 : ^1H NMR spectra of *N,N'*-bis(salicylidene)-1,3-diaminopropane, L3.

A strong singlet peak at 8.30-8.54 ppm for each ligand attributed to the azomethine protons which further confirmed the formation of desired compounds and the spectral data are consistent with the given structure. Gradinaru and his co-workers were reported that the prepared tetradentate Schiff base ligands containing N_2O_2 donor atoms showing one sharp singlet at 7.96-8.77 ppm which corresponded to $-\text{CH}=\text{N}$ moiety (Gradinaru *et*

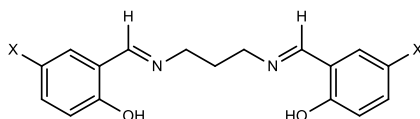
al., 2007). Whereas the azomethine peak for ligands which have been synthesized by Kalaivani and her researchers displayed occurring at 8.37-8.40 ppm (Kalaivani *et al.*, 2014). Thus, all the data are in good agreement with those reported in literature.

The ^1H NMR spectra of ligands also had signals at around 9.85-13.44 ppm which occurred as a singlet due to phenolic proton of hydroxyl oxygen. This observation supports the infrared data.

Table 4.6 : ^1H NMR chemical shifts for ligands L1 to L3.

Ligand	Assignments δ ^1H NMR (ppm)				
	OH	-N=C(H)	Aryl-H	R-CH ₂	-CH ₂ -
L1 (CDCl ₃)	13.38 (s, 2H)	8.30 (s, 2H)	7.35-7.40 (m, 4H) 6.85-6.87 (m, 2H)	3.71-3.74 (m, 4H)	2.09-2.16 (m, 2H)
L2 (CDCl ₃)	13.35 (s, 2H)	8.30 (s, 2H)	7.26-7.20 (m, 4H) 6.92-6.89 (m, 2H)	3.70-3.74 (m, 4H)	2.09-2.15 (m, 2H)
L3 (CDCl ₃)	13.44 (s, 2H)	8.37 (s, 2H)	7.23-7.33 (m, 4H) 6.95-6.97 (m, 2H) 6.88-6.90 (m, 2H)	3.70-3.73 (m, 4H)	2.08-2.15 (m, 2H)

^as = singlet, m = multiplet

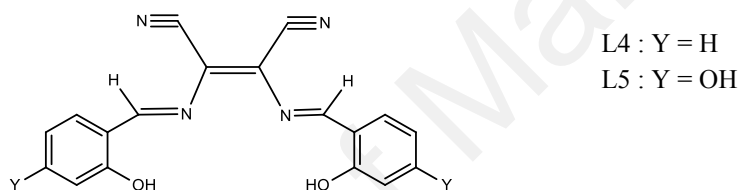


L1 : X = Br
L2 : X = Cl
L3 : X = H

Table 4.7 : ¹H NMR chemical shifts for ligands L4 & L5.

Ligand	Assignments δ ¹ H NMR (ppm)		
	<u>OH</u>	<u>-N=C(H)</u>	Aryl-H
L4 (DMSO)	10.41 (s, 2H)	8.54 (s, 2H)	7.98-8.00 (m, 2H) 7.27-7.31 (m, 2H) 6.82-6.89 (m, 4H)
L5 (DMSO)	9.85 (s, 4H)	8.40 (s, 2H)	7.73-7.75 (m, 2H) 7.47-7.51 (m, 2H) 6.29-6.32 (m, 2H)

^as = singlet, m = multiplet



In the diorganotin(IV) complexes of C1 to C4, the chemical shift for -CH₂-CH₂- group of 1,3-diaminopropane moiety were observed as a multiplet in the range of 3.60-3.73 ppm while the chemical shift for -CH₂- group were exhibited in the range of 2.09-2.14 ppm. For the aromatic proton, there were some increases of integration value in the complexes which proposed that the organotin compound was involved in the formation of complex. This observation indicate that number of protons were increase after complexation occurred. For diorganotin(IV) complexes of C1 to C7, the proton signals of azomethine nitrogen were shifted downfield from 8.30-8.54 ppm to 8.44-8.60 ppm while azomethine proton for complexes of C8 to C10 were shifted upfield in the region of 8.10-8.27 ppm. These results confirmed that the azomethine nitrogen had taken part in the coordination with central tin.

The hydroxyl protons of the ligands were disappeared upon complexation which suggested that deprotonation of OH proton and conforming the bonding to the tin atom except for complex C8 to complex C10 which showed decrease in the integration value of hydroxyl protons. This observation suggested that the bonding of the tin atom to one of the oxygen atoms of the Schiff base ligand through the replacement of one of the phenolic protons. The ^1H NMR spectrum of complexes also showed a new singlet peak in the 1.11-1.98 ppm region. This can be seen in **Fig 4.4** which indicated that Sn-CH₂ proton was attached to the ligands. Also, for complex C7, a singlet peak at 2.23 ppm was found due to the presence of methyl proton that attached at the benzene ring. Overall, the chemical shifts for the ligands and the complexes are found within the expected range.

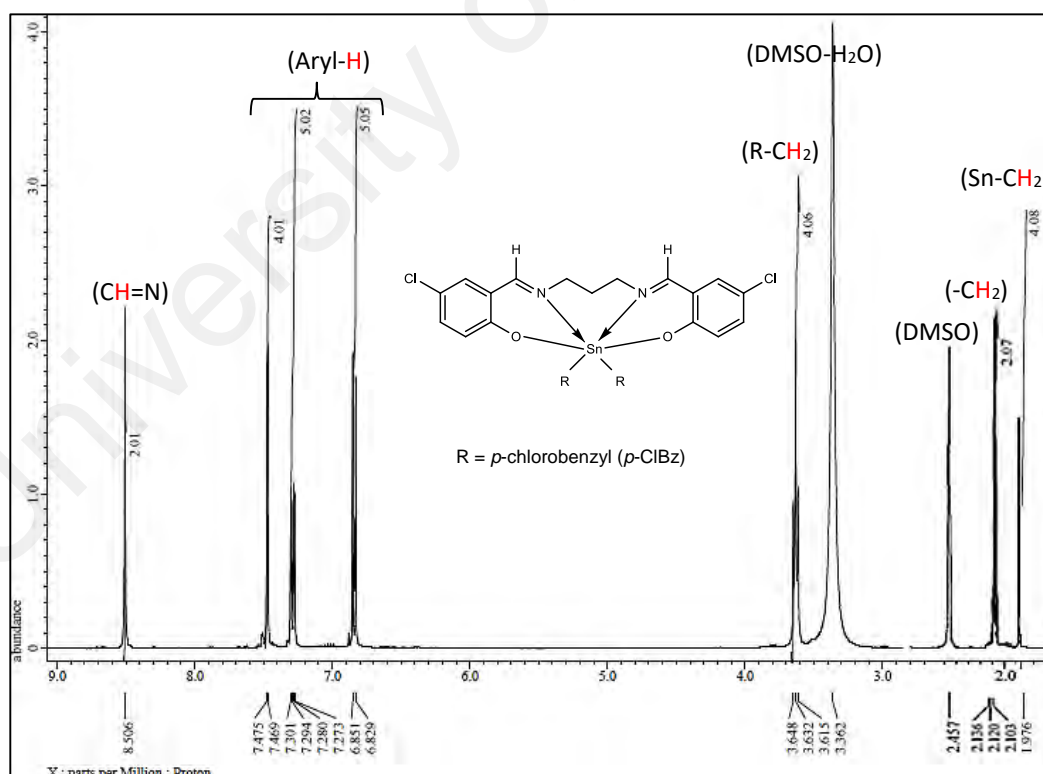
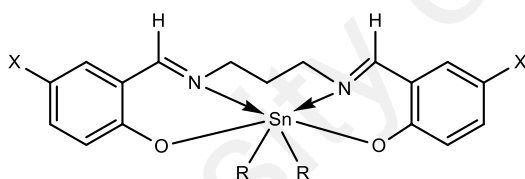


Figure 4.4 : ^1H NMR spectra of N,N' -bis(5-chloro-salicylidene)-1,3-diaminopropane di(*p*-chlorobenzyl)tin, C3.

Table 4.8 : ^1H NMR chemical shifts for complexes C1 to C4.

Complex	Assignments δ ^1H NMR (ppm)				
	-N=C(H)	Aryl-H	R-CH ₂	-CH ₂ -	Sn-CH ₂ -
C1	8.54 (s, 2H)	7.38-7.84 (m, 10H) 6.77-6.97 (m, 4H)	3.60-3.63 (m, 4H)	2.10-2.14 (m, 2H)	1.83 (s, 4H)
C2	8.51 (s, 2H)	7.38-7.63 (m, 10H) 6.78-6.83 (m, 4H)	3.61-3.64 (m, 4H)	2.10-2.14 (m, 2H)	1.97 (s, 4H)
C3	8.51 (s, 2H)	7.27-7.48 (m, 9H) 6.83-6.85 (m, 5H)	3.62-3.65 (m, 4H)	2.10-2.14 (m, 2H)	1.98 (s, 4H)
C4	8.44 (s, 2H)	7.44-7.51 (m, 4H) 7.19-7.36 (m, 10H) 6.88-6.95 (m, 4H)	3.69-3.73 (m, 4H)	2.09-2.13 (m, 2H)	1.27 (s, 4H)

^as = singlet, m = multiplet

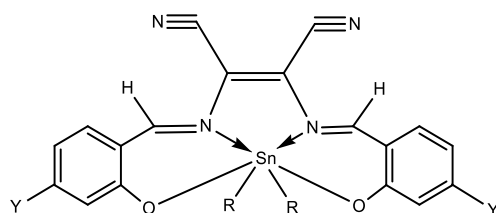


C1: R = *p*-bromobenzyl (*p*-BrBz), X = Br
 C2: R = *p*-fluorobenzyl (*p*-FBz), X = Br
 C3: R = *p*-chlorobenzyl (*p*-ClBz), X = Cl
 C4: R = benzyl (Bz), X = H

Table 4.9 : ¹H NMR chemical shifts for complexes C5 to C10.

Complex	Assignments δ ¹ H NMR (ppm)				
	<u>OH</u>	-N=C(<u>H</u>)	Aryl-H	- <u>CH</u> ₃ -	Sn- <u>CH</u> ₂ -
C5	-	8.59 (s, 2H)	7.48-7.85 (m, 6H) 7.26-7.31 (m, 6H) 6.89-6.94 (m, 4H)	-	1.19 (s, 4H)
C6	-	8.58 (s, 2H)	7.61-7.84 (m, 6H) 7.27-7.35 (m, 6H) 6.87-6.95 (m, 4H)	-	1.18 (s, 4H)
C7	-	8.60 (s, 2H)	7.63-7.87 (m, 6H) 7.06-7.41 (m, 6H) 6.87-6.98 (m, 4H)	2.23 (s, 6H)	1.98 (s, 4H)
C8	9.85 (s, 2H)	8.17 (s, 2H)	7.47-7.79 (m, 6H) 6.99-7.25 (m, 6H) 6.27-6.37 (m, 4H)	-	1.13 (s, 4H)
C9	9.87 (s, 2H)	8.10 (s, 2H)	7.85-7.90 (m, 5H) 7.39-7.47 (m, 5H) 6.24-6.34 (m, 4H)	-	1.11 (s, 4H)
C10	9.92 (s, 2H)	8.27 (s, 2H)	7.74-7.96 (m, 5H) 7.09-7.32 (m, 5H) 6.33-6.42 (m, 4H)	-	1.18 (s, 4H)

^as = singlet, m = multiplet



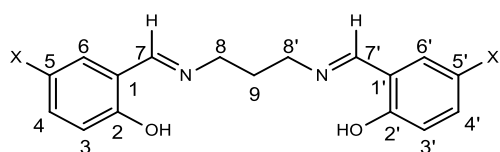
C5: R = *p*-bromobenzyl (*p*-BrBz), Y = H
C6: R = *p*-fluorobenzyl (*p*-FBz), Y = H
C7: R = *p*-methylbenzyl (*p*-CH₃Bz), Y = H
C8: R = *p*-bromobenzyl (*p*-BrBz), Y = OH
C9: R = *p*-chlorobenzyl (*p*-ClBz), Y = OH
C10: R = *p*-fluorobenzyl (*p*-FBz), Y = OH

4.4.2 ^{13}C NMR spectra of ligands and complexes

The ^{13}C NMR of L1 to L3 for the aliphatic carbon of C(8,8') and C(9) were found around 56.9 and 31.5-31.8 ppm respectively and the values were slightly change after formation of complexes. For L3, L4 and their complexes, there were two peaks around 124.8-129.8 ppm and 114.1-114.7 ppm which indicated the presence of C=C and nitrile carbons respectively in the compounds. The chemical shifts for azomethine carbon in the ligands were observed in the range of 159.7-165.7 ppm. Meanwhile, the chemical shift of azomethine carbon for all complexes showed a significant upfield shift in the region of 154.1-158.6 ppm, indicating complexation through azomethine nitrogen (Oztas *et al.*, 2009). The signal which appears in the 163.0-165.6 ppm region for the carbon atom adjacent to the phenolic oxygen in the spectra of free ligands, is observed in the complexes 151.5-164.5 ppm, confirming the coordination of the ligand through phenolic oxygen to the organotin(IV) moiety (Basu *et al.*, 2010). In addition, the ^{13}C NMR chemical shift for the complexes displayed a slight chemical shift between 100-145 ppm for all the aryl carbon as compared to the free ligand. This is due to the electron density transfer from the ligand to the acceptor. The aryl carbons of the ligands and complexes were found in the expected range and were similar to the reported literature values (Gyanakumari *et al.*, 2010; Oztas *et al.*, 2009). In the ^{13}C NMR spectrum of complexes, a new peak around 8.6-9.1 ppm was observed which attributed to the carbon of Sn-CH₂ and this data confirmed the bonding interaction between the organotin compounds and the ligands (Lee *et al.*, 2015).

Table 4.10 : ^{13}C NMR chemical shifts for ligands L1 to L3.

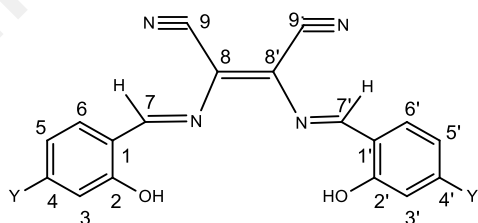
Ligand	Assignments δ ^{13}C NMR (ppm)			
	$\text{C}_{(\text{aromatic})}$	C-7, C-7'	C-8, C-8'	C-9, C-9'
L1 (CDCl_3)	120.1, 164.4, 119.1, 135.1, 110.2, 133.5	160.2	56.9	31.6
L2 (CDCl_3)	123.2, 164.4, 119.4, 132.2, 118.6, 130.4	159.7	56.9	31.5
L3 (CDCl_3)	118.8, 165.6, 117.1, 131.4, 118.8, 132.4	161.2	56.9	31.8



L1 : X = Br
L2 : X = Cl
L3 : X = H

Table 4.11 : ^{13}C NMR chemical shifts for ligands L4 & L5.

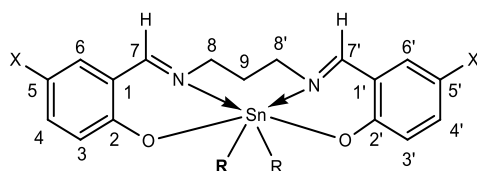
Ligand	Assignments δ ^{13}C NMR (ppm)			
	$\text{C}_{(\text{aromatic})}$	C-7, C-7'	C-8, C-8'	C-9, C-9'
L4 (DMSO)	126.5, 163.0, 121.6, 133.8, 120.1, 131.1	165.7	129.5	114.5
L5 (DMSO)	113.6, 163.8, 102.7, 163.1, 109.2, 134.0	165.7	124.8	114.7



L4 : X = H
L5 : X = OH

Table 4.12 : ^{13}C NMR chemical shifts for complexes C1 to C4.

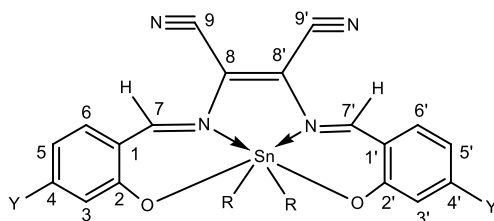
Complex	Assignments δ ^{13}C NMR (ppm)					
	$\text{C}_{(\text{aromatic})}$	$\text{Sn}-\underline{\text{C}}\text{H}_2$	C-7, C7'	C-8, C-8'	C-9, C-9'	R
C1 (DMSO)	124.4, 160.3, 120.4, 133.9, 119.7, 131.2	9.1	154.1	55.2	31.5	109.3, 120.6, 135.5, 109.6, 139.1, 111.3
C2 (DMSO)	128.9, 160.8, 120.5, 133.9, 119.8, 131.3	9.0	154.1	55.2	31.4	109.3, 119.8, 135.5, 109.6, 139.1, 111.2
C3 (DMSO)	128.9, 161.3, 120.5, 133.9, 119.8, 131.3	9.0	154.1	55.9	31.4	109.3, 119.8, 135.5, 109.6, 139.1, 111.2
C4 (CDCl_3)	130.5, 164.5, 118.7, 132.6, 119.4, 132.3	8.6	164.4	56.9	31.6	123.3, 119.4, 137.0, 119.5, 137.0, 118.7



C1: R = *p*-bromobenzyl (*p*-BrBz), X = Br
C2: R = *p*-fluorobenzyl (*p*-FBz), X = F
C3: R = *p*-chlorobenzyl (*p*-ClBz), X = Cl
C4: R = benzyl (Bz), X = H

Table 4.13 : ^{13}C NMR chemical shifts for complexes C5 to C10.

Complex	Assignments δ ^{13}C NMR (ppm)					
	$\text{C}_{(\text{aromatic})}$	$\text{Sn}-\underline{\text{C}}\text{H}_2$	C-7, C-7'	C-8, C-8'	C-9, C-9'	R
C5 (DMSO)	126.5, 153.7, 121.7, 133.7, 120.0, 131.3	9.0	158.6	129.8	116.9	129.0, 125.6, 122.7, 136.9, 138.1, 117.7
C6 (DMSO)	128.9, 160.8, 120.5, 133.9, 119.8, 131.3	9.0	158.6	129.4	114.4	128.8, 128.9, 129.9, 136.9, 139.0, 115.0
C7 (DMSO)	126.4, 153.8, 121.5, 133.9, 120.1, 130.6	9.0	158.6	129.5	114.5	129.1, 126.4, 122.5, 137.1, 142.5, 116.9, 46.3
C8 (DMSO)	114.8, 160.8, 102.9, 163.1, 104.6, 135.2	9.1	154.2	124.8	114.2	127.9, 125.6, 131.3, 132.3, 142.5, 115.7
C9 (DMSO)	113.7, 151.5, 102.9, 160.8, 109.2, 124.8	9.1	154.1	127.8	114.2	129.9, 129.3, 131.0, 131.6, 136.6, 114.8
C10 (DMSO)	115.6, 151.5, 102.7, 163.7, 109.2, 131.9	9.0	154.1	128.9	114.1	130.7, 130.8, 129.0, 129.6, 133.7, 115.4



C5: R = *p*-bromobenzyl (*p*-BrBz), Y = H
C6: R = *p*-fluorobenzyl (*p*-FBz), Y = H
C7: R = *p*-methylbenzyl (*p*-CH₃Bz), Y = H
C8: R = *p*-bromobenzyl (*p*-BrBz), Y = OH
C9: R = *p*-chlorobenzyl (*p*-ClBz), Y = OH
C10: R = *p*-fluorobenzyl (*p*-FBz), Y = OH

4.5 Carbon, Hydrogen and Nitrogen (CHN) Elemental Analysis

The CHN spectra of ligands and complexes can be found in section appendix at page 141. The percentage composition of C, H and N of two new diorganotin(IV) complexes; 2,3-bis((*N*)-(2,4-dihydroxybenzylidene)amino)maleonitrile di(*p*-chlorobenzyl)tin (C9) and 2,3-bis((*N*)-(2,4-dihydroxybenzylidene)amino)maleonitrile di(*p*-fluorobenzyl)tin (C10) were analyzed. Both complexes displayed not more than 0.4% differences of experimental value from theoretical value based on predicted formula. The experimental data found in both complexes stated in **Table 4.14** were in fair agreement with theoretical value. This showed that both complexes were successfully synthesized and pure complexes were obtained (Chow & Lo, 2014).

Table 4.14 : CHN elemental analysis of complexes C9 & C10.

Complex	Empirical formula	Molecular weight (g/mol)	Elemental analysis ^a (%)		
			C	H	N
C9	C ₃₂ H ₂₂ Cl ₂ N ₄ O ₄	716.0	53.59 (53.67)	3.39 (3.10)	7.66 (7.82)
C10	C ₃₂ H ₂₂ F ₂ N ₄ O ₄	683.0	56.17 (56.25)	3.64 (3.25)	8.38 (8.20)

^aactual (calculated)

Due to financial problems, only two complexes can proceed for CHN analysis based on assumption that all ligands and complexes were purified in similar way therefore impurities are eliminated from the end products. Besides that, only one of the two was selected for encapsulation and drug release study.

4.6 Electronic Spectra

The electronic spectra data for the Schiff base ligands and diorganotin(IV) complexes in methanol (MeOH) or dimethylsulfoxide (DMSO) at room temperature and were recorded in the 250-600 nm regions. All the data are presented in **Table 4.15** and **Table 4.16** and the UV-vis absorption spectra of ligands and complexes were shown in

section Appendix at page 136-140. The absorption bands of the Schiff base ligands could be classified into two absorption regions of 207-281 nm and 317-394 nm. There was a slight shift in the spectra of the absorption bands upon complexation; between 215-286 nm and 326-491 nm.

The band between 200-290 nm was assigned as $\pi \rightarrow \pi^*$ electronic transition which occurred in free Schiff bases ligands and the organotin complexes. This $\pi \rightarrow \pi^*$ electronic transition involved the molecular orbitals of the aromatic rings (Ebrahimipour *et al.*, 2015). The presence of peak between 317-394 nm could be attributed to the $n \rightarrow \pi^*$ transitions of the azomethine groups (Mahmoud *et al.*, 2016). From the literature survey, the spectra of the tin complexes were dominated by intense intraligand and charge transfer bands which showed that the tin was capable of forming $d\pi-p\pi$ bonds with ligands containing nitrogen as the donor atom (Ahmad *et al.*, 2002). The tin atom has its 5d orbital completely vacant and hence $Sn \leftarrow N$ bonding can take place by the acceptance of the lone pair of electrons from the azomethine nitrogen of the ligands (Bhanuka & Singh, 2017).

A new band was observed at the 406-486 nm regions in the electronic spectra of complexes and assigned as ligand to metal charge transfer (LMCT). These findings clearly showed the coordination between tin(IV) ion and the ligands (Maurya *et al.*, 1997). Affan and his co-workers made similar observations in the case of organotin(IV) complexes of 2-hydroxyacetophenone-*N*(4)-cyclohexylthiosemicarbazone which showed the new shift of λ_{\max} from the ligand to the complexes at 404–416 nm (Affan *et al.*, 2012).

Table 4.15 : Electronic spectra data of ligands L1 to L5.

Ligand	UV Absorption Spectra λ_{\max} (nm)	
	$n \rightarrow \pi^*$	$\pi \rightarrow \pi^*$
L1	332	210, 251
L2	332	219, 252
L3	317	207, 255
L4	387	263
L5	394	281

Table 4.16 : Electronic spectra data of complex C1 to C10.

Complex	UV Absorption Spectra λ_{\max} (nm)		
	$n \rightarrow \pi^*$	$\pi \rightarrow \pi^*$	LMCT
C1	329	215	411
C2	329	223	406
C3	336	286	413
C4	326	260	419
C5	379	264	483
C6	386	261	484
C7	385	263	484
C8	377	270	486
C9	379	271	486
C10	391	273	486

4.7 X-ray crystallography

Most of the crystals of the complexes were formed very fine needles and the solution for the recrystallization become sticky. Thus, the crystals were not suitable for X-ray crystallography study. A crystal from by-product of complex C10 was unintentionally produced when the complex C10 was left in NMR tube with DMSO as a solvent. It is believed that the by-product was bonded towards DMSO.

4.7.1 Synthesis and crystallization

An attempt was made to prepare complex C10 by condensation of tetradentate Schiff base ligand, 2,3-bis((*N*)-(2-hydroxybenzylidene)amino)maleonitrile with di(*p*-fluorobenzyl)tin dichloride. In **Fig. 4.5**, the compound was dissolved in DMSO-*d*₆ solution in a NMR tube for ¹H NMR spectroscopic characterization. Upon interaction with DMSO-*d*₆, in the context of NMR studies, colourless crystals of the trans-dichloridobis(dimethyl sulfoxide- κ O)bis(4-fluorobenzyl- κ C¹)tin(IV), (I) which was suitable for X-ray crystallographic study was obtained from the slow evaporation.

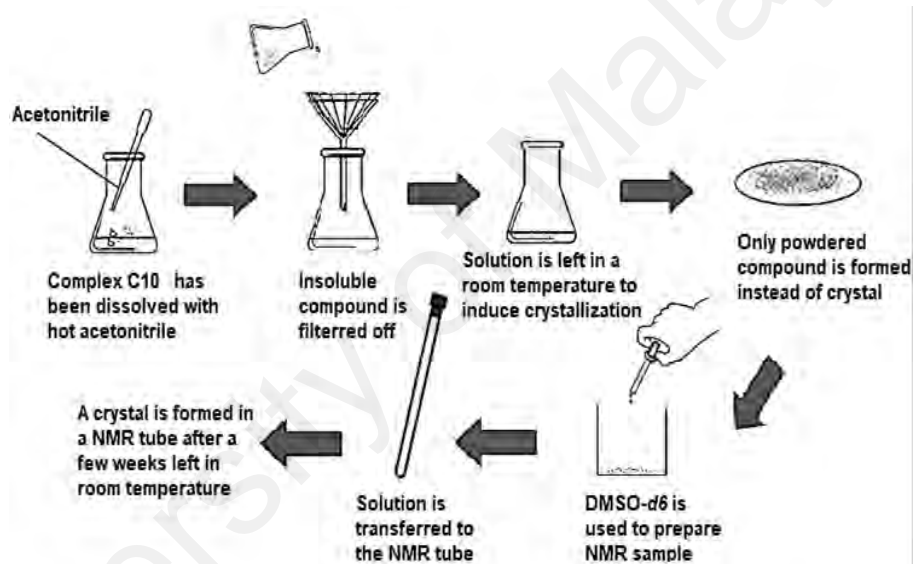


Figure 4.5 : Formation of crystal of by-product of complex C10 in NMR tube.
[Adapted and modified from <https://slideplayer.com/slide/11720866>]

4.7.2 Structural commentary

The molecular structure of (I) in **Fig. 4.6**, has the Sn^{IV} atom situated on a crystallographic centre of inversion. The Sn^{IV} atom is coordinated by monodentate ligands, i.e. chloride, sulfoxide-O and methylene-C atoms. From symmetry, each donor is trans to a like atom resulting in an all-trans-C₂Cl₂O₂ donor set about the Sn^{IV} atom.

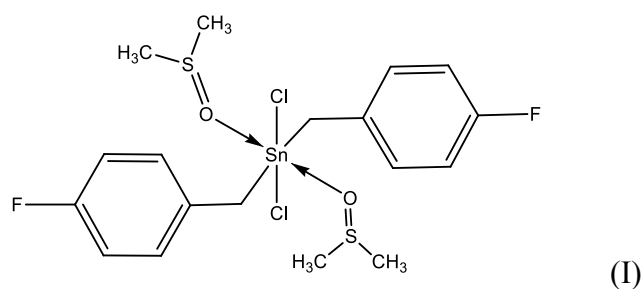


Figure 4.6 : Structure of trans-dichloridobis(dimethyl sulfoxide- κO)bis(4-fluorobenzyl- κC^1)tin(IV).

The donor set defines a distorted octahedral geometry owing, in part, to the disparate Sn-donor atom bond lengths, **Table 4.17**. The angles about the Sn^{IV} atom differ relatively little from the ideal octahedral angles with the maximum deviation of *ca* 6° noted for the C1–Sn–O1 angle, **Table 4.17**.

Table 4.17 : Selected geometric parameters (Å, °).

Atom	Length /Å
Sn–C1	2.1628
Sn–C11	2.5599
Sn–O1	2.2332
Atom	Angle/°
C1–Sn–O1	95.99
C1–Sn–Cl	89.95
C1–Sn–C11	90.05
O1–Sn–C11	90.44
C1–Sn–O1	84.01
O1–Sn–C11	89.56

From the **Fig. 4.7**, the molecular structure of (I), showing the atom-labelling scheme and displacement ellipsoids at the 70% probability level. The Sn^{IV} atom lies on a centre of inversion; unlabelled atoms are related by the symmetry operation $1 - x, 1 - y, 1 - z$.

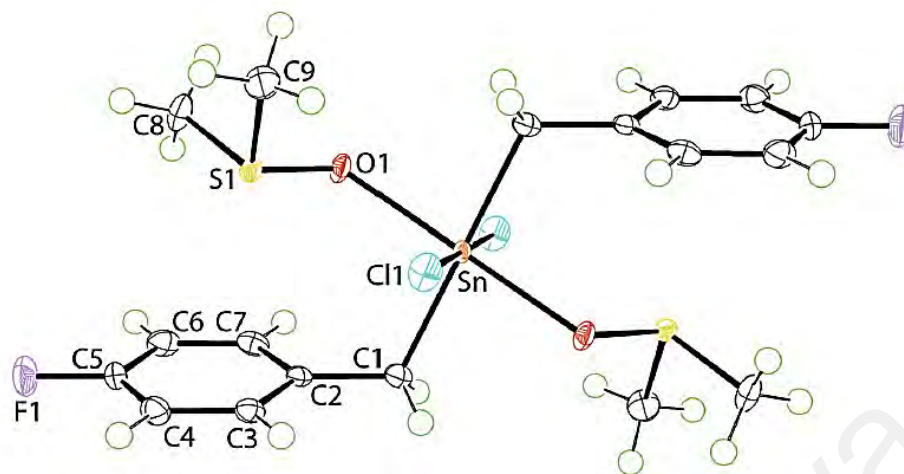


Figure 4.7 : The molecular structure of coordination *trans-dichloridobis(dimethyl sulfoxide- κO)bis(4-fluorobenzyl- κC^1)tin(IV)*.

The crystal data, data collection and structure refinement details of *trans-dichloridobis(dimethyl sulfoxide- κO)bis(4-fluorobenzyl- κC^1)tin(IV)* are presented in **Table 4.18**. Carbon-bound H-atoms were placed in calculated positions (C–H = 0.95–0.99 Å) and were included in the refinement in the riding model approximation, with $U_{\text{iso}}(\text{H})$ set to 1.2–1.5 $U_{\text{eq}}(\text{C})$.

Table 4.18 : Crystallographic and refinement details for trans-dichlorido-bis(dimethyl sulfoxide- κO)bis(4-fluorobenzyl- κC^1)tin(IV)^a.

Empirical formula	[Sn(C ₇ H ₆ F) ₂ Cl ₂ (C ₂ H ₆ OS) ₂]
Formula weight	564.08
Temperature/K	100
Crystal system	Monoclinic
Space group	<i>P</i> 2 ₁ / <i>c</i>
<i>a</i> /Å	8.2363 (1)
<i>b</i> /Å	12.7020 (2)
<i>c</i> /Å	11.4038 (1)
β / °	110.391 (2)
Volume / Å ³	1118.28 (3)
<i>Z</i>	2
Radiation type	Cu <i>K</i> α
Calculated density, <i>D</i> _x (Mgm ⁻³)	1.675
<i>F</i> (000)	564
Absorption coefficient, μ / mm ⁻¹	13.28
Crystal size (mm)	0.24 × 0.12 × 0.10
Reflections collected / unique	2292 / 2228(<i>R</i> _{int} = 0.020)
Refinement method	Full-matrix least-squares on <i>F</i> ²
<i>R</i> [<i>F</i> ² > 2 σ (<i>F</i> ²)], <i>wR</i> (<i>F</i> ²), <i>S</i>	0.018, 0.046, 1.08
Data / restraints / parameters	3865 / 0 / 192
Largest diff. peak and hole (eÅ ⁻³)	0.35 and -0.76

^aComputer programs: CrysAlis PRO (Rigaku Oxford Diffraction, 2015), SHELXS(Sheldrick, 2008), SHELXL2014 (Sheldrick, 2015), and ORTEP-3 for Windows (Farrugia, 2012).

4.7.3 Database survey

From the literature survey, there are three related structures of the general formula R₂SnX₂(DMSO)₂ in the crystallographic literature (Groom et al., 2016). Key bond angles for these are listed in **Table 4.19**. The Me₂SnBr₂(DMSO)₂ compound (Aslanov *et al.*, 1978) is analogous to (I) in that the Sn^{IV} atom is located on a centre of inversion and hence, is an all-*trans* isomer. The two remaining structures have a different arrangements of donor atoms with the common feature being the *trans*-disposition of

the Sn bound organic groups, with the halides and DMSO-O atoms being mutually *cis*, i.e. R=Me and X = Cl (Aslanov *et al.*, 1978; Isaacs & Kennard, 1970) and R = Ph and X = Cl (Sadiq ur *et al.*, 2007).

Table 4.19 : Selected geometric parameters (Å, °) for molecules of the general formula R₂SnX₂(DMSO)₂.

Compound	X-Sn-X	O-Sn-O	C-Sn-C	Reference
Me ₂ SnBr ₂ (DMSO) ₂	180	180	180	(Aslanov <i>et al.</i> , 1978)
Me ₂ SnCl ₂ (DMSO) ₂	95.2	83.7	172.7	(Aslanov <i>et al.</i> , 1978)
Ph ₂ SnCl ₂ (DMSO) ₂	97.43	79.34	172.17	(Sadiq ur <i>et al.</i> , 2007)
(4-FC ₆ H ₄ CH ₂) ₂ SnCl ₂ (DMSO) ₂	180	180	180	This research work

4.8 Cytotoxic Activity

The *in vitro* cytotoxic activity of the Schiff base ligand and its diorganotin(IV) complexes had been evaluated against three human carcinoma cell lines, namely breast (MCF-7), lung (A549) and prostate (PC-3). Only one ligand and selected diorganotin(IV) complexes have been analysed for their anticancer screening.

In the anticancer screening, the Schiff base ligand and their diorganotin(IV) complexes were dissolved in DMSO. The amount of DMSO used did not reveal any cytotoxic activity. MTT assay was used to assess cytotoxicity and cell viability (Alizadeh *et al.*, 2015). *Cis*-platin was used as positive control and the well containing untreated cells was used as the negative control. The cytotoxicity of each sample was expressed as IC₅₀ value which referred to the concentration of test compounds that caused 50% inhibition or cell death as averaged from the three experiments. It was obtained by plotting the graph of percentage inhibition (%) versus the concentration of test compounds in the unit of µg/mL. The IC₅₀ values of the Schiff base ligand, the

diorganotin complexes and reference drugs such as *cis*-platin and paclitaxel are listed in **Table 4.20**. The bar chart showing the comparison of the IC₅₀ value of ligand, L5, with C8, C9 and C10 complexes are displayed in **Fig. 4.8**.

In the present study, *cis*-platin was found to exhibit remarkable growth inhibitory activities with IC₅₀ values ranging from 2.64-16.87 µg/mL. The values are in the acceptable range based on the literature. The IC₅₀ of the *cis*-platin against A549, PC-3 and MCF-7 according to literature are 3.93 µg/mL, 18.30 µg/mL and 8.41 µg/mL respectively (Gumulec *et al.*, 2014; Ma *et al.*, 2016; Mroueh *et al.*, 2015). Every cancer cell line displays different resistance to different diorganotin(IV) complexes.

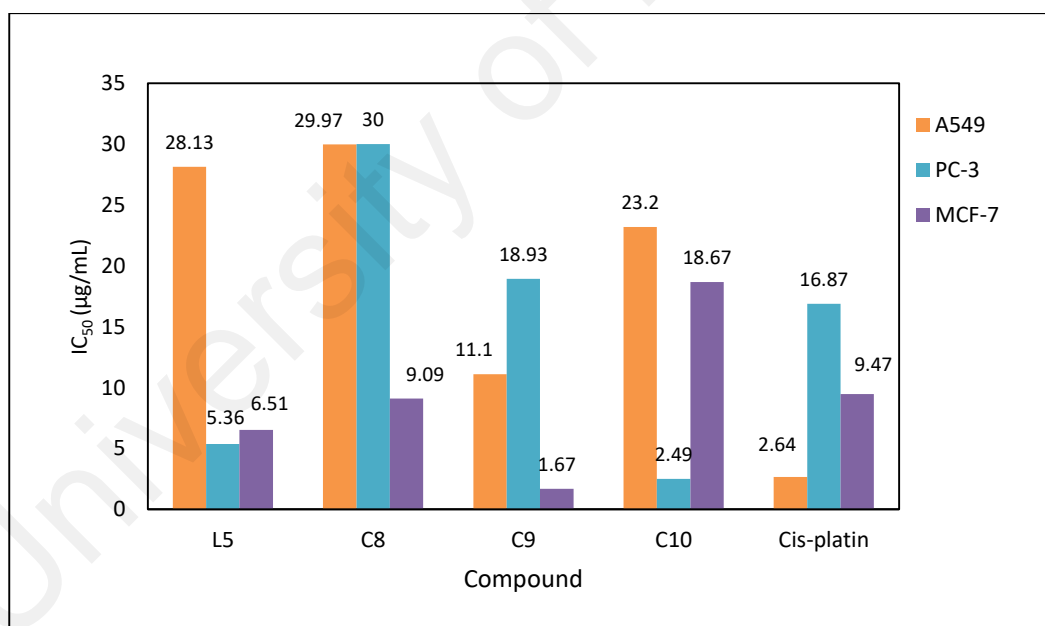


Figure 4.8 : Bar chart showing the comparison of the IC₅₀ value of L5 and its diorganotin(IV) complexes.

The results of *in vitro* cytotoxic effects of complexes C8, C9 and C10 showed that some of these complexes are more potent than *cis*-platin. For example, di-*p*-chlorobenzyltin(IV) complex, C9 showed the most cytotoxicity against MCF-7 as

compared to *cis*-platin. Previous research done by Fani *et al.* showed that monobenzyltin Schiff base complex (IC₅₀ value 2.50 µg/mL) exhibited active in MCF-7, but less active than complex C9 (IC₅₀ value 1.67 µg/mL) (Fani *et al.*, 2015). Also, the results revealed that different complexes showed selective activeness to one cell line but may not be active to another. For example, di-*p*-fluorobenzyltin(IV) complex, C10 demonstrates significant activity for cancer cells PC-3, while exhibiting less activity for cancer cell MCF-7 and A549. However, di-*p*-bromobenzyltin(IV) complex, C8 showed a moderate anticancer activity towards A549 and PC-3 and was only slightly active towards MCF-7.

On the other hand, the ligand itself, L5 showed remarkable cytotoxicity against PC-3 and MCF-7 as compared to other complexes. For A549, all the ligand and complexes exhibit less potent against other reference drugs. The IC₅₀ value of reference drug, for PC-3 showed larger difference about ±14 as compared to complex C10. Hence, this data displayed that complex C10 is the most cytotoxicity against PC-3. This result also showed that the cytotoxicity of ligand was reduced when it coordinated with tin metal. In addition, the substituent groups that attached to the tin metal influenced the cytotoxicity values. As an example, substituent group for C9 which is *p*-chlorobenzyl only exhibited prominent *in vitro* anticancer activity toward MCF-7 but not A549 and PC-3. While for substituent group for C10 which is *p*-fluorobenzyl showed lowest IC₅₀ value for PC-3.

Table 4.20 : Anticancer result of L5 and its complexes.

Compounds	Molecular weight (g/mol)	Cytotoxicity (IC ₅₀ in µg/mL)		
		A549	PC-3	MCF-7
L5	328.0	28.13 ± 0.35	5.36 ± 0.14	6.51 ± 0.22
C8	782.5	29.97 ± 0.06	>30	9.09 ± 0.46
C9	716.0	11.10 ± 0.66	18.93 ± 0.90	1.67 ± 0.06
C10	683.0	23.20 ± 1.11	2.49 ± 0.04	18.67 ± 0.12
<i>Cis-platin</i>	300.0	2.64 ± 0.05	16.87 ± 0.31	9.47 ± 0.27

Based on the data analysis from cytotoxicity activity, further works are needed to enhance this aspect of studies and discover the anticancer mechanism of organotin(IV) complexes. The biological effects of a new chemical compound can often be predicted from its molecular structure using data about other similar compounds. This is because similar compounds may have similar physical and biological properties. There is a relationship between structure and activity, and this principle is referred to as Structure Activity Relationship (SAR) (Hong *et al.*, 2014). The result of SAR studies could be explained the details on why the observations were attained from the cytotoxicity activity. Furthermore, SAR study also can offer information on description of the main molecular features necessary for biological activity and the intermolecular interactions that are actually recognized at the binding site. The cytotoxicity of the complexes also may be connected to the interaction with DNA (Hong *et al.*, 2016). This is because DNA is viewed as one of the most significant targets for antitumoral due to its central role on replication and transcription. Many types of interactions between complexes and DNA are testified, such as major groove binding, intercalation between base-pairs and electrostatic surface binding reactions (Shah *et al.*, 2013; Sirajuddin *et al.*, 2012).

4.9 Encapsulation Studies of Selected Complex

From the anticancer screening result, several organotin(IV) complexes active towards MCF-7 in comparison to A549 and PC-3. Hence, for this research, we prepared a formulation that is suitable for breast cancer treatment. The selected complex which is the one exhibited the best therapeutic activity is further studied for its encapsulation and drug release study. Based on the anticancer screening result, 2,3-bis((N)-(2,4-dihydroxybenzylidene)amino)maleonitrile di(*p*-chlorobenzyl)tin (C9) was selected for drug formulation studies. The properties of the formulation such as the size distribution, zeta potential and encapsulation efficiency are presented and discussed in the next sub-chapter 4.9.1 and 4.9.2 respectively. While the morphology analysis and *in vitro* cytotoxicity study for the formulated drug is described in part 4.9.3 and 4.9.4 respectively.

4.9.1 Particles Size Distribution and Zeta Potential

The summary of the particle size, polydispersity index (PDI) and zeta potential of the complex incorporated in carriers is displayed in **Table 4.21** and the shape of the particle size distribution is shown in **Fig. 4.9**.

Table 4.21 : Particle size distribution, polydispersity index (PDI) and zeta potential of complex C9.

Sample formulation	Size (nm)	Intensity	Polydispersity index (PDI)	Zeta potential (mV)
2,3-bis((N)-(2,4-dihydroxybenzylidene)amino)maleonitrile di(<i>p</i> -chlorobenzyl)tin , C9	128 ± 22	100	0.5 ± 0.1	-16 ± 1

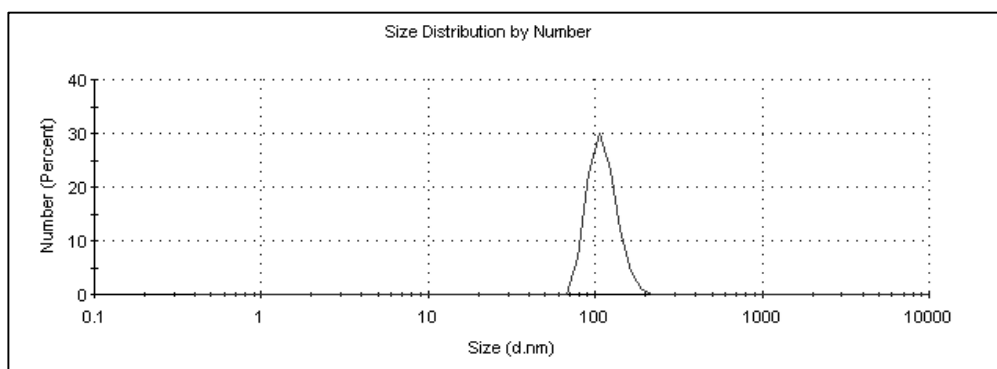


Figure 4.9 : The particle size distribution of the complex C9.

As reported in **Table 4.21**, the particle size distribution of complex C9 incorporated in carriers is 128 ± 22 nm with 100% intensity. It is evident that the size of the prepared hydrophobic drug loaded mixed vesicles are relatively in acceptable range. Based on the evaluation of the reviewed literatures, the particle size for the formulation of hydrophobic drugs such as paclitaxel (PTX) and doxorubicin (DOX) loaded in drug carrier are below 150 nm (Mo *et al.*, 2016). For example, Yoshizawa and his co-workers reported that the size of liposomes enveloped with paclitaxel and polyethylene glycol (PEG) was 105 nm (Yoshizawa *et al.*, 2011). On top of that, Danafar revealed that the average size for the formulation of DOX incorporated in methoxy poly(ethylene glycol)-poly caprolactone (mPEG-PCL) micelle was 134 nm (Danafar *et al.*, 2017). Previous findings have proved that nanoparticles with the size of 100-200 nm would display promising *in vivo* behaviour for the effective enhanced permeability and retention (EPR) effect-based tumour disposition (Gabizon & Papahadjopoulos, 1992; Ishida *et al.*, 1999). Dhand *et al.* reported in her article that the size of drug carrier of 100-200 nm have a better chance to be in the circulatory system for a more extended time (Dhand *et al.*, 2014). Anticancer drugs that are converted into nanoscale size propose some exclusive characters which can lead to upgrade drug efficiency, diminish

the reticuloendothelial system (RES) uptake, sustained drug circulation time in vivo and upgraded drug localization (Litzinger *et al.*, 1994). In order to prevent any occurrences of embolism and immune reactions, the anticancer drugs must be small enough to circulate in human vascular systems. By considering the size of the human blood vessels, blood capillaries which are roughly 5 μm in diameter, anticancer drugs need to be formulated in nanosizes. Blood capillaries may experience severe blockage if the particle size is larger than 5 μm (Müller *et al.*, 2001). Hence, the size of all injectable nanoparticle that are administered intravenously should be less than 5 μm . Furthermore, the phagocytic cells are able to recognise nanoparticles which are greater than 200 nm in size, hence, an immune response and drug bioavailability efficacy will be disrupted (Moghimi *et al.*, 2001). By enhancing permeability and retention effect, nanoparticles with a size less than 200 nm can passively accumulated within tumours. Based on the result obtained, the hydrophobic drug loaded in mixed vesicles (128 nm) formulated in this study would be acceptable.

The information on the polydispersity index (PDI) can be used to predict the stability and tell about the uniformity of the particles (Masarudin *et al.*, 2015). The PDI value reveals the nanoparticle size distribution is within the range of 0.4-0.6, indicating the presence of large size distributions (Tavano *et al.*, 2014). Based on the above reported result, the PDI value was 0.5 ± 0.1 which showed lower particle stability and the existence of aggregated nanoparticles. There are way to maintain a low polydispersity index and avoiding aggregation to occur, such as the preparation methods, the type and concentration of surfactant are examples of the criteria that can be considered (Sharma *et al.*, 2016).

The magnitude of zeta potential offers a suggestion of the colloid system stability. The measurements of the zeta potential are normally used to evaluate the stability of the

colloidal system (Šegota *et al.*, 2006). If the aggregates in a suspension have high positive or negative zeta potentials, they tend to repel each other. However, if the aggregates have low zeta potential, they are ready to flocculate or aggregate. Thus, zeta potential is thought to be a good indicator of the interaction between colloidal aggregates. Nahidah and her co-workers have reported that the higher the surface charge of DTX-CaCO₃NP, the stronger the repellent forces between the particles (Hammadi *et al.*, 2017). Hence, the particles are more stable and no aggregation was occurred.

From the result obtained, the measured zeta potential showed a low negative value which is -16 ± 1 mV. This result indicates that the suspension is unstable in colloidal state. Jiang and her co-workers state that the dividing line between stable and unstable aggregates is usually taken as either +30 mV or -30 mV. That is, aggregates with zeta potential values above ± 30 mV are considered to be stable for colloidal dispersion as the surface charge prevents aggregation of the particles (Jiang *et al.*, 2012). From the literature survey, the nanoparticles should not be kept in a form of liquid suspension and they would be better preserved in a lyophilized form (Abdelwahed *et al.*, 2006). They also need to be reconstituted directly before use. The report also proposed that formulation in colloidal state creates more challenge in stability as compared to dry stage. Hence, a freeze-drying process can be suggested as an alternative to improve the chemical and physical instability of nanoparticles in aqueous medium (Alihosseini *et al.*, 2015). This process is extensively applied for enhancing the stability of colloidal nanoparticles and drying purposes. Soares *et al.* reported that after undergoing freeze-drying process, the negative zeta potentials improved, indicating the nanoparticles have better stabilization and the solid lipid nanoparticles are able to maintain the insulin structure for about six months of storage (Soares *et al.*, 2013).

Despite freeze-drying process is capable in improving the long-term stability of colloidal nanoparticles, this process very slow process depending upon the samples and freeze-drying conditions (Feng *et al.*, 2018). Additionally, freeze-drying of nanoparticles is a very complicated process that involves a major study of formulation and process conditions. Many parameters of the formulation may contribute the success of freeze-drying as the nanoparticles composition (type and concentration of surfactant, type of polymer, type and concentration of cryoprotectants and lyoprotectants, interaction between cryoprotectants and nanoparticles, surface modification of nanoparticles) (Abdelwahed *et al.*, 2006).

4.9.2 Drug Encapsulation Efficiency and Drug Loading

Drug encapsulation efficiency and drug loading are vital parameters to evaluate the properties of any drug formulation. An excellent nanocarrier should have high drug load and encapsulation efficiency.

Table 4.22 : Encapsulation efficiency and drug loading of complex C9.

Percentage Encapsulation Efficiency (%EE)	Percentage Drug Loading (%DL)
>90	90

From the analysis of the data reported in **Table 4.22**, it showed that the prepared vesicles are able to encapsulate more than 90% of the C9 with a drug loading over 90%. Only C9 was tested for the drug formulation study. However, we are expecting that the encapsulation of the other complexes will be similar based on the size of the complexes are not vary from one to the other. The encapsulation process gives an impact on the percentage of drug encapsulation and drug loading. In producing the thin films, larger surface areas are convenient because they accelerate the hydration process of the bilayer

(Kulkarni *et al.*, 1995). Amselem *et al.* examined the encapsulation of doxorubicin in liposomes which applied five different hydration protocols (Amselem *et al.*, 1990). As reported in the literature, the highest percentage of encapsulation and drug loading was attained when a large surface area of thin film was produced. Beside the method used for the encapsulation, the high %EE obtained in this research can also be contributed by the concentration of drug used which is 5mM which is considered appropriate. In addition to that, the %EE of hydrophobic drugs normally higher compared to hydrophilic drugs. Previous study has demonstrated that percentage of encapsulation of drug was found to rise from 80% up to 96% with increasing concentration of docetaxel (Hammadi *et al.*, 2017). Apart from that, Liu *et al.* have found that formulation of paclitaxel with different concentration of 1,2-dilauroylphosphatidylcholine (DLPC) used in the nano-emulsification process has affect %EE from 15% (0.01%, w/v) up to 56% (0.04%, w/v) (Liu *et al.*, 2010).

There are other factors that can enhance encapsulation and drug loading efficiency. One of them is surface charge of nanoparticle on drug loading efficiency. The nanoparticle surface charge is vital for charge-bearing molecules. It has been reported that encapsulation of hydroxocobalamin and doxorubicin was greater with negative charge rather than the neutral charge (Gad, 2008). Moreover, the technique of enlarging the surface area of thin film plays a role to enhance encapsulation and drug loading. Surface area of the thin film can be increased by adding solid contact masses such as glass beads. This has been proven by Mezei and Nugent who had achieved 8-10 times greater encapsulation of hydrophobic drugs when they added glass beads (Mezei & Nugent, 1984). Similarly, Kulkarni and his co-workers obtained 14 times higher encapsulation of colchicine when they used 50 times larger flask and introduced glass beads (Kulkarni *et al.*, 1997). Another factor that can influence the encapsulation efficiency is type of solvent (Morilla *et al.*, 2002). A solvent used for solubilisation and

homogenous mixture is very important for hydrophobic drug, which is poorly water soluble. On one of the previous findings, the encapsulation efficiency of hydrophobic drug, griseofulvin in the nanoparticle increased over 90% when they used several types of solvent for solubilisation (Ong *et al.*, 2016).

4.9.3 Morphology Analysis

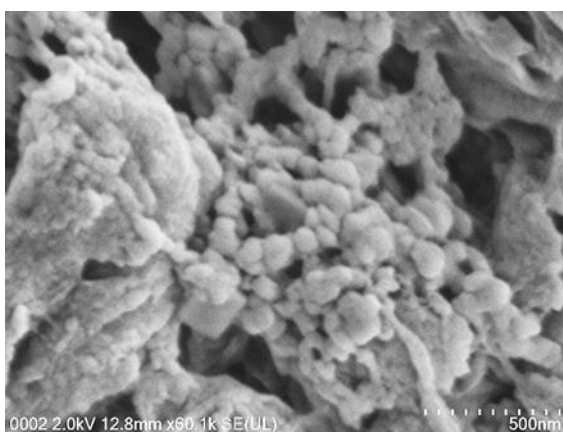


Figure 4.10 : FESEM image of formulation complex C9.

The morphology of formulated drug was examined by FESEM. From the FESEM image in **Fig. 4.10**, it was observed that the formulated drug of complex C9 exhibited a spherical shape. Moreover, most of the particles more exist in a smaller and uniform size. In the design of commercial nanoparticles, shape and surface are the two important elements for efficient drug delivery. From the reported literature, most of the nanoparticles for anticancer drug revealed a fine spherical shape and various degrees of smooth surface (Bandi *et al.*, 2017; Sahoo *et al.*, 2013). Literatures have revealed spherical nanoparticles are more favourable because of several factors including ease of production and controlling data on the effect of nanoparticle shape on bio circulation (Christian *et al.*, 2009; Mitragotri, 2009). As a conclusion, it is generally found that

nanoparticles that are spherical in shape tend to have a long circulation property because they are able to pass through into the cells compared to elongated cylindrical ones (Geng *et al.*, 2007).

4.9.4 *In vitro* Drug Release Study

The drug release profile is another significant goal for nanoparticle formulations. Formulation of released profile for C9 was illustrated in **Fig. 4.11**. The *in vitro* release study was operated in PBS pH 7.4 medium at 37 °C condition in order to mimic the physiological fluid of human body and the body temperature. This study was kinetically analysed according to the zero-order model.

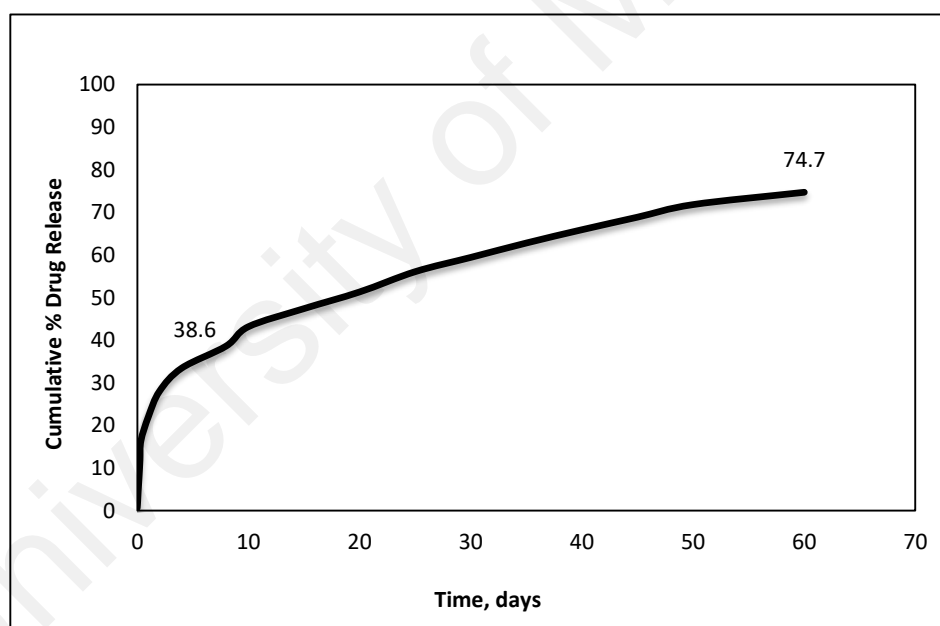


Figure 4.11 : *In vitro* drug release profile of complex C9 formulation in 60 days.

From the **Fig. 4.11**, the release of complex C9 from the nanoparticles displayed biphasic release pattern (Hasan *et al.*, 2013) which consisted an initial faster release phase, followed by a period of slow but continuous release for 10 days. The initial release was about 38.6% at the end of day 8th. Previous research showed that the

hydrophobic drug, PTX encapsulated in polymeric nanoparticles was released about 34.2% in 3 days (Abouelmagd *et al.*, 2015). The early rapid release of hydrophobic drug might be related to the factor of adsorption drug surface in the formulation which promote the spontaneous diffusion in the dissolution medium. It was predictable due to loosely bound on the surface, thus, producing a platform value called burst effect or initial rapid release (Allison, 2008; Magenheim *et al.*, 1993). Among drug-based nanoparticles formulations, burst release effect typically occur and it was widely stated in many reports (Danhier *et al.*, 2009; Xin *et al.*, 2010). In addition, research defined in the previous literature indicates that vesicles formulations containing hydrophobic drug exhibit similar release patterns (Xu *et al.*, 2007). This performance is common for the compounds that able to intermingle with the vesicular carrier bilayer. This capability improves the efficiency of drug loading and offers drug release profiles which results from permeation of drug through the bilayers and the drug maintained in the bilayers (Kulkarni *et al.*, 1995).

For another subsequent 50 days, the remained complex which was captured in the structure was further released in a controlled fashion. Results suggested that the application of vesicles with cationic and non-ionic surfactant prolonged and controlled the C9 release. This is a very important aspect since retarded release and prolonged drug retention are the most significant challenge of an effective drug delivery system (Muzzalupo *et al.*, 2017). The amounts of percentage cumulative drug release were found to be 74.7% for 60 days in phosphate buffered saline pH 7.4 as a medium. A recent studied by Martin *et al.* concluded that paclitaxel incorporated in poly-L-co-D,L-lactic acid (PLDLA) microspheres released 90% of the drug for 30 days period. Thus, the data obtained denote that PLDLA microspheres are promising carriers for paclitaxel (Martins *et al.*, 2014). To sum up, these findings agree with those earlier published in the literature for mixed vesicles that can control the release of drugs (Jiang *et al.*, 2012).

Besides, our reports denote that the sustained release of C9 revealed its potentiality as a drug delivery system that could lessen the contact of healthy tissues, while increasing the accumulation of therapeutic drug in cancer cell.

University of Malaya

CHAPTER 5: CONCLUSIONS

Five multidentate ligands and ten diorganotin(IV) complexes have been successfully prepared and characterized. Three prepared diorganotin(IV) complexes C8, C9 and C10 and one multidentate ligand, L5 were examined for anticancer properties. From the anticancer screening result, all tested ligand and diorganotin(IV) complexes did not show a competitive performance in human lung carcinoma cancer cell line (A549) compared to well-known anticancer drugs such as *cis*-platin and paclitaxel. But complex C10 showed good cytotoxic with reasonable and competitive activity against the tested cell lines for human prostate carcinoma cancer cell line (PC-3) compared to reference drugs *cis*-platin and paclitaxel. Whereas, C9 has shown better therapeutic activity compared to *cis*-platin and paclitaxel for human breast carcinoma cancer cell line (MCF-7). Among all of the complexes, C9 showed the lowest IC₅₀ value. Therefore, C9 complex was further studied for encapsulation and drug release application. From the studies, the particle size distribution of the complex incorporated in carriers was 128 ± 22 nm with 100% intensity and the zeta potential was -16 ± 1 mV. The morphology analysis also showed that the formulated drug exhibited in spherical shape. The percentage encapsulation efficiency and drug loading efficiency obtained were >90% and 90% respectively. Moreover, the amounts of percentage cumulative drug release were found to be 75% for 60 days in phosphate buffered saline pH 7.4 as a medium. The results for the formulation part are in agreement with the properties of common drug formulations. As a conclusion, the results of this research suggest that competitive drug for anticancer chemotherapy treatment can be prepared based on diorganotin(IV) complexes. For a future prospect, the prepared ligands and their corresponding diorganotin(IV) complexes can be evaluated for other biological activities such as antibacterial and antifungal properties. The other several organotin complexes also can be further screened against other types of cancer cell line. In addition, various types of

ligands can be prepared with a different substituent such as using different alkyl chain length to determine the effects on biological activity. For the encapsulation, different methods for the encapsulation or subsequent method after the process of thin film hydration can be applied such as extrusion method to reduce the size and the polydispersity index. Other than that, optimization can be done by as using different type of surfactants and applying various ratio of drug to surfactant to improve the formulation properties.

University of Malaya

REFERENCES

- Abdelwahed, W., Degobert, G., Stainmesse, S., and Fessi, H. (2006). Freeze-drying of nanoparticles: formulation, process and storage considerations. *Advanced Drug Delivery Reviews*, 58(15), 1688-1713.
- Abouelmagd, S. A., Sun, B., Chang, A. C., Ku, Y. J., and Yeo, Y. (2015). Release kinetics study of poorly water-soluble drugs from nanoparticles: are we doing it right? *Molecular Pharmaceutics*, 12(3), 997-1003.
- Affan, M. A., Salam, M. A., Ahmad, F. B., White, F., and Ali, H. M. (2012). Organotin(IV) complexes of 2-hydroxyacetophenone-*N*(4)-cyclohexylthiosemicarbazone (H₂dact): synthesis, spectral characterization, crystal structure and biological studies. *Inorganica Chimica Acta*, 387, 219-225.
- Agarwal, R. K., and Rawat, H. K. (1985). Infrared and thermal studies of tin(IV) halide complexes of substituted amino pyridine *N*-oxides. *Thermochimica Acta*, 90, 355-359.
- Ahmad, F., Parvez, M., Ali, S., Mazhar, M., and Munir, A. (2002). Synthesis And Spectral Studies Of Tri- And Diorganotin(IV) Complexes with 5-Benzoyl-A-Methyl-2-Thiopheneacetic Acid: Crystal Structure Of [(CH₃)₃Sn(C₁₄H₁₁O₃S)]. *Synthesis and Reactivity in Inorganic and Metal-Organic Chemistry*, 32(4), 665-687.
- Ahmed, E. M. (2015). Hydrogel: preparation, characterization, and applications: a review. *Journal of Advanced Research*, 6(2), 105-121.
- Ajloo, D., Shabanpanah, S., Shafaatian, B., Ghadamgahi, M., Alipour, Y., Lashgarbolouki, T., and Saboury, A. A. (2015). Interaction of three new tetradentates Schiff bases containing N₂O₂ donor atoms with calf thymus DNA. *International Journal of Biological Macromolecules*, 77, 193-202.
- Akbarzadeh, A., Rezaei-Sadabady, R., Davaran, S., Joo, S. W., Zarghami, N., Hanifehpour, Y., Samiei, M., Kouhi, M., and Nejati-Koshki, K. (2013). Liposome: classification, preparation, and applications. *Nanoscale Research Letters*, 8(1), 102.
- Ali, I., A. Wani, W., Saleem, K., and Wesselinova, D. (2012). Syntheses, DNA binding and anticancer profiles of L-glutamic acid ligand and its copper(II) and ruthenium(III) complexes. *Medicinal Chemistry*, 9(1), 11-21.
- Ali, M. A., Mirza, A. H., Hamid, M. H. S. A., Bernhardt, P. V., Atchade, O., Song, X., Eng, G., and May, L. (2008). Synthesis, spectroscopic and structural characterization of diphenyltin(IV) complexes of acetone Schiff bases of S-alkyldithiocarbazates. *Polyhedron*, 27(3), 977-984.
- Alihosseini, F., Ghaffari, S., Dabirsiaghi, A. R., and Haghghat, S. (2015). Freeze-drying of ampicillin solid lipid nanoparticles using mannitol as cryoprotectant. *Brazilian Journal of Pharmaceutical Sciences*, 51, 797-802.

- Alizadeh, R., Yousuf, I., Afzal, M., Srivastav, S., Srikrishna, S., and Arjmand, F. (2015). Enantiomeric fluoro-substituted benzothiazole Schiff base-valine Cu(II)/Zn(II) complexes as chemotherapeutic agents: DNA binding profile, cleavage activity, MTT assay and cell imaging studies. *Journal of Photochemistry Photobiology*, 143, 61-73.
- Allison, S. D. (2008). Analysis of initial burst in PLGA microparticles. *Expert Opinion Drug Delivery*, 5(6), 615-628.
- Amini, M. M., Najafi, E., Karami, B., and Khavasi, H. (2016). Synthesis and characterization of a new organotin(IV) complex as a new precursor for preparation SnO₂ nanoparticles. *Inorganic Nano-Metal Chemistry*, 47(3), 332-339.
- Amselem, S., Barenholz, Y., and Gabizon, A. (1990). Optimization and upscaling of doxorubicin-containing liposomes for clinical use. *Journal of Pharmaceutical Sciences*, 79(12), 1045-1052.
- Ananda, K. S., Yiheyis, B. Z., and Nithyakalyani, D. (2014). Synthesis, structural characterization, corrosion inhibition and *in vitro* antimicrobial studies of 2-(5-methoxy-2-hydroxybenzylideneamino) phenol Schiff base ligand and its transition metal complexes. *International Journal of ChemTech Research*, 6(11), 4569-4578.
- Araujo, L. S., Vinicius Melo Novais, M., Salviano Teixeira, C., Honorato-Sampaio, K., Tadeu Pereira, M., Ferreira, L. A., Braga, F. C., and Cristina Oliveira, M. (2013). Preparation, physicochemical characterization, and cell viability evaluation of long-circulating and pH-sensitive liposomes containing ursolic acid. *BioMed Research International*, 2013, 7(1), 46-49.
- Argyriou, A. A., Polychronopoulos, P., Iconomou, G., Chroni, E., and Kalofonos, H. P. (2008). A review on oxaliplatin-induced peripheral nerve damage. *Cancer Treatment Reviews*, 34(4), 368-377.
- Aslanov, L. A., Ioniv, V. M., Attia, W. M., Permin, A. B., and Petrosyan, V. S. (1978). The mutual influence of ligands and the nature of chemical bonds in tin(IV) octahedral complexes. *Journal of Organometallic Chemistry*, 144(1), 39-48.
- Awotwe, D., Zidan, A. S., Rahman, Z., and Habib, M. J. (2012). Evaluation of anticancer drug-loaded nanoparticle characteristics by nondestructive methodologies. *AAPS PharmSciTech*, 13(2), 611-622.
- Balls, P. W. (1987). Tributyltin (TBT) in the waters of a Scottish sea loch arising from the use of antifoulant treated netting by salmon farms. *Aquaculture*, 65, 227-237.
- Bandi, U. M., Philip, K., Reddy, D. B., Swaroopa, A., Prabakaran, L., and Parthasarathy, G. (2017). Formulation and *in vitro* characterization of anticancer drug loaded solid lipid nanoparticles. *International Journal Of Pharmaceutical Sciences and Research*, 8(9), 3808-3812.

- Bangham, A. D., Standish, M. M., and Weissmann, G. (1965). The action of steroids and streptolysin S on the permeability of phospholipid structures to cations. *Journal of Molecular Biology*, 13(1), 253-228.
- Basu, S., Gupta, G., Das, B., and Rao, K. M. (2010). Neutral penta-coordinated diorganotin(IV) complexes derived from ortho-aminophenol Schiff bases: synthesis, characterization and molecular structures. *Journal of Organometallic Chemistry*, 695(18), 2098-2104.
- Batzri, S., and Korn, E. D. (1973). Single bilayer liposomes prepared without sonication. *Biochimica et Biophysica Acta (BBA) - Biomembranes*, 298(4), 1015-1019.
- Bera, A., Ojha, K., and Mandal, A. (2013). Synergistic effect of mixed surfactant systems on foam behavior and surface tension. *Journal of Surfactants and Detergents*, 16(4), 621-630.
- Bernabeu, E., Gonzalez, L., Cagel, M., Gergic, E. P., Moretton, M. A., and Chiappetta, D. A. (2016). Novel soluplus(R)-TPGS mixed micelles for encapsulation of paclitaxel with enhanced *in vitro* cytotoxicity on breast and ovarian cancer cell lines. *Colloids and Surfaces B: Biointerfaces*, 140, 403-411.
- Bhanuka, S., and Singh, H. L. (2017). Spectral, Dft and Antibacterial Studies of Tin(II) Complexes of Schiff Bases Derived from Aromatic Aldehyde and Amino Acids. *Rasayan Journal of Chemistry*, 10(2), 673-681.
- Blanzat, M., Perez, E., Rico-Lattes, I., Prome, D., Prome, J. C., and Lattes, A. (1999). New cationic glycolipids. 1. synthesis, characterization, and biological activity of double-chain and gemini cationic analogues of galactosylceramide (gal β 1cer). *Langmuir*, 15(19), 6163-6169.
- Broido, A. (1969). A simple, sensitive graphical method of treating thermogravimetric analysis data. *Journal of Polymer Science Part A-2: Polymer Physics*, 7(10), 1761-1773.
- Bukhari, I. H., Ahmad, I., Rehman, J., and Shahzadi, S. (2014). Synthesis, characterization and antimicrobial activities of di- and tri organotin(IV) Schiff base complexes. *International Journal of Pharmaceutical Research and Allied Sciences*, 3(4), 62-70.
- Burt, J., Levason, W., and Reid, G. (2014). Coordination chemistry of the main group elements with phosphine, arsine and stibine ligands. *Coordination Chemistry Reviews*, 260, 65-115.
- Butler, J. S., and Sadler, P. J. (2013). Targeted delivery of platinum-based anticancer complexes. *Current Opinion in Chemical Biology*, 17(2), 175-188.
- Cagnoli, M., Alama, A., Barbieri, F., Novelli, F., Bruzzo, C., and Sparatore, F. (1998). Synthesis and biological activity of gold and tin compounds in ovarian cancer cells. *Anticancer Drugs*, 9(7), 603-610.

- Canpolat, E., and Kaya, M. (2004). Studies on mononuclear chelates derived from substituted Schiff-base ligands (part 2): synthesis and characterization of a new 5-bromosalicyliden-*p*-aminoacetophenoneoxime and its complexes with Co(II), Ni(II), Cu(II) and Zn(II). *Journal of Coordination Chemistry*, 57(14), 1217-1223.
- Carnie, S., Israelachvili, J. N., and Pailthorpe, B. A. (1979). Lipid packing and transbilayer asymmetries of mixed lipid vesicles. *Biochimica et Biophysica Acta (BBA) - Biomembranes*, 554(2), 340-357.
- Cervantes, J., Zárraga, R., and Salazar-Hernández, C. (2012). Organotin catalysts in organosilicon chemistry. *Applied Organometallic Chemistry*, 26(4), 157-163.
- Chen, Z., Zhang, A., Wang, X., Zhu, J., Fan, Y., Yu, H., and Yang, Z. (2017). The advances of carbon nanotubes in cancer diagnostics and therapeutics. *Journal of Nanomaterials*, 2017, 1-13.
- Cho, K., Wang, X., Nie, S., Chen, Z. G., and Shin, D. M. (2008). Therapeutic nanoparticles for drug delivery in cancer. *Clinical Cancer Research*, 14(5), 1310-1316.
- Chow, K. M., and Lo, K. M. (2014). Synthesis, spectral characterization and crystal structures of benzyltin complexes with (*E*)-4-chloro-*N'*-(2-hydroxy-4-methoxybenzylidene)benzohydrazide. *Polyhedron*, 8(1), 370-381.
- Christian, D. A., Cai, S., Garbuzenko, O. B., Harada, T., Zajac, A. L., Minko, T., and Discher, D. E. (2009). Flexible filaments for *in vivo* imaging and delivery: persistent circulation of filomicelles opens the dosage window for sustained tumor shrinkage. *Molecular Pharmaceutics*, 6(5), 1343-1352.
- Cima, F., and Ballarin, L. (1999). TBT-induced apoptosis in tunicate haemocytes. *Applied Organometallic Chemistry*, 13(10), 697-703.
- Clogston, J. D., and Patri, A. K. (2011). Zeta potential measurement. *Methods in Molecular Biology*, 697, 63-70.
- Consola, S., Blanzat, M., Perez, E., Garrigues, J. C., Bordat, P., and Rico-Lattes, I. (2007). Design of original bioactive formulations based on sugar-surfactant/non-steroidal anti-inflammatory cationic self-assemblies: a new way of dermal drug delivery. *Chemistry*, 13(11), 3039-3047.
- Cui, J. X., Li, C. L., Deng, Y. J., Wang, Y. L., and Wang, W. (2006). Freeze-drying of liposomes using tertiary butyl alcohol/water cosolvent systems. *International Journal of Pharmaceutics*, 312(1-2), 131-136.
- Danafar, H., Rostamizadeh, K., Davaran, S., and Hamidi, M. (2017). Co-delivery of hydrophilic and hydrophobic drugs by micelles: a new approach using drug conjugated PEG-PCL Nanoparticles. *Drug Development and Industrial Pharmacy*, 43(11), 1908-1918.

- Danhier, F., Lecouturier, N., Vroman, B., Jerome, C., Marchand-Brynaert, J., Feron, O., and Preat, V. (2009). Paclitaxel-loaded PEGylated PLGA-based nanoparticles: *in vitro* and *in vivo* evaluation. *Journal of Controlled Release*, 133(1), 11-17.
- Dawara, L., and Singh, R. V. (2011). Synthesis, spectroscopic characterization, antimicrobial, pesticidal and nematocidal activity of some nitrogen-oxygen and nitrogen-sulfur donor coumarins based ligands and their organotin(IV) complexes. *Applied Organometallic Chemistry*, 25, 643-652.
- de Sousa, G. F., Lang, L. S., Manso, L. C. C., Deflon, V. M., Filgueiras, C. A. L., and Niquet, E. (2005). Mono-organotin(IV) complexes with 2-acetylpyridine 3-hexamethyleneiminylthiosemicarbazone (HACHexim). The crystallographic structures of [SnX(Ahexim)Cl₂] (X=Me, Ph). *Journal of Molecular Structure*, 753(1-3), 22-26.
- de Vos, D., Willem, R., Gielen, M., van Wingerden, K. E., and Nooter, K. (1998). The development of novel organotin anti-tumor drugs: structure and activity. *Metal-based Drugs*, 5(4), 179-188.
- Deamer, D. (1978). Preparation and properties of ether-injection liposomes. *Annals of the New York Academy of Sciences*, 308(1), 250-258.
- Deamer, D., and Bangham, A. D. (1976). Large volume liposomes by an ether vaporization method. *Biochimica et Biophysica Acta (BBA) - Biomembranes*, 443(3), 629-634.
- Devi, J., and Suman. (2017). Synthesis, characterization and antimicrobial evaluation of Schiff base complexes derived from [2,2'-(ethylenedioxy)bis(ethylamine)] and 5-chlorosalicylaldehyde. *Der Pharma Chemica*, 9(10), 89-92.
- Dey, D. K., Saha, M. K., Das, M. K., Bhartiya, N., Bansal, R. K., Rosair, G., and Mitra, S. (1999). Synthesis and characterization of diorganotin(IV) complexes of tetradentate Schiff bases: crystal structure of *n*-Bu₂Sn(Vanophen). *Polyhedron*, 18(20), 2687-2696.
- Dhand, C., Prabhakaran, M. P., Beuerman, R. W., Lakshminarayanan, R., Dwivedi, N., and Ramakrishna, S. (2014). Role of size of drug delivery carriers for pulmonary and intravenous administration with emphasis on cancer therapeutics and lung-targeted drug delivery. *RSC Advances*, 4(62), 32673-32689.
- Dieter, W., Heike, B., and Hans-Werner, R. (1983). Polymeric Schiff's base chelates and their precursors, 4^a). Syntheses of schiff's base chelates from diaminomaleonitrile and investigation of their activity for the valence isomerisation of quadricyclane to norbornadien. *Macromolecular Chemistry and Physics*, 184(8), 763-778.
- Discher, D. E., and Eisenberg, A. (2002). Polymer vesicles. *Science*, 297(5583), 967-973.
- Dong, Y., and Feng, S. S. (2005). Poly(d,l-lactide-co-glycolide)/montmorillonite nanoparticles for oral delivery of anticancer drugs. *Biomaterials*, 26(30), 6068-6076.

- Doyle, C. D. (1961). Estimating thermal stability of experimental polymers by empirical thermogravimetric analysis. *Analytical Chemistry*, 33(1), 77-79.
- Dubey, R. K., Singh, A. P., and Patil, S. A. (2014). Synthesis, spectroscopic characterization and DNA cleavage studies of dibutyltin(IV) complexes of bidentate Schiff bases. *Inorganica Chimica Acta*, 410, 39-45.
- Dutta, R. (2007). Drug carriers in pharmaceutical design: Promises and progress. *Current Pharmaceutical Design*, 13(7), 761-769.
- Ebrahimipour, S. Y., Sheikhshoae, I., Castro, J., Haase, W., Mohamadi, M., Foro, S., Sheikhshoae, M., and Esmaeili-Mahani, S. (2015). A novel cationic copper(II) Schiff base complex: synthesis, characterization, crystal structure, electrochemical evaluation, anticancer activity, and preparation of its metal oxide nanoparticles. *Inorganica Chimica Acta*, 430, 245-252.
- El-Batanoney, M., Abdel-Moghny, T., and Ramzi, M. (1999). The effect of mixed surfactants on enhancing oil recovery. *Journal of Surfactants and Detergents*, 2(2), 201-205.
- Eldem, T., Speiser, P., and Hincal, A. (1991). Optimization of spray-dried and congealed lipid micropellets and characterization of their surface morphology by scanning electron microscopy. *Pharmaceutical Research*, 8(1), 47-54.
- Elerman, Y., Kabak, M., and Atakol, O. (1993). An *N,N'*-bis(salicylidene)-1,3-propanediamine-nickel complex. *Acta Crystallographica Section C Crystal Structure Communications*, 49(11), 1905-1906.
- Elmali, A., Zeyrek, C. T., Elerman, Y., and Svoboda, I. (2000). [N,N'-Bis(5-bromosalicylidene)-1,3-diaminopropane]nickel(II) and [N,N'-bis(5-chlorosalicylidene)-1,3-diaminopropane]copper(II). *Acta Crystallographica Section C Crystal Structure Communications*, 56(11), 1302-1304.
- Fani, S., Kamalidehghan, B., Lo, K. M., Hashim, N. M., Chow, K. M., and Ahmadipour, F. (2015). Synthesis, structural characterization, and anticancer activity of a monobenzyltin compound against MCF-7 breast cancer cells. *Drug Design, Development and Therapy*, 9, 6191-6201.
- Farokhzad, O. C., and Langer, R. (2009). Impact of nanotechnology on drug delivery. *ACS Nano*, 3(1), 16-20.
- Feng, J., Zhang, Y., McManus, S. A., Ristroph, K. D., Lu, H. D., Gong, K., White, C. E., and Prud'homme, R. K. (2018). Rapid Recovery of Clofazimine-Loaded Nanoparticles with Long-Term Storage Stability as Anti-Cryptosporidium Therapy. *ACS Applied Nano Materials*, 1(5), 2184-2194.
- Frye, A. H., Horst, R. W., and Paliobagis, M. A. (1964). The chemistry of poly(vinyl chloride) stabilization. V. Organotin stabilizers having radioactively tagged Y groups. *Journal of Polymer Science Part A: General Papers*, 2(4), 1801-1814.

- Fu, X., Ping, Q., and Gao, Y. (2005). Effects of formulation factors on encapsulation efficiency and release behaviour *in vitro* of huperzine A-PLGA microspheres. *Journal of Microencapsulation*, 22(7), 705-714.
- Gabizon, A., and Papahadjopoulos, D. (1992). The role of surface charge and hydrophilic groups on liposome clearance *in vivo*. *Biochimica et Biophysica Acta (BBA) - Biomembranes*, 1103(1), 94-100.
- Gabriel, N. E., and Roberts, M. F. (1984). Spontaneous formation of stable unilamellar vesicles. *Biochemistry*, 23(18), 4011-4015.
- Gad, S. C. (2008). *Pharmaceutical Manufacturing Handbook: Production and Processes*: Wiley.
- Gasser, G., Ott, I., and Metzler-Nolte, N. (2011). Organometallic anticancer compounds. *Journal of Medicinal Chemistry*, 54(1), 3-25.
- Gaubert, A., Clement, Y., Bonhomme, A., Burger, B., Jouan-Rimbaud Bouveresse, D., Rutledge, D., Casabianca, H., Lanteri, P., and Bordes, C. (2016). Characterization of surfactant complex mixtures using raman spectroscopy and signal extraction methods: application to laundry detergent deformation. *Analytica Chimica Acta*, 915, 36-48.
- Geng, Y., Dalhaimer, P., Cai, S., Tsai, R., Tewari, M., Minko, T., and Discher, D. E. (2007). Shape effects of filaments versus spherical particles in flow and drug delivery. *Nature Nanotech.*, 2(4), 249-255.
- Ghosh, S., Ray, A., Pramanik, N., and Ambade, B. (2016). Can a cationic surfactant mixture act as a drug delivery vehicle? *Comptes Rendus Chimie*, 19(8), 951-954.
- Gibbs, P. E., and Bryan, G. W. (2009). Reproductive failure in populations of the dogwhelk, *nucella lapillus*, caused by imposex induced by tributyltin from antifouling paints. *Journal of the Marine Biological Association of the United Kingdom*, 66(04), 767-777.
- Gireesh, T., Kuldeep, C., and Pramod, K. (2013). Liposomal current status, evaluation and recent advances. *International Journal of Current Pharmaceutical Research*, 5(3), 4-14.
- Gradinaru, J., Forni, A., Druta, V., Tessore, F., Zecchin, S., Quici, S., and Garbalau, N. (2007). Structural, spectral, electric-field-induced second harmonic, and theoretical study of Ni(II), Cu(II), Zn(II), and VO(II) complexes with [N₂O₂] unsymmetrical schiff bases of S-methylisothiosemicarbazide derivatives. *Inorganic Chemistry*, 46(3), 884-895.
- Gumulec, J., Balvan, J., Sztalmachova, M., Raudenska, M., Dvorakova, V., Knopfova, L., Polanska, H., Hudcova, K., Ruttkay-Nedecky, B., Babula, P., Adam, V., Kizek, R., Stiborova, M., and Masarik, M. (2014). Cisplatin-resistant prostate cancer model: differences in antioxidant system, apoptosis and cell cycle. *International Journal of Oncology*, 44(3), 923-933.

- Gyanakumari, C., Mounika, K., and Pragathi, A. (2010). Synthesis, characterization and biological activity of a schiff base derived from 3-ethoxy salicylaldehyde and 2-amino benzoic acid and its transition metal complexes. *Journal of Scientific Research*, 2(3), 513-524.
- Hammadi, N. I., Abba, Y., Hezmee, M. N. M., Razak, I. S. A., Jaji, A. Z., Isa, T., Mahmood, S. K., and Zakaria, M. (2017). Formulation of a sustained release docetaxel loaded cockle shell-derived calcium carbonate nanoparticles against breast cancer. *Pharmaceutical Research*, 34(6), 1193-1203.
- Hasan, A. A., Madkor, H., and Wageh, S. (2013). Formulation and evaluation of metformin hydrochloride-loaded niosomes as controlled release drug delivery system. *Drug Delivery*, 20(3-4), 120-126.
- Hill, K., and Rhode, O. (1999). Sugar-based surfactants for consumer products and technical applications. *Lipid - Fett*, 101(1), 25-33.
- Holeček, J., Nádvorník, M., Handlíř, K., and Lyčka, A. (1983). ^{13}C and ^{119}Sn NMR study of some four- and five-coordinate triphenyltin(IV) compounds. *Journal of Organometallic Chemistry*, 241(2), 177-184.
- Holeček, J., Nádvorník, M., Handlíř, K., and Lyčka, A. (1986). ^{13}C and ^{119}Sn NMR spectra of Di-*n*-butyltin(IV) compounds. *Journal of Organometallic Chemistry*, 315(3), 299-308.
- Hong, M., Chang, G., Li, R., and Niu, M. (2016). Anti-proliferative activity and DNA/BSA interactions of five mono- or di-organotin(IV) compounds derived from 2-hydroxy-*N'*-(2-hydroxy-3-methoxyphenyl)methylidene]-benzohydrazone *New Journal of Chemistry*, 40(9), 7889-7900.
- Hong, M., Geng, H., Niu, M., Wang, F., Li, D., Liu, J., and Yin, H. (2014). Organotin(IV) complexes derived from Schiff base *N'*-[(1E)-(2-hydroxy-3-methoxyphenyl)methylidene]pyridine-4-carbohydrazone: synthesis, *in vitro* cytotoxicities and DNA/BSA interaction. *European Journal of Medicinal Chemistry*, 86, 550-561.
- Hong, M., Yin, H., Zhang, X., Li, C., Yue, C., and Cheng, S. (2013). Di- and tri-organotin(IV) complexes with 2-hydroxy-1-naphthaldehyde 5-chloro-2-hydroxybenzoylhydrazone: Synthesis, characterization and *in vitro* antitumor activities. *Journal of Organometallic Chemistry*, 724, 23-31.
- Hunter, B. K., and Reeves, L. W. (1968). Chemical shifts for compounds of the group IV elements silicon and tin. *Canadian Journal of Chemistry*, 46(8), 1399-1414.
- Hussen, R. S. D., and Heidelberg, T. (2016). Drug carriers in cancer therapy: administration, formulation and characterization. *International Journal of Pharmacy Review and Research*, 5(4), 37-45.
- Isaacs, N. W., and Kennard, C. H. L. (1970). Crystal structure of *cis*-dichloro-*cis*-bis(dimethylsulphoxide)-*trans*-di-methyltin(IV). *Journal of the Chemical Society A: Inorganic, Physical, Theoretical*, 2(1), 1257.

- Ishida, O., Maruyama, K., Sasaki, K., and Iwatsuru, M. (1999). Size-dependent extravasation and interstitial localization of polyethyleneglycol liposomes in solid tumor-bearing mice. *International Journal of Pharmaceutics*, 190(1), 49-56.
- Jabir, N. R., Tabrez, S., Ashraf, G. M., Shakil, S., Damanhour, G. A., and Kamal, M. A. (2012). Nanotechnology-based approaches in anticancer research. *International Journal of Nanomedicine*, 7, 4391-4408.
- Jain, R., Singh, R., and Kaushik, N. K. (2013). Synthesis, characterization, and thermal and antimicrobial activities of some novel organotin(IV): purine base complexes. *Journal of Chemistry*, 2013, 1-12.
- Jiang, Y., Li, F., Luan, Y., Cao, W., Ji, X., Zhao, L., Zhang, L., and Li, Z. (2012). Formation of drug/surfactant catanionic vesicles and their application in sustained drug release. *International Journal of Pharmaceutical*, 436(1-2), 806-814.
- Jiskoot, W., Teerlink, T., Beuvery, E. C., and Crommelin, D. J. A. (1986). Preparation of liposomes via detergent removal from mixed micelles by dilution. *Pharmaceutisch Weekblad Scientific Edition*, 8(5), 259-265.
- Kabak, M., Elmali, A., Kavlakoglu, E., Elerman, Y., and Durlu, T. N. (1999). [N,N'-Bis(5-bromosalicylidene)-1,3-diaminopropane]copper(II). *Acta Crystallographica Section C Crystal Structure Communications*, 55(10), 1650-1652.
- Kalaivani, P., Saranya, S., Poornima, P., Prabhakaran, R., Dallemer, F., Vijaya Padma, V., and Natarajan, K. (2014). Biological evaluation of new nickel(II) metallates: Synthesis, DNA/protein binding and mitochondrial mediated apoptosis in human lung cancer cells (A549) via ROS hypergeneration and depletion of cellular antioxidant pool. *European Journal of Medicinal Chemistry*, 82(7), 584-599.
- Kalshetty, B. M., Karabasannavar, S. S., Gani, R. S., and Kalashetti, M. B. (2013). Synthesis, characterization and antimicrobial study of some organometallic complexes of multidentate Schiff bases derived from 3-aldehydosalicylic acid at various pH ranges. *Drug Invention Today*, 5(2), 105-112.
- Kaur, G., Garg, T., Rath, G., and Goyal, A. K. (2016). Archaeosomes: an excellent carrier for drug and cell delivery. *Drug Delivery*, 23(7), 2497-2512.
- Kendre, K. L., Pande, G., and Pingalkar, S. R. (2014). Synthesis and characterization of lanthanide complex derived from tetradentate Schiff base and its antimicrobial activity *Der Chemica Sinica*, 5(4), 12-16.
- Khan, M. I., Kaleem Baloch, M., and Ashfaq, M. (2004). Biological aspects of new organotin(IV) compounds of 3-maleimidopropionic acid. *Journal of Organometallic Chemistry*, 689(21), 3370-3378.
- Khandani, M., Sedaghat, T., Erfani, N., Haghshenas, M. R., and Khavasi, H. R. (2013). Synthesis, spectroscopic characterization, structural studies and antibacterial and

antitumor activities of diorganotin complexes with 3-methoxysalicylaldehyde thiosemicarbazone. *Journal of Molecular Structure*, 1037, 136-143.

Kianfar, H. A., and Abroshan, I. (2013). Spectrophotometric study of complexation between some salen type schiff bases and dimethyltin(IV) dichloride. *Chemical Science Transactions*, 2(S1), S17-S24.

Kostova, I., and Saso, L. (2013). Advances in research of Schiff-base metal complexes as potent antioxidants. *Current Medicinal Chemistry*, 20(36), 4609-4632.

Kratz, F. (2008). Albumin as a drug carrier: design of prodrugs, drug conjugates and nanoparticles. *Journal of Control Release*, 132(3), 171-183.

Kreuter, J. (1994). Drug targeting with nanoparticles. *European Journal of Drug Metabolism and Pharmacokinetics*, 19(3), 253-256.

Kulkarni, S. B., Betageri, G. V., and Singh, M. (1995). Factors affecting microencapsulation of drugs in liposomes. *Journal of Microencapsulation*, 12(3), 229-246.

Kulkarni, S. B., Singh, M., and Betageri, G. V. (1997). Encapsulation, stability and *in vitro* release characteristics of liposomal formulations of colchicine. *Journal of Pharmacy and Pharmacology*, 49(5), 491-495.

Kumar, S., Dhar, D. N., and Saxena, P. N. (2009). Applications of metal complexes of Schiff bases. *Journal of Scientific & Industrial Research*, 68(3), 181-187.

Kurtaran, R., Yildirim, L. T., Azaz, A. D., Namli, H., and Atakol, O. (2005). Synthesis, characterization, crystal structure and biological activity of a novel heterotetranuclear complex: $[\text{NiLPb}(\text{SCN})_2(\text{DMF})(\text{H}_2\text{O})]_2$, bis- $\{[\mu\text{-N,N}'\text{-bis}(\text{salicylidene})\text{-1,3-propanediaminato-aqua-nickel(II)](\text{thiocyanato}) (\mu\text{-thiocyanato})(\mu\text{-N,N}'\text{-dimethylformamide})\text{lead(II)}\}$. *Journal Inorganic Biochemistry*, 99(10), 1937-1944.

Laouini, A., Jaafar-Maalej, C., Limayem-Blouza, I., Sfar, S., Charcosset, C., and Fessi, H. (2012). Preparation, characterization and applications of liposomes: state of the art. *Journal of Colloid Science and Biotechnology*, 1(2), 147-168.

Lee, S. M., Sim, K. S., and Lo, K. M. (2015). Synthesis, characterization and biological studies of diorganotin(IV) complexes with tris[(hydroxymethyl)aminomethane] Schiff bases. *Inorganica Chimica Acta*, 429, 195-208.

Leovac, V. M., Jevtovic, V. S., Jovanovic, L. S., and Bogdanovic, G. A. (2005). Metal complexes with Schiff-base ligands - pyridoxal and semicarbazide-based derivatives. *Journal of the Serbian Chemical Society*, 70(3), 393-422.

Li, G. J., and Shen, J. R. (2000). A study of pyridinium-type functional polymers. IV. Behavioral features of the antibacterial activity of insoluble pyridinium-type polymers. *Journal of Applied Polymer Science*, 78(3), 676-684.

- Li, J., Yin, H., and Hong, M. (2011). Synthesis, characterization, and crystal structure of a diorganotin(IV) complex with 2-oxo-2-phenylacetic acid 4-hydroxybenzohydrazone. *ISRN Organic Chemistry, 2011*, 432-437.
- Lin, C. C., and Metters, A. T. (2006). Hydrogels in controlled release formulations: network design and mathematical modeling. *Advanced Drug Delivery Reviews, 58*(12-13), 1379-1408.
- Litzinger, D. C., Buiting, A. M. J., Van Rooijen, N., and Huang, L. (1994). Effect of liposome size on the circulation time and intraorgan distribution of amphipathic poly(ethylene glycol)-containing liposomes. *Biochimica et Biophysica Acta (BBA) - Biomembranes, 1190*(1), 99-107.
- Liu, Y., Pan, J., and Feng, S. S. (2010). Nanoparticles of lipid monolayer shell and biodegradable polymer core for controlled release of paclitaxel: effects of surfactants on particles size, characteristics and *in vitro* performance. *International Journal of Pharmaceutical, 395*(1-2), 243-250.
- Ma, J., Wang, Q., Yang, X., Hao, W., Huang, Z., Zhang, J., Wang, X., and Wang, P. G. (2016). Glycosylated platinum(IV) prodrugs demonstrated significant therapeutic efficacy in cancer cells and minimized side-effects. *Dalton Trans, 45*(29), 11830-11838.
- Magenheim, B., Levy, M. Y., and Benita, S. (1993). A new *in vitro* technique for the evaluation of drug release profile from colloidal carriers - ultrafiltration technique at low pressure. *International Journal of Pharmaceutical, 94*(1-3), 115-123.
- Mahmoud, W. H., Deghadi, R. G., and Mohamed, G. G. (2016). Novel Schiff base ligand and its metal complexes with some transition elements. Synthesis, spectroscopic, thermal analysis, antimicrobial and *in vitro* anticancer activity. *Applied Organometallic Chemistry, 30*(4), 221-230.
- Martin, C. S., Gouveia-Caridade, C., Crespilho, F. N., Constantino, C. J. L., and Brett, C. M. A. (2015). Nickel- *N,N'*-bis(salicylidene)-1,3-propanediamine (Ni-Salpn) film-modified electrodes. Influence of electrodeposition conditions and of electrode material on electrochemical behaviour in aqueous solution. *Electrochimica Acta, 178*(2), 80-91.
- Martins, K. F., Messias, A. D., Leite, F. L., and Duek, E. A. R. (2014). Preparation and characterization of paclitaxel-loaded PLDLA microspheres. *Materials Research, 17*, 650-656.
- Masarudin, M. J., Cutts, S. M., Evison, B. J., Phillips, D. R., and Pigram, P. J. (2015). Factors determining the stability, size distribution, and cellular accumulation of small, monodisperse chitosan nanoparticles as candidate vectors for anticancer drug delivery: application to the passive encapsulation of [(14)C]-doxorubicin. *Nanotechnology, Science and Applications, 8*, 67-80.
- Masroor, S. (2017). Azomethine as potential corrosion inhibitor for different metals and alloys: Review. *Journal of Bio- and Tribo-Corrosion, 3*(3), 1-16.

- Maurya, M. R., Jayaswal, M. N., Puranik, V. G., Chakrabarti, P., Gopinathan, S., and Gopinathan, C. (1997). Dioxomolybdenum(VI) and dioxotungsten(VI) complexes of isomeric ONO donor ligands and the X-ray crystal structure of $[\text{MoO}_2(o\text{-OC}_6\text{H}_4\text{CH}=\text{NCH}_2\text{C}_6\text{H}_4\text{O})(\text{MeOH})]_2 \cdot \text{MeOH}$. *Polyhedron*, 16(23), 3977-3983.
- Mazzaferro, S., Bouchemal, K., and Ponchel, G. (2013). Oral delivery of anticancer drugs I: general considerations. *Drug Discovery Today*, 18(1-2), 25-34.
- McWhinney, S. R., Goldberg, R. M., and McLeod, H. L. (2009). Platinum neurotoxicity pharmacogenetics. *Molecular Cancer Therapeutics*, 8(1), 10-16.
- Menger, F. M., Binder, W. H., and Keiper, J. S. (1997). Cationic surfactants with counterions of glucuronate glycosides. *Langmuir*, 13(12), 3247-3250.
- Meure, L. A., Foster, N. R., and Dehghani, F. (2008). Conventional and dense gas techniques for the production of liposomes: a review. *AAPS PharmSciTech*, 9(3), 798-809.
- Mezei, M., and Nugent, F. J. (1984). Method of encapsulating biologically active materials in multilamellar lipid vesicles (MLV): Google Patents.
- Mishra, A. K., Manav, N., and Kaushik, N. K. (2005). Organotin(IV) complexes of thiohydrazones: synthesis, characterization and antifungal study. *Spectrochimica Acta Part A: Molecular and Biomolecular Spectroscopy*, 61(13-14), 3097-3101.
- Mitragotri, S. (2009). In drug delivery, shape does matter. *Pharmaceutical Research*, 26(1), 232-234.
- Mo, J., Eggers, P. K., Yuan, Z. X., Raston, C. L., and Lim, L. Y. (2016). Paclitaxel-loaded phosphonated calixarene nanovesicles as a modular drug delivery platform. *Scientific Reports*, 6, 79-90.
- Moghimi, S. M., Hunter, A. C., and Murray, J. C. (2001). Long-circulating and target-specific nanoparticles: theory to practice *Pharmacological Reviews*, 53(2), 283-318.
- Mohamed, G. G., Omar, M. M., and Ibrahim, A. A. (2009). Biological activity studies on metal complexes of novel tridentate Schiff base ligand, spectroscopic and thermal characterization. *European Journal of Medicinal Chemistry*, 44(12), 4801-4812.
- Morilla, M. J., Benavidez, P., Lopez, M. O., Bakas, L., and Romero, E. L. (2002). Development and *in vitro* characterization of a benzimidazole liposomal formulation. *International Journal of Pharmaceutical*, 249(1-2), 89-99.
- Mosmann, T. (1983). Rapid colorimetric assay for cellular growth and survival: application to proliferation and cytotoxicity assays. *Journal of Immunological Methods*, 65(1-2), 55-63.

- Mousa, S. A., and Bharali, D. J. (2011). Nanotechnology-based detection and targeted therapy in cancer: nano-bio paradigms and applications. *Cancers*, 3(3), 2888-2903.
- Mroueh, M., Daher, C., Hariri, E., Demirdjian, S., Isber, S., Choi, E. S., Mirtamizdoust, B., and Hammud, H. H. (2015). Magnetic property, DFT calculation, and biological activity of *bis*[(μ (2)-chloro)chloro(1,10-phenanthroline)copper(II)] complex. *Chemico-Biological Interactions*, 231, 53-60.
- Müller, R. H., Jacobs, C., and Kayser, O. (2001). Nanosuspensions as particulate drug formulations in therapy. Rationale for development and what we can expect for the future. *Advance Drug Delivery Reviews*, 47(1), 3-19.
- Muñoz-Flores, B. M., Santillán, R., Farfán, N., Álvarez-Venicio, V., Jiménez-Pérez, V. M., Rodríguez, M., Morales-Saavedra, O. G., Lacroix, P. G., Lepetit, C., and Nakatani, K. (2014). Synthesis, X-ray diffraction analysis and nonlinear optical properties of hexacoordinated organotin compounds derived from Schiff bases. *Journal of Organometallic Chemistry*, 769, 64-71.
- Muzzalupo, R., Perez, L., Pinazo, A., and Tavano, L. (2017). Pharmaceutical versatility of cationic niosomes derived from amino acid-based surfactants: skin penetration behavior and controlled drug release. *International Journal of Pharmaceutical*, 529(1-2), 245-252.
- Nádvorník, M., Holeček, J., Handlíř, K., and Lyčka, A. (1984). The ^{13}C and ^{119}Sn NMR spectra of some four- and five-coordinate tri-*n*-butyltin(IV) compounds. *Journal of Organometallic Chemistry*, 275(1), 43-51.
- Nakanishi, T., Fukushima, S., Okamoto, K., Suzuki, M., Matsumura, Y., Yokoyama, M., Okano, T., Sakurai, Y., and Kataoka, K. (2001). Development of the polymer micelle carrier system for doxorubicin. *Journal of Controlled Release*, 74(1-3), 295-302.
- Nath, M., Saini, P. K., and Kumar, A. (2010). New di- and triorganotin(IV) complexes of tripodal Schiff base ligand containing three imidazole arms: synthesis, structural characterization, anti-inflammatory activity and thermal studies. *Journal of Organometallic Chemistry*, 695(9), 1353-1362.
- Nath, M., Vats, M., and Roy, P. (2013). Tri- and diorganotin(IV) complexes of biologically important orotic acid: synthesis, spectroscopic studies, *in vitro* anti-cancer, DNA fragmentation, enzyme assays and *in vivo* anti-inflammatory activities. *European Journal of Medicinal Chemistry*, 59, 310-321.
- Nornoo, A. O., and Chow, D. S. (2008). Cremophor-free intravenous microemulsions for paclitaxel II. stability, *in vitro* release and pharmacokinetics. *International Journal of Pharmaceutics*, 349(1-2), 117-123.
- Okawara, R., and Wada, M. (1967). Structural Aspects of Organotin Compounds. In F. G. A. Stone & R. West (Eds.), *Advances in Organometallic Chemistry* (Vol. 5, pp. 137-167): Academic Press.

- Ong, S. G., Ming, L. C., Lee, K. S., and Yuen, K. H. (2016). Influence of the encapsulation efficiency and size of liposome on the oral bioavailability of griseofulvin-loaded liposomes. *Pharmaceutics*, 8(3), 25-32.
- Osoyole, A. A., Kolawole, G. A., and Fagade, O. E. (2005). Synthesis, physicochemical, and biological properties of nickel(II), copper(II), and zinc(II) complexes of an unsymmetrical tetradentate Schiff base and their adducts. *Synthesis and Reactivity in Inorganic, Metal-Organic, and Nano-Metal Chemistry*, 35(10), 829-836.
- Otera, J. (1981). ^{119}Sn Chemical Shifts in five- and six-coordinate organotin chelates. *Journal of Organometallic Chemistry*, 221(1), 57-61.
- Otera, J., Hinoishi, T., and Okawara, R. (1980). ^{119}Sn chemical shifts in seven-coordinate organotin compounds. *Journal of Organometallic Chemistry*, 202(4), C93-C94.
- Oztaş, N. A., Yenisehirli, G., Ancin, N., Oztaş, S. G., Özcan, Y., and Ide, S. (2009). Synthesis, characterization, biological activities of dimethyltin(IV) complexes of Schiff bases with *ONO*-type donors. *Spectrochimica Acta Part A: Molecular and Biomolecular Spectroscopy*, 72(5), 929-935.
- Papadopoulos, N., Limniou, M., Koklamanis, G., Tsarouxas, A., Roilidis, M., and Bigger, S. W. (2001). Spec UV-Vis: An ultraviolet-visible spectrophotometer simulation. *Journal of Chemical Education*, 78(11), 1560-1565.
- Pellerito, C., D'Agati, P., Fiore, T., Mansueto, C., Mansueto, V., Stocco, G., Nagy, L., and Pellerito, L. (2005). Synthesis, structural investigations on organotin(IV) chlorin-e6 complexes, their effect on sea urchin embryonic development and induced apoptosis. *Journal of Inorganic Biochemistry*, 99(6), 1294-1305.
- Pellerito, L. (2002). Organotin(IV) $^{n+}$ complexes formed with biologically active ligands: equilibrium and structural studies, and some biological aspects. *Coordination Chemistry Reviews*, 224(1-2), 111-150.
- Perez-Herrero, E., and Fernandez-Medarde, A. (2015). Advanced targeted therapies in cancer: drug nanocarriers, the future of chemotherapy. *European Journal of Pharmaceutics and Biopharmaceutics*, 93, 52-79.
- Peruzynska, M., Szlag, S., Trzeciak, K., Kurzawski, M., Cendrowski, K., Barylak, M., Roginska, D., Piotrowska, K., Mijowska, E., and Drozdziak, M. (2016). *In vitro* and *in vivo* evaluation of sandwich-like mesoporous silica nanoflakes as promising anticancer drug delivery system. *International Journal of Pharmaceutics*, 506(1-2), 458-468.
- Poller, R. C. (1970). *The chemistry of organotin compounds* Academic Press.
- Pramanik, A., Laha, D., Dash, S. K., Chattopadhyay, S., Roy, S., Das, D. K., Pramanik, P., and Karmakar, P. (2016). An *in vivo* study for targeted delivery of copper-organic complex to breast cancer using chitosan polymer nanoparticles. *Materials Science & Engineering. C, Materials for Biological Applications*, 68, 327-337.

- Prasad, K. S., Kumar, L. S., Prasad, M., and Revanasiddappa, H. D. (2010). Novel organotin(IV)-Schiff base complexes: synthesis, characterization, antimicrobial activity, and DNA interaction studies. *Bioinorganic Chemistry and Applications*, 2(3), 15-19.
- Prausnitz, M. R., and Langer, R. (2008). Transdermal drug delivery. *Nature Biotechnology*, 26(11), 1261-1268.
- Pruchnik, F. P., Bańbuła, M., Ciunik, Z., Latocha, M., Skop, B., and Wilczok, T. (2003). Structure, properties and cytostatic activity of tributyltin aminoarylcaboxylates. *Inorganica Chimica Acta*, 356, 62-68.
- Pupo, E., Padrón, A., Santana, E., Sotolongo, J., Quintana, D., Dueñas, S., and Hardy, E. (2005). Preparation of plasmid DNA-containing liposomes using a high-pressure homogenization-extrusion technique. *Journal of Control Release*, 104, 37-43.
- Quan, Z., Chen, S., and Li, S. (2001). Protection of copper corrosion by modification of self-assembled films of schiff bases with alkanethiol. *Corrosion Science*, 43(6), 1071-1080.
- Rabab, K. (2016). Transdermal drug delivery: Benefits and challenges. *Journal of Applied Pharmacy*, 8(1), 438-450.
- Ran, R., Liu, Y., Gao, H., Kuang, Q., Zhang, Q., Tang, J., Fu, H., Zhang, Z., and He, Q. (2015). PEGylated hyaluronic acid-modified liposomal delivery system with anti-gamma-glutamylcyclotransferase siRNA for drug-resistant MCF-7 breast cancer therapy. *Journal of Pharmaceutical Sciences*, 104(2), 476-484.
- Ray, P. C., Tummanapalli, J. M. C., and Gorantla, S. R. (2011). Process for the large-scale production of Stavudine. . *Google Patents*.
- Rehman, T. U., and Zahid, M. (2016). Synthesis and characterization of diphenyltin (IV) complexes with cyclopropane and cyclopentane carboxylic acids. *International Journal of Current Research and Review*, 8(1), 46-50.
- Rehman, W., Badshah, A., Khan, S., and Tuyet le, T. A. (2009). Synthesis, characterization, antimicrobial and antitumor screening of some diorganotin(IV) complexes of 2-[(9H-Purin-6-ylimino)]-phenol. *European Journal of Medicinal Chemistry*, 44(10), 3981-3985.
- Rehman, W., Yasmeen, R., Rahim, F., Waseem, M., Guo, C. Y., Hassan, Z., Rashid, U., and Ayub, K. (2016). Synthesis biological screening and molecular docking studies of some tin(IV) Schiff base adducts. *Journal of Photochemistry Photobiology*, 164, 65-72.
- Rezl, V., and Janák, J. (1973). Elemental analysis by gas chromatography. *Journal of Chromatography A*, 81(2), 233-260.
- Ricci, M., Giovagnoli, S., Blasi, P., Schoubben, A., Perioli, L., and Rossi, C. (2006). Development of liposomal capreomycin sulfate formulations: effects of

formulation variables on peptide encapsulation. *International Journal of Pharmaceutics*, 311(1-2), 172-181.

Rocha, C. S., de Morais, B. P., Rodrigues, B. L., Donnici, C. L., de Lima, G. M., Ardisson, J. D., Takahashi, J. A., and Bitzer, R. S. (2016). Spectroscopic and X-ray structural characterization of new organotin carboxylates and their *in vitro* antifungal activities. *Polyhedron*, 117, 35-47.

Rogolino, D., Carcelli, M., Bacchi, A., Compari, C., Contardi, L., Fisicaro, E., Gatti, A., Sechi, M., Stevaert, A., and Naesens, L. (2015). A versatile salicyl hydrazonic ligand and its metal complexes as antiviral agents. *Journal of Inorganic Biochemistry*, 150, 9-17.

Sadiq ur, R., Saeed, S., Ali, S., Shahzadi, S., and Helliwell, M. (2007). Dichloridobis(dimethyl sulfoxide- κ O)diphenyltin(IV). *Acta Crystallographica Section E Structure Reports Online*, 63(7), 1788.

Safran, S. A., Pincus, P., and Andelman, D. (1990). Theory of spontaneous vesicle formation in surfactant mixtures. *Science*, 248(4953), 354-356.

Sahoo, S. K., Sahoo, S. U. K., Behera, A., Patil, S. V., and Panda, S. K. (2013). Formulation, *in vitro* drug release study and anticancer activity of 5-fluorouracil loaded gellan gum microbead. *Drug Research*, 70(1), 123-127.

Sailaja, S., Reddy, K. R., Rajasekharan, M. V., Hureau, C., Riviere, E., Cano, J., and Girerd, J. J. (2003). Synthesis, structure, and magnetic properties of [MnIII(salpn)NCS]_n, a helical polymer, and the dimer [MnIII(salpn)NCS]₂. Weak ferromagnetism in [MnIII(salpn)NCS]_n related to the strong magnetic anisotropy in Jahn-Teller MnIII (salpnH₂ = *N,N'*-bis(salicylidene)-1,3-diaminopropane). *Inorg Chem*, 42(1), 180-186.

Sainorudin, M. H., Sidek, N. M., Ismail, N., Rozaini, M. Z. H., Harun, N. A., Sabiqah Tuan Anuar, T. N., Abd Rahman Azmi, A. A., and Yusoff, F. (2015). Synthesis, characterization and biological activity of organotin(IV) complexes featuring di-2-ethylhexyldithiocarbamate and *N*-methylbutyldithiocarbamate as ligands. *GSTF Journal of Chemical Sciences (JChem)*, 2(1), 1-9.

Salam, M. A., Affan, M. A., Saha, R., Ahmad, F. B., and Sam, N. (2012). Synthesis, characterization and *in vitro* antibacterial studies of organotin(IV) complexes with 2-hydroxyacetophenone-2-methylphenylthiosemicarbazone (H₂)_{dampt}. *Bioinorganic Chemistry and Applications*, 2012, 698-705.

Salmela, L., and Washington, C. (2014). A continuous flow method for estimation of drug release rates from emulsion formulations. *International Journal of Pharmaceutics*, 472(1-2), 276-281.

Saxena, A. K. (1987). Organotin compounds: toxicology and biomedical applications. *Applied Organometallic Chemistry*, 1(1), 39-56.

Šegota, S., Heimer, S., and Težak, Đ. (2006). New catanionic mixtures of dodecyldimethylammonium bromide/sodium dodecylbenzenesulphonate/water. *Colloids Surf., A*, 274(1-3), 91-99.

- Senapati, P. C., Sahoo, S. K., and Sahu, A. N. (2016). Mixed surfactant based (SNEDDS) self-nanoemulsifying drug delivery system presenting efavirenz for enhancement of oral bioavailability. *Biomedicine & Pharmacotherapy*, 80, 42-51.
- Senthilraja, P., and Kathiresan, K. (2015). *In vitro* cytotoxicity MTT assay in Vero, HepG2 and MCF-7 cell lines study of marine yeast. *Journal of Applied Pharmaceutical Science*, 080-084.
- Shagisultanova, G. A., and Ardasheva, L. P. (2003). Electrochemical synthesis of thin films of polymers derived from [NiSalen] and [NiSalphen]. *Russian Journal of Applied Chemistry*, 76(10), 1626-1630.
- Shah, F. A., Sirajuddin, M., Ali, S., Abbas, S. M., Tahir, M. N., and Rizzoli, C. (2013). Synthesis, spectroscopic characterization, X-ray structure and biological screenings of organotin(IV) 3-[(3,5-dichlorophenylamido)]propanoates. *Inorganica Chimica Acta*, 400(2), 159-168.
- Shaji, J., and Patole, V. (2008). Protein and Peptide drug delivery: oral approaches. *Indian Journal of Pharmaceutical Sciences*, 70(3), 269-277.
- Sharma, A. K., Gothwal, A., Kesharwani, P., Alsaab, H., Iyer, A. K., and Gupta, U. (2017). Dendrimer nanoarchitectures for cancer diagnosis and anticancer drug delivery. *Drug Discovery Today*, 22(2), 314-326.
- Sharma, N., Madan, P., and Lin, S. (2016). Effect of process and formulation variables on the preparation of parenteral paclitaxel-loaded biodegradable polymeric nanoparticles: a co-surfactant study. *Asian Journal of Pharmaceutical Sciences*, 11(3), 404-416.
- Shi, Z., Chen, J., and Yin, X. (2013). Effect of anionic-nonionic-mixed surfactant micelles on solubilization of PAHs. *Journal of the Air & Waste Management Association*, 63(6), 694-701.
- Shujah, S., Zia ur, R., Muhammad, N., Shah, A., Ali, S., Meetsma, A., and Hussain, Z. (2014). Homobimetallic organotin(IV) complexes with hexadentate Schiff base: synthesis, crystal structure and antimicrobial studies. *Journal of Organometallic Chemistry*, 759, 19-26.
- Shujha, S., Shah, A., Zia Ur, R., Muhammad, N., Ali, S., Qureshi, R., Khalid, N., and Meetsma, A. (2010). Diorganotin(IV) derivatives of *ONO* tridentate Schiff base: synthesis, crystal structure, *in vitro* antimicrobial, anti-leishmanial and DNA binding studies. *European Journal of Medicinal Chemistry*, 45(7), 2902-2911.
- Shyamal, M., Panja, A., and Saha, A. (2014). Five new mononuclear zinc(II) complexes with a tetradentate *N*-donor Schiff base: synthesis, structures and influence of anionic coligands on the luminescence behaviour and supramolecular interactions. *Polyhedron*, 69, 141-148.
- Silva, A. L., and Bordado, J. C. (2004). Recent developments in polyurethane catalysis: catalytic mechanisms review. *Catalysis Reviews*, 46(1), 31-51.

- Singh, J., Jain, K., Mehra, N. K., and Jain, N. K. (2016). Dendrimers in anticancer drug delivery: mechanism of interaction of drug and dendrimers. *Artificial Cells, Nanomedicine, and Biotechnology*, 44(7), 1626-1634.
- Singh, R., and Lillard, J. W., Jr. (2009). Nanoparticle-based targeted drug delivery. *Experimental and Molecular Pathology*, 86(3), 215-223.
- Sirajuddin, M., Ali, S., Haider, A., Shah, N. A., Shah, A., and Khan, M. R. (2012). Synthesis, characterization, biological screenings and interaction with calf thymus DNA as well as electrochemical studies of adducts formed by azomethine [2-((3,5-dimethylphenylimino)methyl)phenol] and organotin(IV) chlorides. *Polyhedron*, 40(1), 19-31.
- Sirajuddin, M., Tariq, M., and Ali, S. (2015). Organotin(IV) carboxylates as an effective catalyst for the conversion of corn oil into biodiesel. *Journal of Organometallic Chemistry*, 779, 30-38.
- Sisido, K., Takeda, Y., and Kinugawa, Z. (1961). Direct synthesis of organotin compounds. i. di- and tribenzyltin chlorides. *Journal of the American Chemical Society*, 83(3), 538-541.
- Smith, J. D. B. (1997, 22-25 Sep 1997). *Organotin amine complexes as latent catalysts for epoxy resins*. Paper presented at the Proceedings: Electrical Insulation Conference and Electrical Manufacturing and Coil Winding Conference.
- Soares, S., Fonte, P., Costa, A., Andrade, J., Seabra, V., Ferreira, D., Reis, S., and Sarmento, B. (2013). Effect of freeze-drying, cryoprotectants and storage conditions on the stability of secondary structure of insulin-loaded solid lipid nanoparticles. *International Journal of Pharmaceutical*, 456(2), 370-381.
- Song, X. Q., Zapata, A., and Eng, G. (2006). Organotins and quantitative-structure activity/property relationships. *Journal of Organometallic Chemistry*, 691(8), 1756-1760.
- Stano, P., Bufali, S., Pisano, C., Bucci, F., Barbarino, M., Santaniello, M., Carminati, P., and Luisi, P. L. (2004). Novel camptothecin analogue (gimatecan)-containing liposomes prepared by the ethanol injection method. *Journal of Liposome Research*, 14(1-2), 87-109.
- Storm, G., and Etten, E. (1997). Biopharmaceutical aspects of lipid formulations of amphotericin B. *European Journal of Clinical Microbiology & Infectious Diseases*, 16(1), 64-73.
- Sutradhar, K. B., and Amin, M. L. (2014). Nanotechnology in cancer drug delivery and selective targeting. *ISRN Nanotechnology*, 2014, 1-12.
- Suydam, F. H. (1963). The C=N Stretching Frequency in Azomethines. *Analytical Chemistry*, 35(2), 193-195.
- Szoka, F., and Papahadjopoulos, D. (1978). Procedure for preparation of liposomes with large internal aqueous space and high capture by reverse-phase evaporation. *Proceedings of the National Academy of Sciences*, 75(9), 4194-4198.

- Takahashi, M., and Iwamoto, T. (1981). Synthesis of the metal complexes of the Schiff base derived from 2,3-diamino-cis-2-butenedinitrile and salicylaldehyde. *Journal of Inorganic and Nuclear Chemistry*, 43(2), 253-256.
- Tan, Y., Whitmore, M., Li, S., Frederik, P., and Huang, L. (2002). LPD nanoparticles- novel non viral vector for efficient gene delivery. *Methods in Molecular Medicine*, 69, 73-81.
- Tanwar, H., and Sachdeva, R. (2016). Transdermal drug delivery system: a review. *International Journal Of Pharmaceutical Sciences and Research*, 7(6), 2274-2290.
- Tavano, L., Pinazo, A., Abo-Riya, M., Infante, M. R., Manresa, M. A., Muzzalupo, R., and Perez, L. (2014). Cationic vesicles based on biocompatible diacyl glycerol-arginine surfactants: physicochemical properties, antimicrobial activity, encapsulation efficiency and drug release. *Colloids Surf B Biointerfaces*, 120, 160-167.
- They, C., Ostrowski, M., and Segura, E. (2009). Membrane vesicles as conveyors of immune responses. *Nature Reviews Immunology*, 9(8), 581-593.
- Tiwari, G., Tiwari, R., Sriwastawa, B., Bhati, L., Pandey, S., Pandey, P., and Bannerjee, S. K. (2012). Drug delivery systems: an updated review. *International Journal of Pharmaceutical Investigation*, 2(1), 2-11.
- Tomalia, D. A., and Fréchet, J. M. J. (2002). Discovery of dendrimers and dendritic polymers: a brief historical perspective. *Journal of Polymer Science Part A: Polymer Chemistry*, 40(16), 2719-2728.
- Tripathi, A., and Melo, J. S. (2015). Preparation of a sponge-like biocomposite agarose-chitosan scaffold with primary hepatocytes for establishing an *in vitro* 3D liver tissue model. *Royal Society of Chemistry Advances*, 5(39), 30701-30710.
- Tümer, M., Köksal, H., Sener, M. K., and Serin, S. (1999). Antimicrobial activity studies of the binuclear metal complexes derived from tridentate schiff base ligands. *Transition Metal Chemistry*, 24(4), 414-420.
- Varela-Ramirez, A., Costanzo, M., Carrasco, Y. P., Pannell, K. H., and Aguilera, R. J. (2011). Cytotoxic effects of two organotin compounds and their mode of inflicting cell death on four mammalian cancer cells. *Cell Biology and Toxicology*, 27(3), 159-168.
- Varshney, A., Tandon, J. P., and Crowe, A. J. (1986). Synthesis and structural studies of tin(II) complexes of semicarbazones and thiosemicarbazones. *Polyhedron*, 5(3), 739-742.
- Wang, X., and Guo, Z. (2013). Targeting and delivery of platinum-based anticancer drugs. *Chemical Society Reviews*, 42(1), 202-224.
- Wohrie, D., and Buttner, P. (1985). Polymeric schiff's base chelates and their precursors 8^a), some cobalt chelates as catalysts for the isomerization of quadrycyclyane to norbornadiene. *Polymer Bulletin*, 13(1), 57-64.

- Wong, J., Brugger, A., Khare, A., Chaubal, M., Papadopoulos, P., Rabinow, B., Kipp, J., and Ning, J. (2008). Suspensions for intravenous (IV) injection: a review of development, preclinical and clinical aspects. *Advanced Drug Delivery Reviews*, 60(8), 939-954.
- Wu, H., Liu, S., Xiao, L., Dong, X., Lu, Q., and Kaplan, D. L. (2016). Injectable and pH-responsive silk nanofiber hydrogels for sustained anticancer drug delivery. *ACS Applied Materials & Interfaces*, 8(27), 17118-17126.
- Wu, Y., Wang, L., Qing, Y., Yan, N., Tian, C., and Huang, Y. (2017). A green route to prepare fluorescent and absorbent nano-hybrid hydrogel for water detection. *Scientific Reports*, 7(1), 4380-4389.
- Xin, H., Chen, L., Gu, J., Ren, X., Wei, Z., Luo, J., Chen, Y., Jiang, X., Sha, X., and Fang, X. (2010). Enhanced anti-glioblastoma efficacy by PTX-loaded PEGylated poly(varepsilon-caprolactone) nanoparticles: *in vitro* and *in vivo* evaluation. *International Journal of Pharmaceutics*, 402(1-2), 238-247.
- Xu, J., Zhang, S., Machado, A., Lecommandoux, S., Sandre, O., Gu, F., and Colin, A. (2017). Controllable microfluidic production of drug-loaded PLGA nanoparticles using partially water-miscible mixed solvent microdroplets as a precursor. *Scientific Reports*, 7(1), 4794-4799.
- Xu, Q., Tanaka, Y., and Czernuszka, J. T. (2007). Encapsulation and release of a hydrophobic drug from hydroxyapatite coated liposomes. *Biomaterials*, 28(16), 2687-2694.
- Yang, Y., Hong, M., Xu, L., Cui, J., Chang, G., Li, D., and Li, C. (2016). Organotin(IV) complexes derived from Schiff base *N*'-[(1E)-(2-hydroxy-3-methoxyphenyl)methylidene]pyridine-3-carbohydrazone: synthesis, *in vitro* cytotoxicities and DNA/BSA interaction. *Journal of Organometallic Chemistry*, 804(15), 48-58.
- Yardan, A., Hopa, C., Yahsi, Y., Karahan, A., Kara, H., and Kurtaran, R. (2015). Two new heterodinuclear Schiff base complexes: synthesis, crystal structure and thermal studies. *Spectrochimica Acta Part A: Molecular and Biomolecular Spectroscopy*, 137(4), 351-356.
- Yassin, A. E. B., Anwer, M. K., Mowafy, H. A., El-Bagory, I. M., Bayomi, M. A., and Alsarra, I. A. (2010). Optimization of 5-fluorouracil solid-lipid nanoparticles: a preliminary study to treat colon cancer. *International Journal of Medical Sciences*, 7(6), 398-408.
- Yearwood, B., Parkin, S., and Atwood, D. A. (2002). Synthesis and characterization of organotin Schiff base chelates. *Inorganica Chimica Acta*, 333(1), 124-131.
- Yin, H., Yue, C., Hong, M., Cui, J., Wu, Q., and Zhang, X. (2012). Synthesis, structural characterization and *in vitro* cytotoxicity of diorganotin(IV) diimido complexes. *European Journal of Medicinal Chemistry*, 58(2), 533-542.
- Yin, H. D., Chen, S. W., Li, L. W., and Wang, D. Q. (2007). Synthesis, characterization and crystal structures of the organotin(IV) compounds with the Schiff base

ligands of pyruvic acid thiophene-2-carboxylic hydrazone and salicylaldehyde thiophene-2-carboxylic hydrazone. *Inorganica Chimica Acta*, 360(7), 2215-2223.

Yin, H. D., Hong, M., Wang, Q. B., Xue, S. C., and Wang, D. Q. (2005). Synthesis and structural characterization of diorganotin(IV) esters with pyruvic acid isonicotinyl hydrazone and pyruvic acid salicylhydrazone Schiff bases. *Journal of Organometallic Chemistry*, 690(6), 1669-1676.

Yoshizawa, Y., Kono, Y., Ogawara, K., Kimura, T., and Higaki, K. (2011). PEG liposomalization of paclitaxel improved its *in vivo* disposition and anti-tumor efficacy. *International Journal of Pharmaceutics*, 412(1-2), 132-141.

Zarracino, R. G., Quinones, J. R., and Herbert, H. (2000). Preparation and structural characterization of six new diorganotin(IV) complexes of the $R_2Sn(SalceanH_2)$ and $R_2Sn(SalceanH_2)$ type ($R=Me, nBu, Ph$). *Journal of Organometallic Chemistry*, 664(1-2), 188-200.

Zhang, Y., Yang, M., Portney, N. G., Cui, D., Budak, G., Ozbay, E., Ozkan, M., and Ozkan, C. S. (2008). Zeta potential: a surface electrical characteristic to probe the interaction of nanoparticles with normal and cancer human breast epithelial cells. *Biomedical Microdevices*, 10(2), 321-328.

Zhao, H., Liu, Q., Cai, Y., and Zhang, F. (2008). Effects of water on the structure and properties of F-doped SnO_2 films. *Materials Letters*, 62(8-9), 1294-1296.

Zucali, R., Uslenghi, C., Kenda, R., and Bonadonna, G. (1976). Natural history and survival of inoperable breast cancer treated with radiotherapy and radiotherapy followed by radical mastectomy. *Cancer*, 37(3), 1422-1431.

LIST OF PUBLICATIONS AND PAPERS PRESENTED

Amin, N. A. B. M., Hussen, R. S. D., Lee, S. M., Halcovitch, N. R., Jotani, M. M., & Tiekink, E. R. T. (2017). trans-Di-chlorido-*bis*-(dimethyl sulfoxide-kappaO)*bis*-(4-fluoro-benzyl-kappaC1)tin(IV) : crystal structure and Hirshfeld surface analysis. *Acta Crystallographica Section E: Crystallographic Communications*, 73(Pt 5), 667-672.

University of Malaya